THE EFFECTS OF INSERTS ON FLOW BEHAVIOR OF COHESIVE BULK SOLIDS IN A MODEL BIN

BY

BIN HAO

A Thesis
Submitted to the Faculty of Graduate Studies
in partial fulfillment of the requirements
for the degree of
MASTER OF SCIENCE

DEPARTMENT OF BIOSYSTEMS ENGINEERING
UNIVERSITY OF MANITOBA
WINNIPEG, MANITOBA

THE UNIVERSITY OF MANITOBA

FACULTY OF GRADUATE STUDIES

*****

COPYRIGHT PERMISSION PAGE

THE EFFECTS OF INSERTS ON FLOW BEHAVIOR OF COHESIVE BULK SOLIDS IN A MODEL BIN

BY

BIN HAO

A Thesis/Practicum submitted to the Faculty of Graduate Studies of The University of Manitoba in partial fulfillment of the requirements of the degree of

MASTER OF SCIENCE

I hereby declare that I am the sole author of this thesis.

I authorize the University of Manitoba to lend this thesis to other institutions and/or individuals for the purpose of scholarly research.

Bin Hao

I further authorize the University of Manitoba to reproduce this thesis by photocopying or by other means, in total or in part, at the request of other institutions and/or individuals for the purpose of scholarly research.

Bin Hao

ABSTRACT

Experiments were performed to investigate the effects of inserts on flow behavior of cohesive materials stored in a two-dimensional wedge-shaped model bin. A hopper half angle of 60 degrees and an opening of 38 mm were employed in the tests. A video camera was used to record images of flow patterns of the stored material during discharge. A computer image processing tool was used to analyze the acquired images to determine the influence of inserts on flow patterns and velocity profiles. The discharge rate was measured by using transducers. A computer-controlled data acquisition unit was used to record data.

The tests were performed without inserts, with fixed inserts, and with rotating inserts installed in the bin. For the tests with fixed inserts, the heights of the inserts were 83, 174, 261, and 450 mm from the bin outlet to the bottom of the insert, and for the tests with rotating inserts, the heights of the inserts were 53 and 174 mm from the bin outlet to the bottom of the insert. Each test was repeated three times.

The introduction of the fixed insert at a height of 216 mm and the rotating insert at a height of 174 mm improved the flow quality to the point where the bin was emptied without human intervention. Inserts caused significant changes to flow patterns and velocity profiles. Flow was improved more by increasing the insert height from 83 to 261 mm and from 53 to 174 mm for the fixed insert and for the rotating insert, respectively. Compared to the flow rate without inserts, the average flow rate increased 15% and 28% for the fixed insert at 174 mm and at 261 mm, respectively, and 21% for the rotating insert at the height of 174 mm. No

further improvement in flow was observed by increasing the height of the fixed insert after 261 mm. The rotating insert performed better than the fixed inserts did in improving material flow.

ACKNOWLEDGEMENT

Throughout my thesis project, I received encouragement and assistance from many individuals and I would like to thank them for their kindness and inspiration.

First, I want to acknowledge Dr. Q. Zhang, my advisor, for initially intriguing me with this topic. His positive attitude and guidance always encouraged me to go further and it was most sincerely appreciated. Thank you also to Dr. M. G. Britton and Dr. N. Sepehri for their time evaluating my thesis and for their invaluable suggestions.

Others, whose help I wish to acknowledge, are Mr. J. Putnam, Mr. D. Bourns, Mr. M. McDonald, Mr. J. Philip, and all of my friends and fellow students.

Finally, my wife Y. Sun's patience and encouragement are also acknowledged.

TABLE OF CONTENTS

LIST OF TABLES

LIST OF FIGURES

1. INTRODUCTION

Handling and storage of bulk solid materials such as grain, flour, animal foodstuffs, fertilizer and various industrial powders play an essential role in the agriculture and food industry. Gravity discharge of bulk solids is commonly used in many industries to unload materials from storage facilities. In gravity discharge, materials flow toward the outlet located at the bin bottom when the discharge gate is opened. Flow problems of stored materials often occur because of improper design of the bin. The most common flow problems include arching, rathole, and segregation. Arching results in irregularities in flow patterns. When an arch or rathole is broken either on its own or by manual intervention, the resulting collapse of materials can contain enough force to damage the bin.

Gaylord and Gaylord (1984) have reported that the type of flow pattern in bins depends on the shape of the bin, the roughness of its interior surfaces and the properties of stored materials. Several patterns of flow during discharge are possible. Two principal modes of flow are mass flow and funnel flow. The terminologies used in this study to describe the flow of chop feed are those defined in the ASAE Engineering Practice dealing with loads exerted by free flowing grains on bins (ASAE 1989). Funnel flow is defined as "flow from a bin in which all grain movement occurs through a central core with no movement occurring along the bin wall." Mass flow is described as "flow from a bin in a manner such that movement occurs along all or part of the bin wall" (ASAE 1989).

Various methods have been used to change the flow mode. Extremely cohesive bulk solids, such as clays or caked salt, may have flow properties that require very large bin outlets to prevent a stable material arch from forming. Flow aid devices such as vibrators and air

blasters are also used to break arches. However, because cohesive materials are sensitive to the over-compaction caused by these devices, they may be unsuitable in some cases. The bin insert is an alternative. Inverted cones and pyramids have been used for years in this regard but with limited success. Selection and installation of a 'correct' device can provide a quick, practical solution to the problem of a poorly flowing hopper. The selection of a 'wrong' device may have the reverse effect and lead to more problems than it solves.

In this study, experiments were conducted on a wedged-shape bin to examine the effects of inserts on flow behavior of cohesive materials.

2. LITERATURE REVIEW

2.1 Formation of arching

Laforge and Boruff (1964) studied the formation of an arch by observing the movements of particles in a model bin. Their observations revealed that converging particle flow paths could best be described as turbulence in which particles collided and rebounded, resulting in erratic movements inward, outward, and upward, as well as downward, and thus the periodic breaking of a temporary arch could be observed. They thought that internal pressures within the mass of materials in a hopper compacted cohesive materials into a solid mass, and thus an arch formed over the hopper opening. They pointed out that these pressures were not uniform throughout the mass, and were not equal in all directions as in liquids.

Jenike (1964) proposed a predictive model to determine the minimum dimension of the opening of a bin to prevent an arch or a dome from forming. An arch and a dome were defined by the flow channels in which blockages formed. An arch formed if the channel was wedged-shaped and a dome if it was a conical channel. He assumed that the blockage consisted of self-supporting arches or domes so that the upper and lower boundaries were free surfaces. The minor principal stress (normal to the free surfaces) was zero at any section, and the corresponding major principal stress was tangential to the arch. Because the maximum shear stress for this stress state was on planes at 45° with the principal direction and was equal to one-half of the major principal stress, the maximum span of an arch which could be self-supporting under this stress state was attained when the shear stresses on the vertical sections at the abutments were equal to their maximum values. He postulated that this condition was realized when the major principal stress at the abutments equalled the

unconfined yield strength of the solid and acted at 45° with the horizontal. Therefore, the following equations to predict the minimum dimension of the bin opening were derived:

1) For a wedge-shaped bin, the rectangular opening width was:

$$b = \frac{f_c}{g\gamma} \tag{2-1}$$

2) For a conical bin, the diameter of a circular opening was:

$$d = \frac{2f_c}{g\gamma} \tag{2-2}$$

where:

b = minimum width of a rectangular opening (m),

g = gravitational acceleration (m/s^2),

f_c = unconfined yield strength of solid (Pa),

γ = bulk density of solid (kg/m^3),

d = minimum diameter of a circular opening (m).

Eqns. (2-1) and (2-2) were correct only for θ=0. Jenike (1964) argued that the required outlet diameter was also a function of the hopper half angle θ, and thus, his solution gave values of b for wedge hoppers varying essentially linearly from $\frac{2f_c}{g\gamma}$ at θ=0 to $\frac{1.3f_c}{g\gamma}$ at θ=60°, and values of d for conical hoppers ranged from $\frac{2f_c}{g\gamma}$ at θ=0 to $\frac{2.6f_c}{g\gamma}$ at θ=40°.

2.2 Flow patterns

Flow patterns of granular materials have been observed by many researchers (O'Callaghan 1960; Giunta 1969; Brown and Richards 1970; Bransby and Blair-Fish 1974; Moriyama 1983; McLean et al. 1985; Schwab et al. 1989; Bucklin et al. 1991). In most cases, the flow patterns were observed visually or photographically in model bins constructed of clear plastic, or by using x-ray techniques to observe the density changes of the material and the movement of steel balls embedded in the granular mass. The researchers agreed that two distinct flow patterns, mass flow and funnel flow existed.

O'Callaghan (1960) used photographic techniques to study flow patterns of grains (wheat and barley) in rectangular model bins. He observed that the failure lines between the stationary and moving grain were not straight lines as were generally assumed when the grain was discharged through a central outlet. Based on the principles of soil mechanics, his observations of rupture lines between the stationary and moving grain were best described by logarithmic spirals.

Schwab et al. (1989) studied the effects of the depth of grain on flow patterns. They carried out tests by discharging wheat from the central outlet of a full scale steel bin which was 4.08 m in diameter and with a maximum possible H/D ratio (the depth of grain in the bin to the diameter of the bin cross-section) of 5.0. They found that a funnel flow occurred when the ratio of H/D was less than 1.55, and a mass flow occurred when the ratio of H/D was greater than 2.6. Bucklin et al. (1991) conducted similar studies. They observed flow patterns of corn and wheat during discharge from four clear plastic flat bottom model bins. The types of flow were obtained by varying the grain depth. When the ratio of H/S (the grain depth to

the distance across the bin) was less than 1.25, wheat and corn always discharged in funnel flow. For $1.25 \leq H/S < 2.5$, wheat discharged in a transition state between funnel flow and mass flow, called intermediate flow. For $2.5 \leq H/S < 3.5$, wheat discharged in either intermediate or mass flow. Wheat always discharged in mass flow for $H/S = 3.5$. For $1.25 \leq H/S < 3.5$, corn discharged in uncertain flow patterns. Although the effects of the depth of grain in the bin on flow patterns indeed existed, the predictions of flow patterns were only limited for few experimental materials.

Moriyama (1983) investigated the effects of filling methods on flow patterns in a half cylindrical bin with a glass board in the front. The central and peripheral filling were used in his tests. The results showed that when the bulk solids were poured into the central part of a bin, a perfect mass flow could be attained during discharge. Inversely, when the bulk solids were peripherally filled to the central part of the bin, a funnel flow could occur during the discharge.

Giunta (1969) observed flow patterns of starch, coal and iron ore in a cylindrical bin 0.46 m in diameter and 0.6 m in height. Based on his observations, he developed boundaries to define the flow channel in a flat bottom bin as shown in Fig. 2.1 and the mathematical expression in Eqn. (2-3):

$$2R = d + \frac{2(\tan\theta)(H - \frac{AD}{2})}{1 + A\tan\theta} \qquad (2\text{-}3)$$

where:

R = minimum radius of the boundaries between flowing and nonflowing materials (m),

d = diameter of the discharge opening (m),

θ = angle made by the flow boundary at the edge of the opening (degrees),

H = depth of materials in the bin (m),

A = dimensionless flat bottom bin factor, and

D = bin diameter (m).

McLean et al. (1985) developed different expressions which described the geometric boundaries of the flow channel for free flowing materials (Fig. 2.2), and expressed them mathematically as:

$$\theta_{min} = \frac{\pi}{4} - 0.5\cos^{-1}\left(\frac{1-\sin\delta}{2\sin\delta}\right) \tag{2-4}$$

$$\theta_E = \theta_{min} + \frac{\pi}{18} \tag{2-5}$$

$$\theta_{max} = \left(\frac{5\pi}{36}\right)\exp\left(\frac{-36\left(\delta - \frac{\pi}{6}\right)}{5\pi}\right) \tag{2-6}$$

where:

θ_{min} = minimum value of the half angle of flow zones,

δ = effective angle of the internal friction,

θ_E = expected value of the half angle of flow zones, and

θ_{max} = maximum value of the half angle of flow zones.

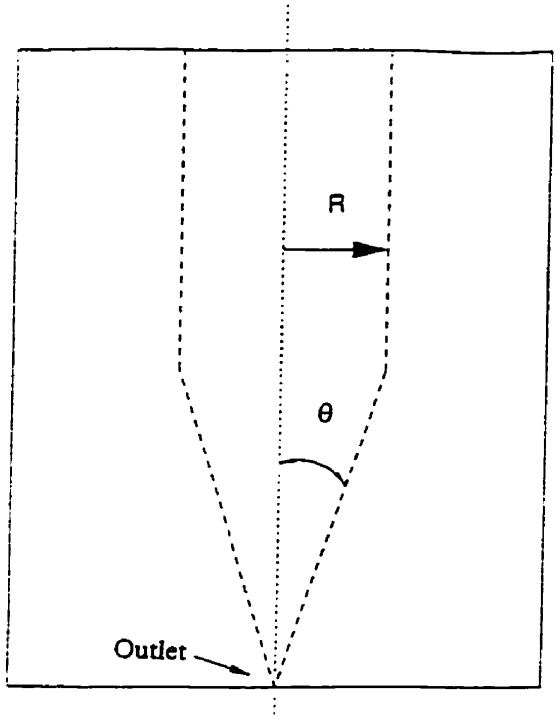

Fig. 2.1 Flow channels predicted by Giunta (1969)

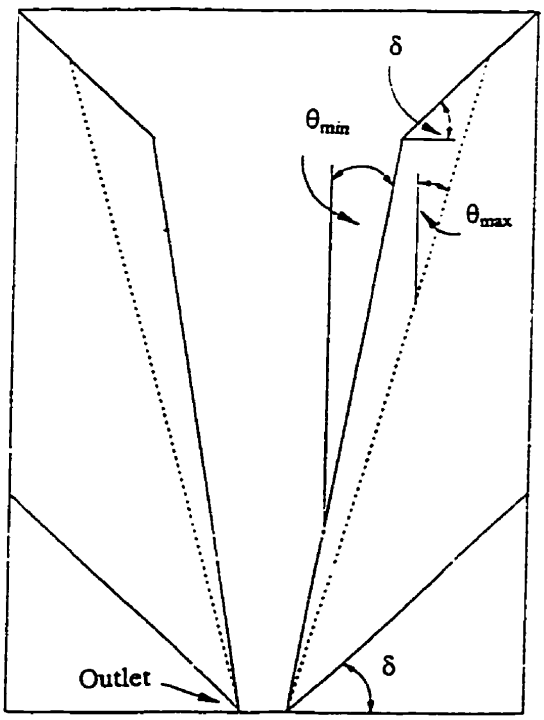

Fig. 2.2 Flow patterns predicted by McLean et al. (1985)

Bucklin et al. (1991) examined the above theoretical predictions of flow patterns. They observed flow patterns by discharging wheat and corn from two 1.2 m tall plexiglass bins. They indicated that McLean's method predicted a better estimate of flow patterns for wheat and corn than Giunta's method did.

Jenike and Leser (1964) indicated that the conditions of mass flow depended on three parameters: wall friction, internal friction, and hopper half angle. Any factor which affected one of these three parameters could have an effect on the flow mode. A similar conclusion was drawn by Gaylord and Gaylord (1984). They concluded that for mass flow to occur, the hopper walls would need to be sufficiently steep and smooth to assure sliding of the solid along the wall.

2.3 Observations of velocity profiles

Tüzün and Nedderman (1983) investigated velocity profiles around obstacles in a planar bunker with a float glass front. The bunker with a rectangular cross-section was about 1.8 m tall and the width between the side walls was adjustable from 152 to 508 mm. One or two obstacles were inserted axially at different heights within the bunker during each test. These obstacles were constructed of perspex and were either of the square or the equilateral triangle shapes with sides of about half the bunker width. Mustard seeds and polyethylene pellets were discharged separately through a central slot orifice in the bunker. The velocity distribution within the bulk materials was obtained by photography of marker particles through the smooth glass front wall of the bunker. The velocity profiles obtained without the obstacles were compared with those obtained with the obstacles. They found that flow patterns were dependant on the magnitude of velocities within the bunker, and the prediction

of particle velocities within the bulk materials was equally important to the calculation of the prevailing stress field within the bunker.

Some researchers (Kotchanova 1971; McCabe 1974; Bransby and Blair-Fish 1974) obtained velocity profiles by stopping the flow, locating the markers placed in the materials and restarting the flow. However, other researchers (Brown and Hawksley 1947; Zenz and Othmer 1960) indicated that the velocity and some features of flow patterns could be affected by stopping the flow intermittently.

The velocity distribution in a converging channel was studied in some detail by Johanson (1964), and a practical application of this work was presented by Johanson and Royal (1982), but they were only interested in calculating the sliding velocity along the wall.

No researchers have reported a successful method of examining the effects of inserts on velocity profiles, nor to relate velocity profiles to flow patterns.

2.4 Discharge rates

Johanson (1965) conducted tests to study the discharge rate of bulk solids from storage structures, and then developed a predictive model for the maximum discharge rate. The tests were performed in rectangular bins with wedge hoppers and in cylindrical bins with conical hoppers. He found that the shape of the bin cross section affected the flow channel but not the flow rate. He postulated that materials at the hopper opening formed a continuously failing arch. The principal stress in the arch was equal to the unconfined compressive strength of the materials. Based on this postulation, the following formulas for calculating the maximum flow rate of frictional, cohesive granular solids were derived:

1) For a wedge hopper:

$$Q_m = \gamma A \sqrt{\frac{bg}{2\tan\theta}\left(1 - \frac{f_c}{P_1}ff\right)} \qquad (2\text{-}7)$$

2) For a conical hopper:

$$Q_m = \gamma A \sqrt{\frac{dg}{4\tan\theta}\left(1 - \frac{f_c}{P_1}ff\right)} \qquad (2\text{-}8)$$

where:

γ = bulk density (kg/m^3),

A = area of outlet (m^2),

Q_m = maximum flow rate (kg/s),

P_1 = consolidation pressure (Pa),

f_c = unconfined compressive strength (Pa),

b = width of the discharge slot (m),

d = diameter of the orifice of a conical hopper (m),

g = gravitational acceleration (m/s^2), and

ff = flow factor.

In order to examine the adequacy of the above formulae, Johanson (1965) conducted full-scale tests with Lac Jeannine concentrate, venezuelan ore fines, and dolomite. The experimental results showed that in all cases a good agreement with predicted values was obtained. It should be noted, however, that his experimental verification was only for bins with material flowing along the hopper walls.

Most of researchers concentrated their studies only on the discharge rate without an insert. However, an insert may have influences on the discharge rate by varying flow patterns.

2.5 Major factors affecting flow behavior

2.5.1 Properties of stored materials

Many researchers (Shamlou 1988; Reisner and Rothe 1971; Gaylord and Gaylord 1984; Safarian and Harris 1985) have reported that the design of flow patterns in bulk solids storage and handling equipment requires knowledge of the bulk properties of materials. The important properties include the effective angle of internal friction, the angle of wall friction, the flow factor, and the flow function.

Jenike (1964) indicated that for an arch to occur in a flow channel, the solid had to be consolidated to such a degree that it developed sufficient strength to support the weight of the arch. Hence, the higher the consolidating pressure in a channel, and the lower the major principle pressure acting in an arch, the lower the flowability of the channel. This was expressed by the flow factor:

$$ff = \frac{\bar{\sigma}_1}{\sigma_1} \tag{2-9}$$

where:

ff = flow factor,

$\bar{\sigma}_1$ = consolidating pressure in a channel (Pa), and

σ_1 = major principle pressure in an arch (Pa).

Jenike (1964) thought that during flow the particles were first brought closer together, as pressures increased, then farther apart, as pressures decreased. The ratio of the major principle pressure to the minor principle pressure was almost constant if the material had a constant moisture content and temperature. This property of bulk solids is usually expressed by the following relationship:

$$\frac{\sigma_1}{\sigma_2} = \frac{1 + \sin\delta}{1 - \sin\delta} \tag{2-10}$$

where:

σ_1 = major principle pressure (Pa),

σ_2 = minor principle pressure (Pa), and

δ = effective angle of internal friction (degrees).

The effects of the effective angle of internal friction and the angle of wall friction on flow have been studied by many researchers (Schweds 1983; Ooms and Roberts 1984; Roberts 1988 and 1991; Carson and Marinelli 1994). Schweds (1983) concluded that the distinction between mass flow and funnel flow was determined by the bin geometry and flow properties, and the governing parameter was the angle of friction between solids and wall material. Roberts (1991) obtained a similar conclusion that, of the various parameters affecting the performance of a hopper, friction at the boundary surface had, in most cases, the major influence. Ooms and Roberts (1984) also indicated that the angle of wall friction had significant influences on designs of flow patterns both in conical and plane-flow bins. For a given geometry, a small increase in the wall friction angle would change a mass flow hopper into a funnel flow hopper. Carson and Marinelli (1994) stated that the effective angle of the internal friction and the angle of the wall friction were important parameters characterizing

the flow properties of a solid. They concluded that the lower the angle of wall friction, the less steep the hopper walls needed to obtain mass flow. This conclusion was in agreement with that drawn by Ooms and Roberts (1985). Carson and Marinelli (1994) also indicated that many variables such as consolidation pressure, moisture content, particle size and shape, temperature, and storage time would affect the values of these angles. Typically as the consolidation pressure increased, the effective angle of internal friction increased.

The flow function was a property of the bulk material. Jenike (1964) defined the flow function as the slope of the plot of the unconfined yield strength against the consolidation pressure. He used the ratio of the unconfined yield strength to the consolidation pressure to classify powder: when the ratio was between 2 and 4, the material was defined as a cohesive material; when the ratio was between 4 and 10, the material was defined as a slightly flowing material; and when the ratio was more than 10, the material was defined as a free flowing material.

The combination of the effective angle of internal friction, the angle of wall friction, the flow factor, and the flow function have been used as the main design criteria in determining the flow mode (funnel or mass flow) in storage bins (Gaylord and Gaylord 1984; Safarian and Harris 1985).

It also should be noted that the effective angle of the internal friction varied along the depth of the stored material because the distribution of the bulk density was not uniform along the whole height of the storage equipment. Stewart (1968) studied the effect of the specific weight on internal friction properties of sorghum grain. He reported that the specific weight of grain was definitely a factor to be considered in determining the internal friction angle of

sorghum grain. He observed a highly significant increase in the internal friction angle with increasing specific weight.

2.5.2 Bin configuration

It is well known that the cross section of the bin or hopper, the hopper angle, and the discharge outlet have significant influences on flow patterns. The success of a bin operation depends largely on the design of these factors. The shape of the upper part of the hopper is usually that of the cross section of the bin. The symmetrical, conical hopper attached to a bin with a circular cross section is commonly used. A hopper can change the flow direction of the stored material and force it to converge and flow through the smaller opening of the hopper. Gaylord and Gaylord (1984) indicated that how the material flowed and converged toward the opening depended almost entirely on the shape of the hopper and the smoothness of its walls.

2.6 Flow promoting devices: inserts

In many cases, it is impractical or impossible to design a bin or hopper that would be self-emptying. An improvement can be achieved by providing flow enhancing devices. Gaylord and Gaylord. (1984) defined many devices as flow inducers such as air blasters, gas entrainments, vibrators, chain slingers and bin inserts. Johanson (1966) suggested that inserts of an appropriately chosen shape when placed at a certain critical height above the silo outlet would considerably reduce the size of stagnant zones observed in a funnel-flow bunker and thus enhance flow behaviour. Jenike (1964) indicated that an insert could also be employed to redistribute the stresses in the flow channel. He thought that because the self-perpetuated

over-consolidation of flowing materials could not develop due to the influences of inserts, the stable arch or dome formation near a hopper outlet would not occur.

Tüzün and Nedderman (1983) investigated the effects of obstacles in a bunker on the formation of arches; the details of their tests have been described in section 2.3. They observed that obstacles increased the wall stresses of filling, but decreased them during flow. They concluded that stable arches, once formed, were frequently observed to give rise to sporadic discharge behavior or indeed in some cases, to completely stop the discharge. Formation of arches would sometimes be prevented by allowing the material to flow in a cascading manner onto successive stress-breaking inserts placed at different heights along the bunker.

Despite the wide-scale use of various types of inserts in industrial bunkers, very little is currently understood about the flow mechanism of bulk solids around inserts.

2.7 Model testing

Most of the observations of flow patterns have been made with small-scale model tests. Cutress (1966) discussed the use of scale models to reproduce arching in cohesive materials, and came to the conclusion that it was doubtful whether an increase in the bulk density (for example, by compaction) could compensate for the reduction of the span of a cohesion arch (full width of a slot or the radius of a circular aperture) by the scale factor of the model. They indicated that in any case after flow had taken place, the bulk density was a characteristic of the flow system and was no longer an independent variable. The consolidation pressure of the system itself was the only agent that would influence the bulk

density, but in a model bin this pressure was almost certain to be too small.

However, influence of test scale on flow behavior and the effect of the bulk density on flow patterns have not been reported in the literature.

3. OBJECTIVES

From the literature cited in the above review, it is clear that the study of the effects of inserts on flow behavior is a complex subject. When analysing flow patterns, many factors need to be considered, many of which are still little understood. Although research has shown that inserts can enhance the flow behavior of cohesive materials stored in bins, more work is still needed to investigate how the flow behavior is affected by inserts during the discharge of stored cohesive materials.

The objectives of this study are:

1) to investigate the influences of mechanical "inserts" on discharge rates, flow patterns, and the formation of arching, and

2) to study the effects of the mounting locations and mounting methods of inserts on flow behavior of cohesive materials.

4. METHODOLOGY

4.1 Major hypothesis

Frequently, inverted cone-shaped inserts were placed above outlets in cylindrical bins with conical hoppers. In this study, the spatial system of a cylindrical bin with a conical insert was modelled by a two-dimensional bin to allow for observation and recording of flow patterns inside the bin. This two-dimensional bin with a triangular insert modelled a rectangular section of a circular bin with a conical insert (Fig. 4.1).

4.2 Experimental equipment

4.2.1 Main frame and bin base

A triangular steel frame was used as a base to support the model bin (Fig. 4.2). The entire weight of the bin structure and feed was placed on this base. Because the maximum load carried by the bin base was 7 kN, which was less than half of the 15 kN design load for the base, the bending deflections in the bin base should be less than the maximum deflection of 1 mm as designed by Pokrant (1983). The bin base was suspended from a main support frame by three steel rods 9.5 mm in diameter and 2400 mm in length. Each rod was cut near the top and a load transducer was placed in the break to measure the total weight of the stored bin.

4.2.2 Model bin

The bin walls were made of three pieces of plywood and a piece of transparent plexiglass. The plexiglass wall was at the front of the bin. The bin was 2400 mm tall, and was rectangular in the cross section with a width of 400 mm and a length of 1000 mm. On the front and rear walls of the model bin, holes were drilled for mounting inserts. The bin hopper

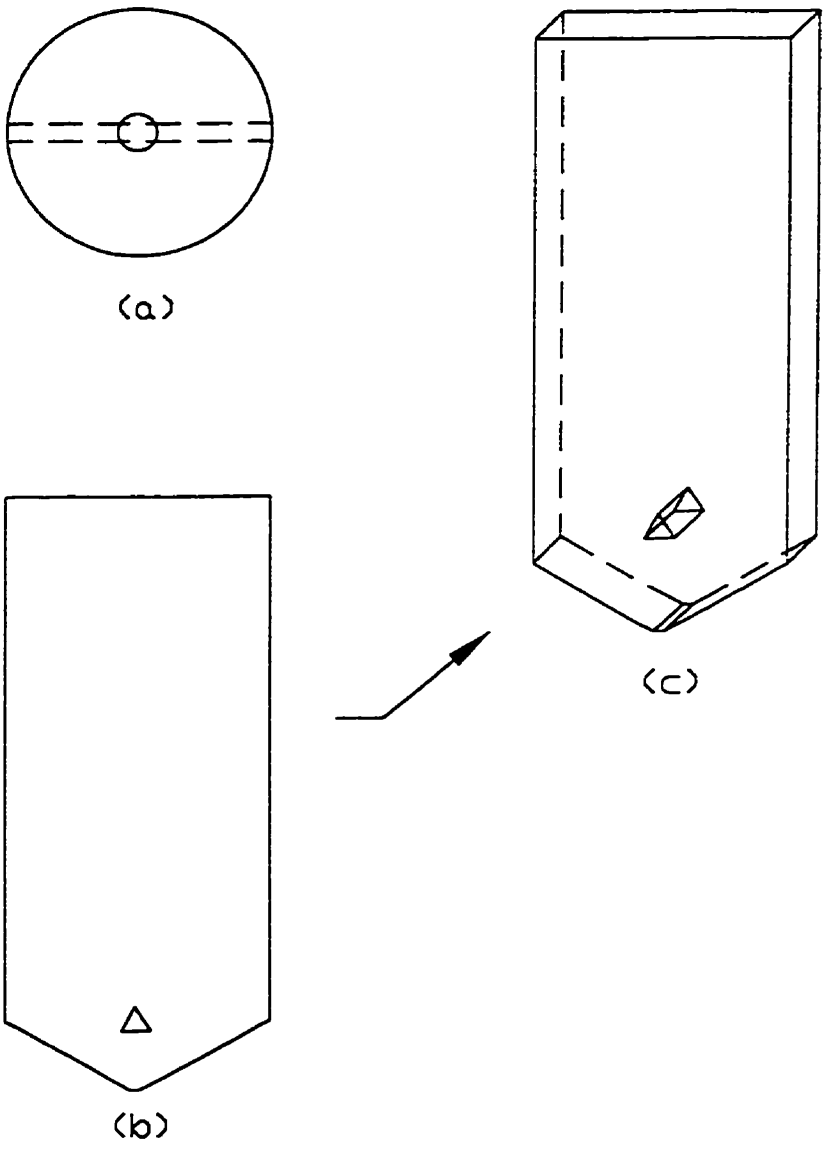

Fig. 4.1 **Schematics of the model for a conical bin with a cone insert. a) top view, b) front view, and c) model bin**

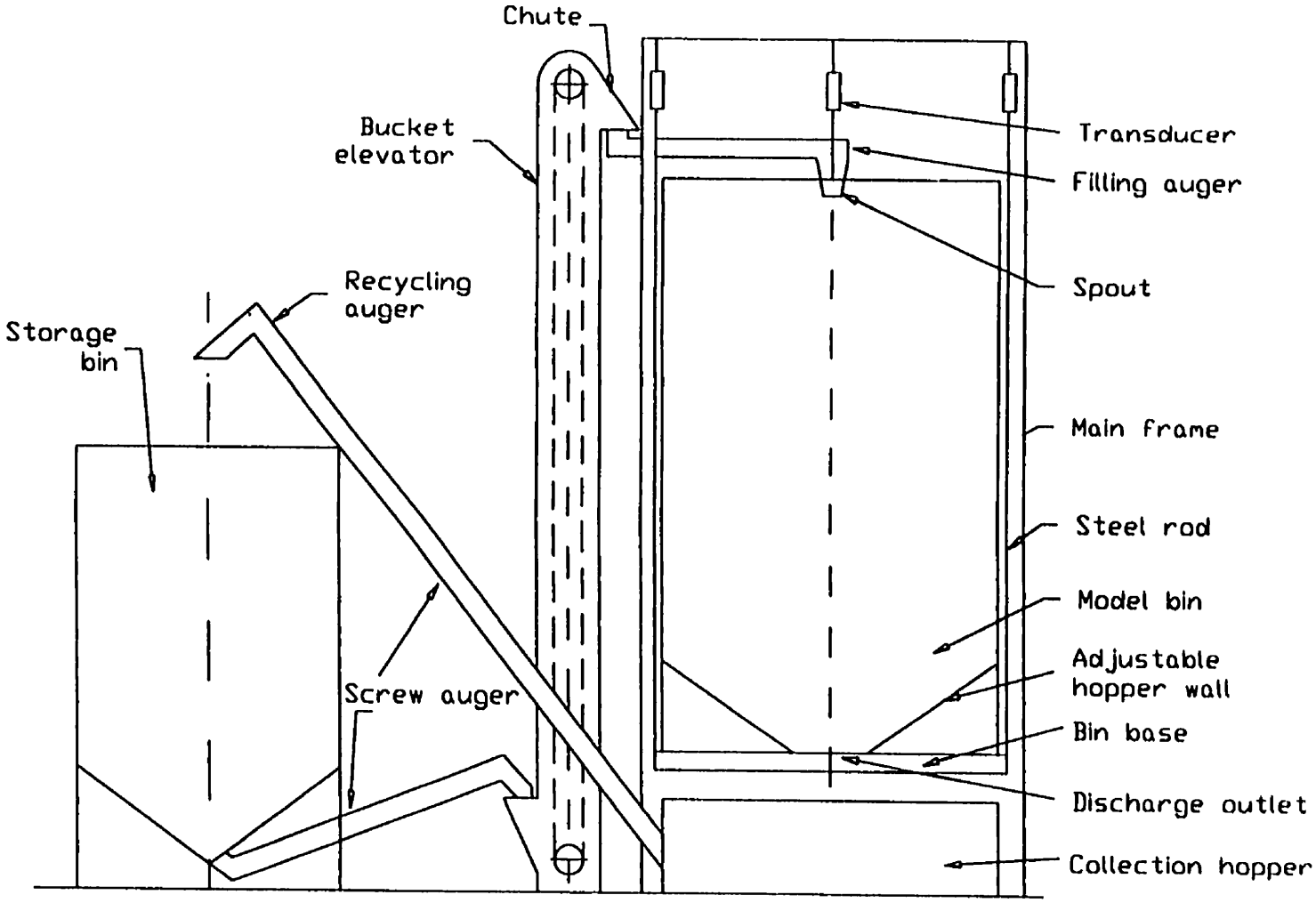

Fig. 4.2 Schematic of model bin testing system

was constructed by putting two plywood plates inside the bin and the hopper half angle could be adjusted from 30° to 90° by changing the length of the plywood plates.

In order to obtain the same friction on all the inside surfaces of the bin, the plywood walls were all lined with plexiglass similar to the front wall. To minimize the influence of the wall deformations on flow, three parallel rows of angle iron bars were mounted horizontally on the front and rear walls to gird the walls. The maximum deflection was less than 1% of the width of the model bin. The deflection was measured by calculating the movement of the marking point in the plug of the insert related to the rear wall of the bin.

A sliding gate opening was used to control discharge. In this research, an opening of 3.8 mm was used.

4.2.3 Insert

A triangular-shaped insert was constructed from plexiglass. The insert was 400 mm long with a triangular cross-section of 100 mm on all three sides. Three holes were drilled at each end of the insert (Fig. 4.3). The hole at the top was used to mount the insert so that it could swing sideways. Tests were also performed when the bottom holes were used to fix the insert in the bin firmly. The insert was mounted at 53, 83, 130, 174, 261, 350, and 450 mm measured from the base of the insert to the bin outlet.

4.2.4 Material handling

A screw auger connected to the chute of a bucket elevator was mounted on the top of the main frame to provide consistent central filling of chop feed (Fig. 4.2). The bucket elevator was fed by another screw auger. The filling rate was 0.6 kg/s. This rate was obtained by adjusting the outlet opening of the storage bin and the speed of the bottom screw auger.

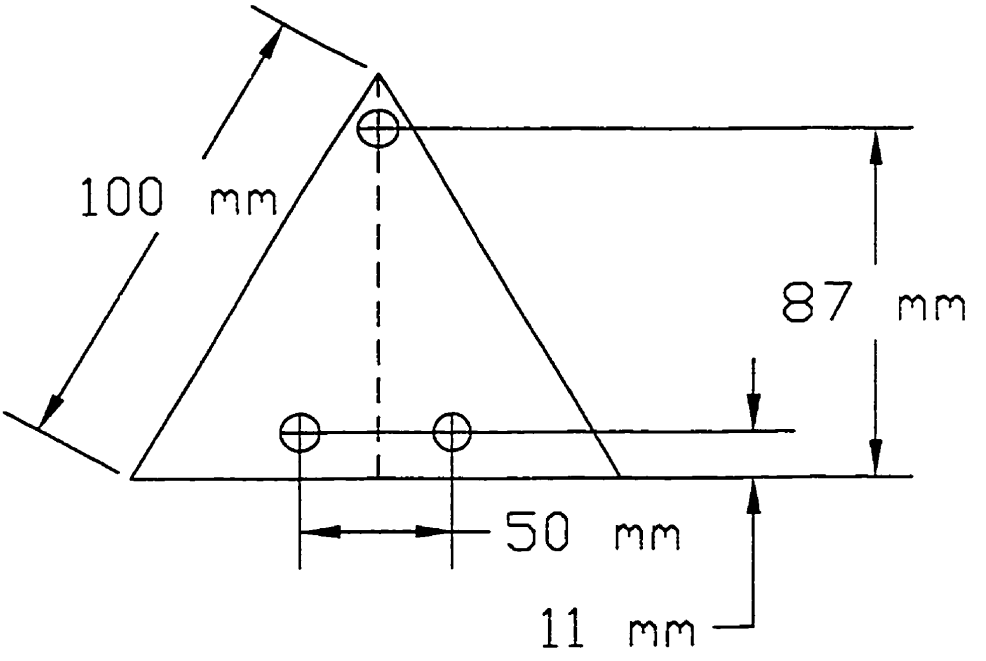

Fig. 4.3 Schematic of bin insert

The discharged feed was collected in a collection hopper beneath the bin, and another screw auger was used to convey the feed back to the storage bin (Fig. 4.2). After each test, the storage bin was covered by a plastic sheet to prevent the feed from changing moisture content.

4.3 Instrumentation

4.3.1 Load transducers

Three transducers designed by Shan (1996) were used for measuring feed loads. Each of the three transducers had a maximum load capacity of 5 kN. The mounting brackets allowed each transducer to rotate to a plumb position thus assuring that the applied load was vertical. The transducer was capable of measuring both static and fluctuating loads.

The transducers were calibrated using dead weights from 0 to 4.2 kN. A typical calibration curve for a transducer is shown in Fig. 4.4. All calibration equations were linear, with R^2>99.99 (Appendix A).

4.3.2 Data acquisition unit and computer system

A high-speed data acquisition unit (HP 3852A, Hewlett-Packard), controlled by a PC computer, was used to record outputs from three transducers. The system was capable of taking 20 readings per second for each of 3 channels with a 6.5 digital resolution. In this study, a recording rate of one reading per second per channel was used.

4.3.3 Flow pattern measurements

4.3.3.1 Arrangements of marking lines

Solid and broken marking lines were added to the test bin to mark the feed levels so that the flow patterns were made visible along the front wall of the bin. The pulverized black

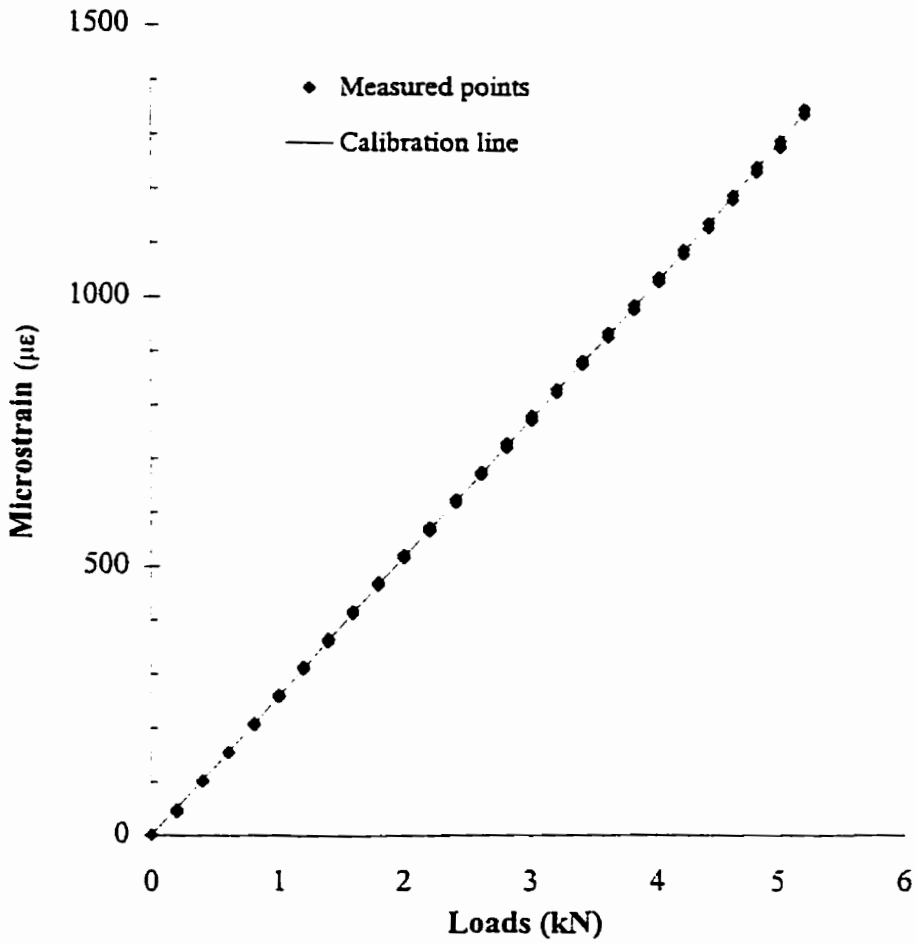

Fig. 4.4 Typical calibration curve of a transducer.

charcoal was used to make marking lines. The arrangement of solid marking lines and broken marking lines is shown in Fig. 4.5. The marking lines were made by placing black powder on the free surface of feed in the bin during filling. Marking lines began with a broken line and then a solid line from the bin bottom, alternately. Eight layers were marked for one test. The vertical space between the two adjacent lines were 100 mm at the hopper section and 300 mm apart at the section above the bin transition. Each broken line consisted of five sequences, about 200 mm apart in the horizontal direction, and these segments divided the feed into five columns vertically (Fig. 4.5).

A special filling bar was used to place black powder into the bin to make marking lines. The bar was designed so that the length of the bar was adjustable to ensure that it worked effectively in the small space between the bin top and the ceiling of the room. A small hopper was fixed at the end of the filling bar.

An experiment was run to examine whether the movements of the solid marking lines reflected the flow of feed. A thin layer of coloured feed was placed beneath a solid marking line in the middle level of the bin. When the bin was fully filled, it was allowed to settle for 30 minutes. After 30 minutes of settling, the feed was discharged. The observation of the movement of the marking line and coloured feed confirmed that they moved together in parallel during discharge. This showed that marking lines reflected the flow of feed.

4.3.3.2 Image processing system

The image processing system consisted of a VHS camcorder (Panasonic Omnimovie PV-950-KHS), a Video Cassette Recorder (VCR, SLV-975 HF, SONY Corporation), and a computer with a video digitizing board (the Intel Smart Video Recorder III board, Intel

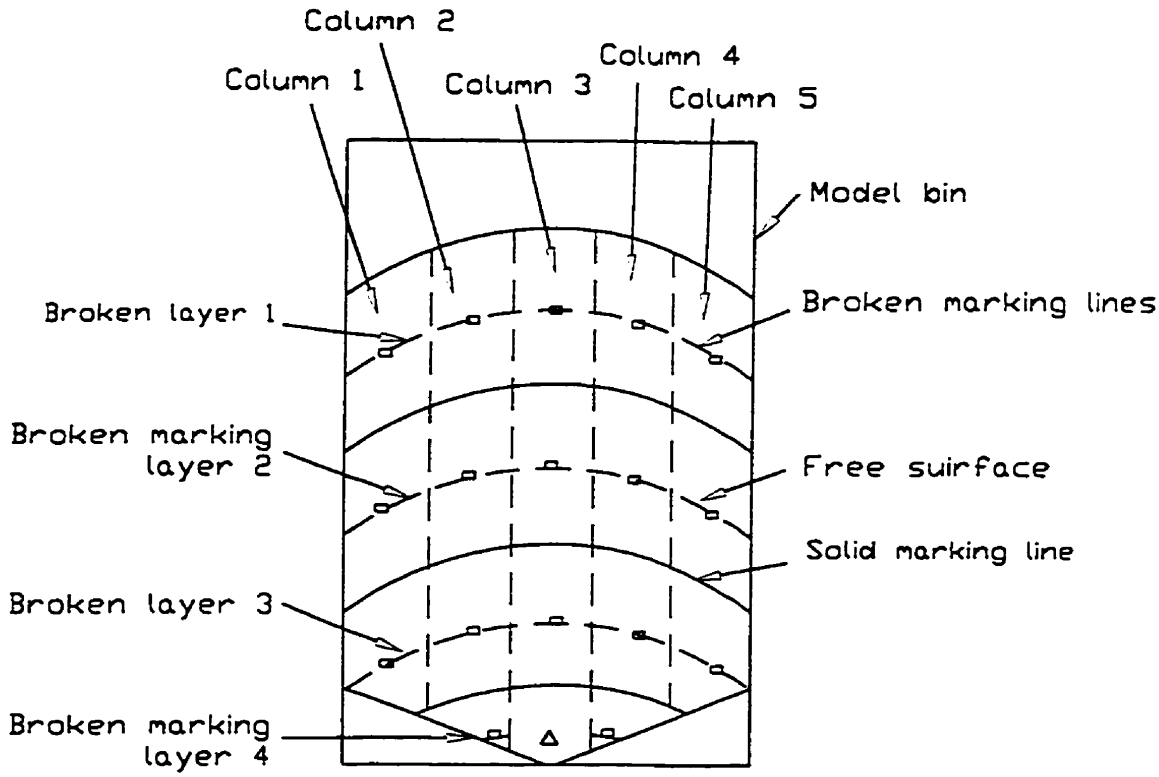

Fig. 4.5 Marking lines in the bin for measuring velocities

Corporation, Hillsboro, OR). Feed movement in the bin was recorded by the video camera mounted in a tripod at the front of the bin. The whole bin was confined in the camera view by adjusting the height and the magnification ratio of the video camera as well as the distance between the camera lens and the front wall of the bin. To minimize distortion of pictures, a level was used to level the video camera, the video camera lens was set to face directly at the bin wall at a 3 m distance, and the height of the video camera was adjusted to equal the centre level of the bin. The type of video cassettes used in the tests was VHS tape. A standard tape play speed of 120 minutes was chosen. Video signals were EIA Standard (525 lines, 60 fields) NTSC colour signals.

By using the VCR with a timer, the video images were played back frame by frame in a rate ranging from 1 to 30 frames per second. In order to ensure that the time used in the calculation of velocity was correct, a digital quartz timer (Micronta, New York) was used to calibrate the timers of the video camera and the VCR. During the calibration of the video camera timer, the quartz timer was put on the front of the bin. The times given by the video camera and by the quartz timer were recorded in the same picture. No difference was found between the two timers.

To check the accuracy of the timer in the VCR, the tape containing the picture with two times was played by the VCR. The calibration was performed for one hour by capturing two pictures at the very beginning of the tape and two near the end of the tape. Time elapsed in the VCR was obtained by using the timer in the VCR. The difference was less than 2 second within one hour of playing.

Video images from the VCR were digitized by the video capture board and captured by using Asymetrix DVP Capture (Asymetrix Corporation). The captured images were processed to change contrast, tint, saturation, or brightness to obtain high quality images. The processed images were then saved in bitmap files. CORE Draw 7 (Corel Corporation and Corel Corporation Limited, New York) was used to further process images to determine the movements of the materials in the bin.

4.4 Materials

Chop feed was used as the test material. The composition and some physical properties of chop feed are listed in Table 4.1 and Table 4.2, respectively. The bulk density of the chop feed was calculated by dividing the measured in-bin mass by the volume of the feed. The moisture content of the chop feed was determined by the air-oven method as recommended by ASAE Standards (ASAE 1990). The angle of repose was determined by emptying a small surge hopper into a 1.5 m wide by 1.0 m high by 0.1 m deep box with a clear front. The angle was determined by measuring the cone of the feed. A modified direct shear apparatus was used to measure the angle of internal friction of the feed and the friction angle between the feed and the bin wall. Details of the modified shear apparatus were discussed by Kieper (1992). To minimize the time effect on feed behavior, the minimum shearing speed of 0.5 mm per minute was used in all tests. A load cell was used to measure the shear force, and a Linear Variable Differential Transducer (LVDT) was used to monitor the horizontal motion of the shear box. The load cell was calibrated using dead weights from 0.045 to 0.054 kN with R^2>99.99% (Appendix A). The LVDT was calibrated using a dial gauge in the deflections ranging from 0 to 60 mm with R^2>99.99% (Appendix B). The data

acquisition system for the shear test consisted of computer and data acquisition instrumentation (HP 3852A, Hewlett-Packard). Cohesion was obtained by extrapolating the yield locus to get an intersection on the plot of shear stress vs normal stress (Brown and Richards 1970). The yield locus is shown in Fig. 4.6.

Table 4.1 Composition of chop feed

Material	Content (%)
Crushed barley	59.1
Soya-meal	12
Canola meal	10
Calcium carbonate	8.25
Tallow	6.4
Fish meal	2
Vitamin premix	1
Calcium phosphate	0.75
Mineral premix	0.5

Table 4.2 Physical properties of the chop feed used in experiments

Bulk density, kg/m^3	638.9[!](21.28)[*]
Angle of internal friction, degrees	27.2[!](0.51)[*]
Angle of wall friction, degrees	10.5[!](0.18)[*]
Angle of repose, degrees	29[!](0.48)[*]
Cohesion, kPa	1.6[!](0.31)[*]
Moisture content, % wb.	10.8[!](0.1)[*]

[!]Means of three measurements.

[*]Values in the parentheses are standard deviations.

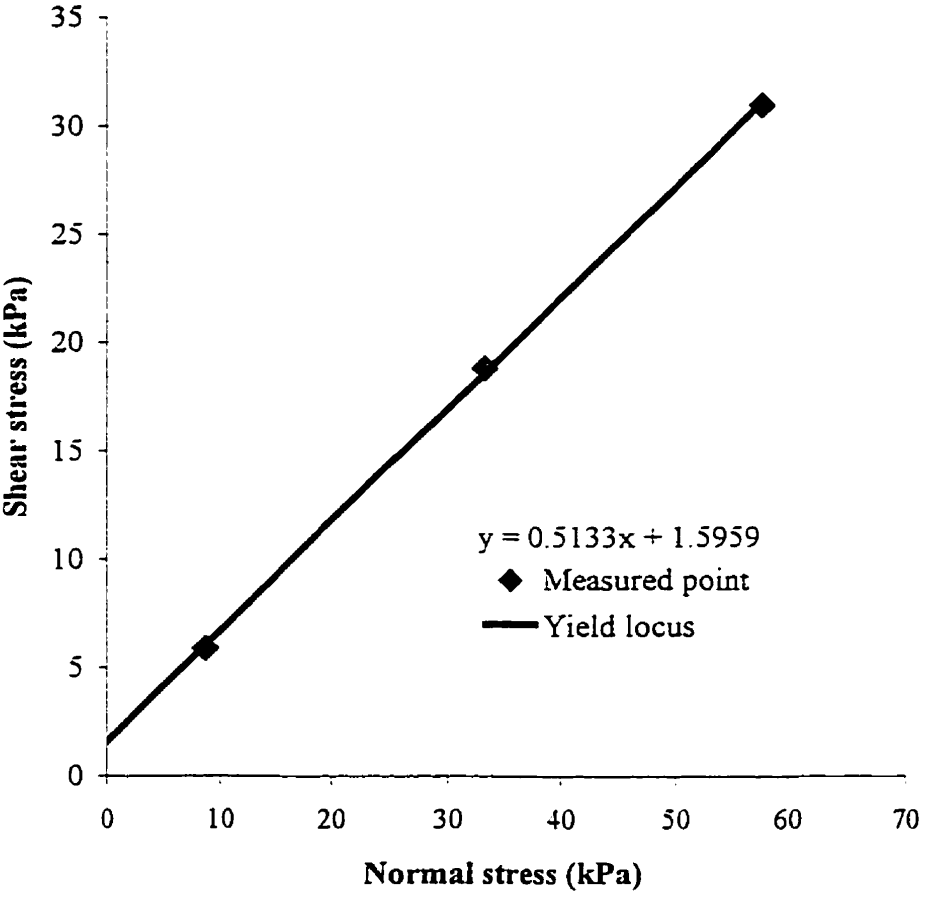

Fig. 4.6 Yield locus of chop feed

4.5 Testing procedure

4.5.1 Experimental design

Test configurations are summarized in Table 4.3.

Table 4.3 Experimental design

Test number	Insert	Insert location	
		Level	Height* (mm)
P	none	none	none
F1	fixed	1	83
F2	fixed	2	174
F3	fixed	3	261
F4	fixed	4	450
R1	rotating	1	53
R2	rotating	2	174

*Measured from bin outlet to the bottom of inserts.

Three repetitions of each of the seven test configurations made up one test series. To eliminate the error in setting bin configurations, each series of tests were completed before the next configuration were tested.

The first series of tests were conducted with no flow enhancing device present. Four series of tests with a fixed insert at four levels (Fig. 4.7) were run. The lowest location was 83 mm at level 1. This was the level where the insert could be placed as close to the discharge outlet as was physically possible. The gap between the hopper wall and the bottom of the insert was 5 mm greater than the width of the outlet opening. Level 2 was located 174 mm above the outlet. For level 3 the insert was placed 261 mm above the outlet so that the tip of the insert was at the level of the bin hopper transition. For level 4 the insert was placed

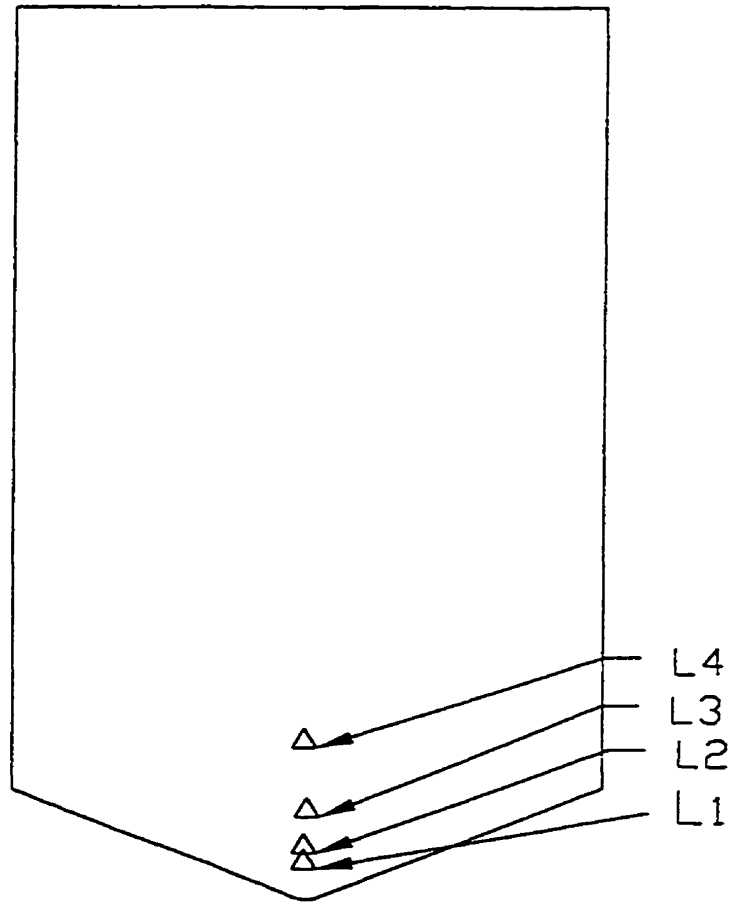

Fig. 4.7 **Locations of the fixed insert in the bin. Locations L1, L2, L3, and L4 were at heights of 83, 174, 261 and 450 mm, respectively.**

entirely above the bin hopper transition level, or 450 mm above the outlet. The last two series of tests were run with a rotating insert at two levels (Fig. 4.8). For level 1 the rotating insert was placed 53 mm above the outlet. For level 2 the rotating insert was set 174 mm above the outlet. It was initially planned to run three repetitions of the tests with the rotating insert at level 1, but as each test in this series required an extensive amount of time and the data appeared to be quite similar between test series, the number of repetitions was reduced to two.

4.5.2 Settling tests

Since the strength of cohesive materials could be significantly increased by time consolidation, thus reducing the flowability of the material (Jenike 1964), it was necessary to consider the effect of time in this study although it was not a primary variable.

A marker was placed in the feed close to the top free surface along the front wall. After the bin was fully filled, the movement of the marker was recorded by the video camera for 120 minutes, which was the maximum recording time of a VHS tape. The images were analysed to determine how much consolidation had occurred during the settling period. Three repetitions were run. The maximum displacement of the marker near the top surface was 8 mm within 30 minutes of settling. Little movement was found from 30 to 120 minutes for all three settling tests. The mean displacement of the three settling tests was 7 mm with a standard deviation of 1.53. It seemed that the feed needed less than 30 minutes to stabilize after it was filled into the bin.

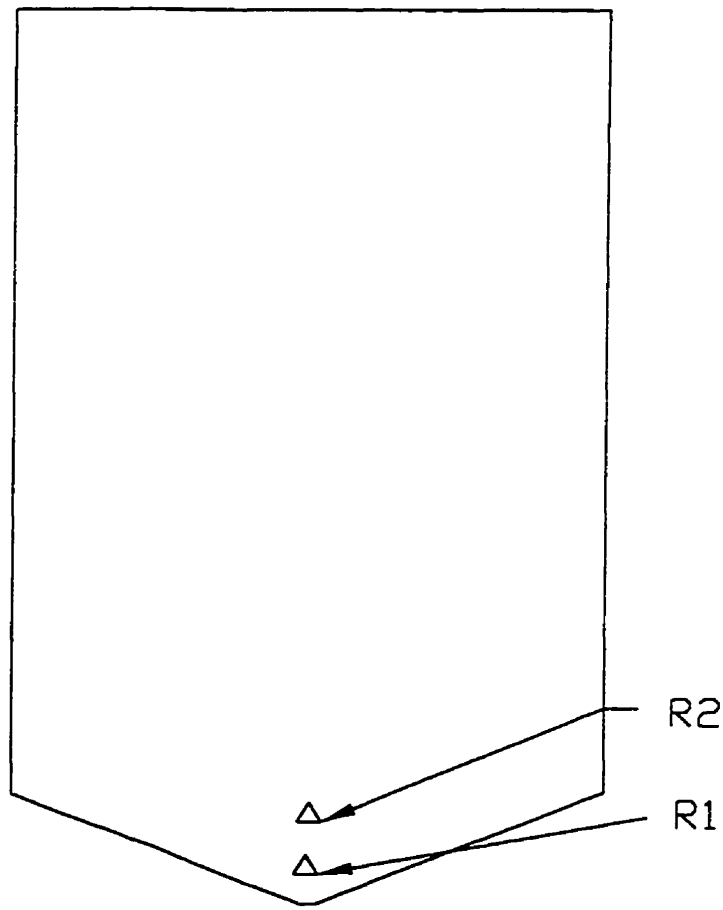

Fig. 4.8 **Locations of the rotating insert in the bin. Locations R1 and R2 were at heights of 53 and 174 mm, respectively.**

4.5.3 Tests for lighting arrangements

All light sources were installed symmetrically to the front wall so that uniform lighting was achieved on the front wall. The arrangements of the light bulbs were determined experimentally by adjusting locations of light sources and diffusion directions to achieve high quality images. Two sheets of black paper were used as a background on both sides of the bin.

For each lighting arrangement, the images were recorded and analysed. By comparing the images obtained in the different arrangements the final arrangement was selected.

4.5.4 Test steps

After the bin was filled and allowed to settle for 30 minutes, the lighting system was switched on. The video camera was set to record. The data acquisition system was initiated and the reference load of zero was taken. The readings were taken at a rate of one reading per second per channel.

A test name was entered into the computer to name the test data. Characters were used to identify bin configurations and test replication numbers. The first character was given in P, F, or R, for tests without an insert, tests with a fixed insert, and tests with a rotating insert, respectively. The letter was followed by a number 1, 2, 3, or 4 for insert locations. The last character A, B, or C was used to represent the repetitions of tests.

After a test was completed, the video tape was played back to check whether high quality images were obtained, and then the data were checked to ensure that all expected data were collected.

4.6 Data analysis

4.6.1 Flow rate

The raw data of microstrains were initially obtained from load transducers. According to the calibration equations for the transducers listed in Appendix A, the raw data were converted to loads applied on each transducer. The total mass of feed in the model bin was calculated by adding up the loads applied on the three transducers. The flow rate was obtained by dividing the change of the load by time.

4.6.2 Calculations of velocities

Velocity calculation was based on the movements of the marking lines in the feed. First, the relative coordinates of broken marking lines in one image frame were recorded in a raw data table with the corresponding time (Table 4.4). The sequent frames were analysed in the same way. The raw data were the converted from pixel to mm by using a coordinate scale in images. The velocity of a point was determined from the coordinates of the point in two consecutive image frames (time between the two frames $\Delta T = 1/30s$).

Table 4.4 Positions of broken marking lines[1]

Test series number: Time: Unit: pixel

Item	Column 1**		Column 2**		Column 3**		Column 4**		Column 5**	
Layer 1*	X_{11}	Y_{11}	X_{12}	Y_{12}	X_{13}	Y_{13}	X_{14}	Y_{14}	X_{15}	Y_{15}
Layer 2*	X_{21}	Y_{21}	X_{22}	Y_{22}	X_{23}	Y_{23}	X_{24}	Y_{24}	X_{25}	Y_{25}
Layer 3*	X_{31}	Y_{31}	X_{32}	Y_{32}	X_{33}	Y_{33}	X_{34}	Y_{34}	X_{35}	Y_{35}
Layer 4*			X_{42}	Y_{42}			X_{44}	Y_{44}		

[1](X_{ij}, Y_{ij}) was defined as the relative location of the marking line in the horizontal and vertical directions for the marking line at layer i and column j in the relative coordinate used in the image processing tools.

*Layers of broken marking lines corresponding to Fig. 4.5 were defined as layer 1, 2, 3, and 4 from top to bottom in the feed.

**Columns were represented by numbers of 1, 2, 3, 4, and 5 in an order of columns from the left to the right as defined in Fig.4.5.

For example, when point (X_{ij}, Y_{ij}) moved from (X_0, Y_0) to (X_1, Y_1) during the period of ΔT, the velocity vectors were calculated as follow:

$$V_x = \frac{X_1 - X_0}{\Delta T} \tag{4.1}$$

$$V_y = \frac{Y_1 - Y_0}{\Delta T} \tag{4.2}$$

$$V_{ij} = \sqrt{V_x^2 + V_y^2} \tag{4.3}$$

where:

V_x = horizontal velocity of point (X_{ij}, Y_{ij}),

V_y = vertical velocity of point (X_{ij}, Y_{ij}), and

V_{ij} = velocity vector of point (X_{ij}, Y_{ij}).

5. RESULTS AND DISCUSSION

5.1 Effects of inserts on flow rates

Reisner (1971) stated that when a bin with a free flowing material was emptied through a vertical opening in the bottom, the material flowed at a constant rate during the entire process of discharge. Therefore, the plot of discharge loads vs. discharge time should have a constant slope if feed flowed freely out of the bin.

No constant slopes were found in the plots of discharge loads vs. discharge time for feed flow (Fig. 5.1). Instead, fluctuations of the slopes were observed. Roberts et al.(1990) indicated that cohesion was the major factor out of all the parameters affecting the gravity flow performance of bins. This factor was thus considered to be the main reason for a decreasing flow rate or for making the flow rate inconsistent in the tests.

Fig. 5.1 showed that some slopes in the plots were zero during the initial and intermediate period of feed discharge, that is, the flow rate was zero. Obviously, a zero flow rate meant that arching had occurred in the bin. Arches were found in all the tests except the test with a fixed insert at level 3 and the test with a rotating insert at level 2. Table 5.1. shows some of the flow characteristics observed in the tests.

It was necessary to break the arch to restore the flow when arch occurred in the bin during the test. When feed from the top layer collapsed down to the bottom of the bin, the feed in the low part of the bin obtained high strength due to compacting from the collapsed feed.

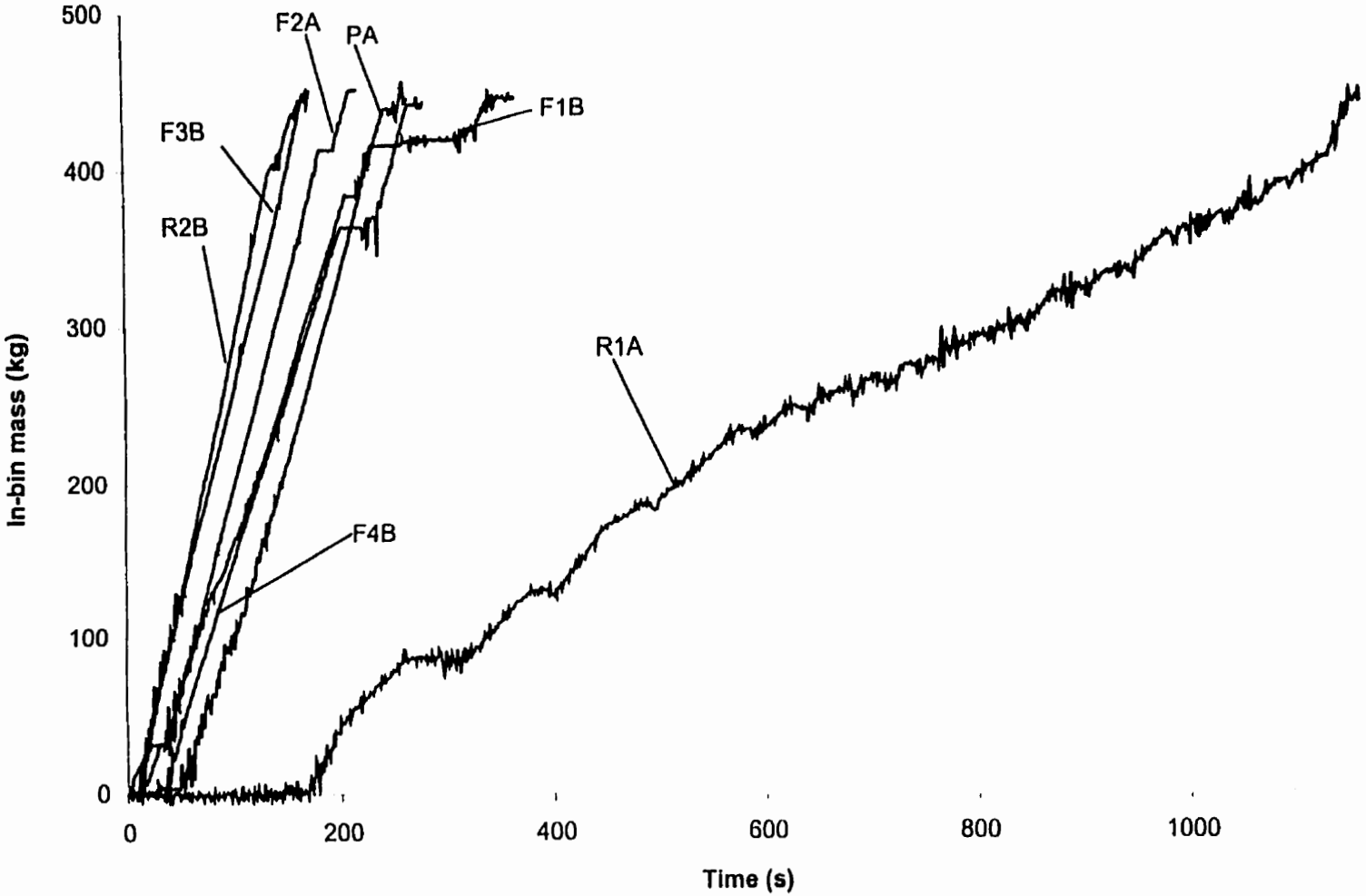

Fig. 5.1 Variation of in-bin feed mass during discharge. PA-without inserts, F1B-fixed insert at level 1 in repetition B, F2A-fixed insert at level 2 in repetition A, F3B-fixed insert at level 3 in repetition B, F4B-fixed insert at level 4 in repetition B, R1A-rotating insert at level 1 in repetition A, and R2B-rotating insert at level 2 in repetition B.

Table 5.1 Flow characteristics*

Test No.	Times of arching formation	Average flow rate (kg/s)	Standard deviation of flow rate
PA	3	1.93	2.14
F1	2	1.48	0.70
F2	1	2.22	1.64
F3	0	2.79	0.69
F4	1	2.06	2.28
R1	9	0.52	1.77
R2	0	2.33	5.28

*Mean values from three measurements except test R1 from two measurements.

The average flow rate was calculated from the total mass of the feed in the bin and the total time required to empty the bin. The time of flow stoppage was also included in calculations of the average flow rates. Although the time required to break an arch had influences on the calculations of the flow rates, it was thought that man-made factors could also reflect the effectiveness of the inserts. The better the insert promoted the flow, the less the man-made factor affected the time needed to break an arch, and thus, the higher the flow rate.

Compared with the flow rate of 1.93 kg/s for the tests without inserts, the flow rates increased to 2.22 (15%), 2.79 (45%), and 2.06 kg/s (7%) for the tests with a fixed insert at level 2, 3, and 4, and increased to 2.33 (21%) kg/s for the tests with a rotating insert at level 2; However, the flow rates decreased to 1.48 (23%) and 0.57 kg/s (73%) for the tests with a fixed insert at level 1 and for the tests with a rotating insert at level 1, respectively (Fig.

5.2). The best mounting locations for enhancing the flow were found at 261 mm for the fixed insert and 174 mm for the rotating insert, respectively.

Lower flow rates for the insert locations closer to the outlet might be attributed to the smaller perpendicular gaps between the insert and the hopper wall. For the fixed insert at level 1, the gap between the bottom of the insert and the hopper wall was 48 mm. This gap was close to the 38 mm width of the outlet of the bin. It seemed that when the gap between the insert and the hopper wall was close to the opening of the discharge outlet, the arching would occur, causing the flow rate to decrease. It should be noted that the gap between the rotating insert and the hopper wall changed as the insert rotated. The gap change may be calculated from the geometric relationship as follows (Fig. 5.3).

$$\frac{S + G_0}{S\cos\phi + H + \frac{L}{2}\tan\phi} = \cos\theta \qquad (5\text{-}1)$$

$$\Delta G = AD\sin\frac{\theta}{2} \qquad (5\text{-}2)$$

$$AD = 2DO\sin\frac{\theta}{2} \qquad (5\text{-}3)$$

When S = 100 mm, L = 38 mm, θ = 300, the following equations (5-4) to (5-6) are obtained:

$$G_0 = 0.886H - 24.027 \qquad (5\text{-}4)$$

$$\Delta G = 200\sin^2\frac{\theta}{2} \qquad (5\text{-}5)$$

$$G = G_0 + \Delta G \qquad (5\text{-}6)$$

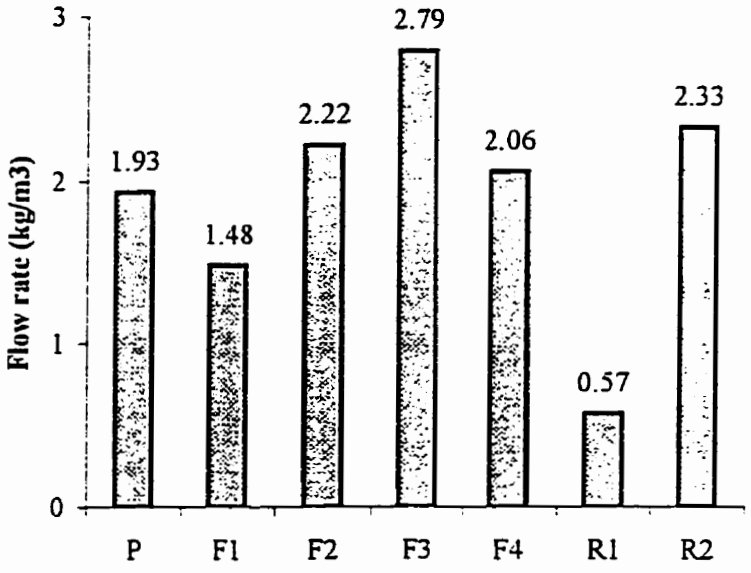

Fig. 5.2 **Average flow rates of feed in the bins without inserts (P), with fixed inserts at levels 1 to 4 (F1 to F4), and with rotating inserts at levels 1 to 2 (R1 to R2).**

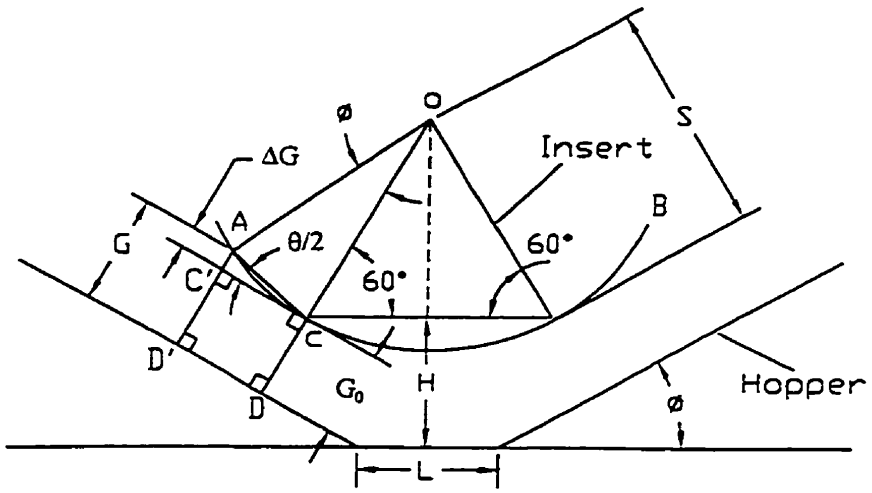

Fig. 5.3 **The geometric relationship of the rotation angle of the insert and the gap between the insert and the hopper walls**

where:

S = side length of insert section (mm),

L = width of the bin outlet (mm),

ϕ = angle of hopper wall to the horizontal direction (degrees),

G_0 = gap between the insert and the hopper wall when the insert is at the neutral position (mm),

H = height of the insert bottom above the bin opening when the insert is at the neutral position (mm),

ΔG = change of the gap between the insert bottom and the hopper wall (mm),

G = gap between the insert and the hopper wall when the insert rotates (mm), and

θ = swinging angle of the insert.

When the insert was rotating clockwise within 4°, the gaps on both sides of the insert increased (Fig. 5.4). Counter-clockwise rotations within 4° caused the gaps to decrease. No matter if the gap was increased or decreased, the insert rotation helped break arching. This inference was proven by comparing the flow characteristics for a rotating insert and the flow characteristics for a fixed insert at level 2. Although both inserts were at the same location, the flow stoppage was not found in the tests with the rotating insert.

5.2 Effects of inserts on flow patterns and velocity profiles

5.2.1 Tests without inserts

For the tests without inserts, the flow of chop feed created a stable arch or rathole across the hopper outlet after 30, 15, and 70 seconds of discharge for three tests, respectively.

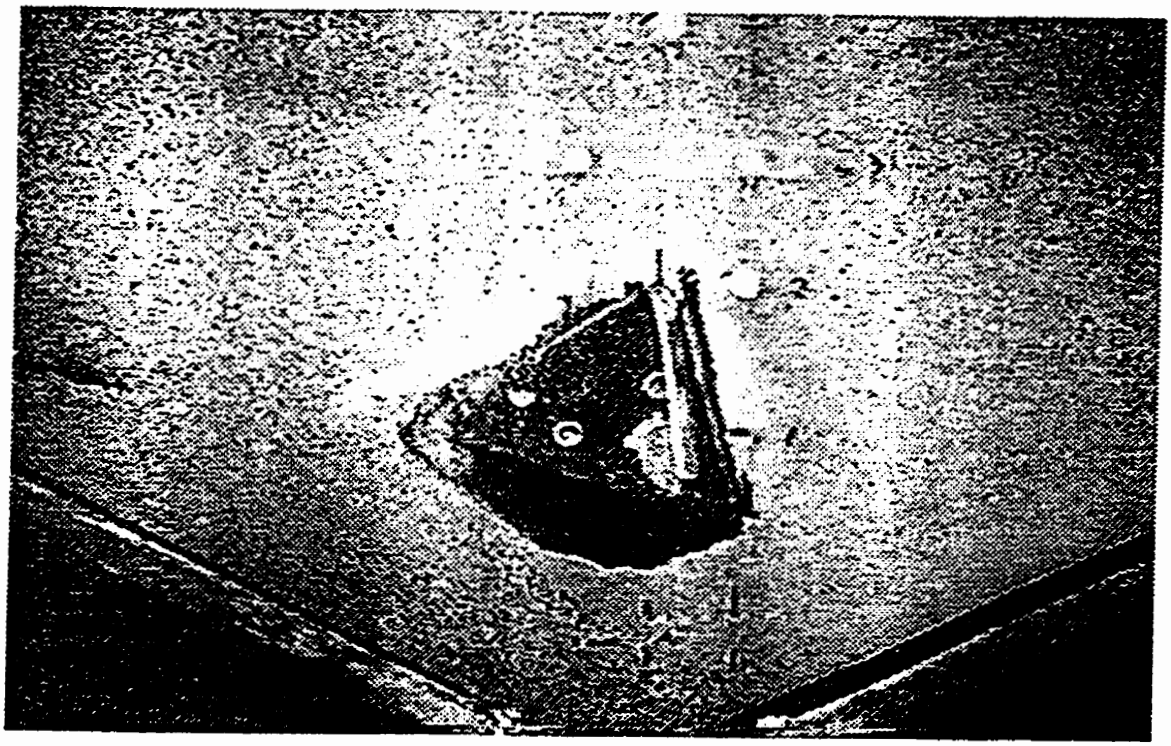

Fig. 5.4 Initial rotation of the insert before discharge.

The mean of the time of arch or rathole happening for three tests was 38 seconds with a standard deviation of 28. This demonstrated that the flow patterns were irregular without insert.

The typical flow patterns are shown in Figs. 5.5a-n, with Fig. 5.5a depicting the full bin before discharge. In the first 15 seconds of discharge, the flow pattern was funnel flow. An approximately 166 mm wide flow funnel was formed (Fig. 5.5b). The feed in the central area of the bin moved downward with a maximum velocity of 91 mm/s. At 30 seconds of discharge when the feed in the flow channel was completely discharged (Fig. 5.5c), the flow channel developed into a stable rathole through the bin with a height of 2000 mm and a width of 166 mm. About a 417 mm thick layer of chop feed along the side walls of the bin remained stationary after the stable rathole formed. When the rat hole was manually broken feed collapses into the channel and arching occurred above the outlet (Fig. 5.5d). After several instances of human intervention a new flow funnel was developed (Figs. 5.5e-f). About 104 seconds of discharge an arch occurred again across the outlet of the bin (Fig. 5.5g). With human intervention, the feed started to flow again. Figs. 5.5h-m show that the flow still tended to be funnel flow, with feed sliding along the free surface and filling in the flow channel. No feed movement was observed in the feed along the bin walls. At 210 seconds of discharge an arch occurred again as shown in Fig. 5.5n. Once again manual intervention had to be applied to break the arch to empty the bin.

The flow patterns in this configuration were unacceptable because the feed had to be manually assisted out of the bin. Poor flow was due to cohesion of the material and the bin configuration. The cohesive property of chop feed increased the strength of the falling arch,

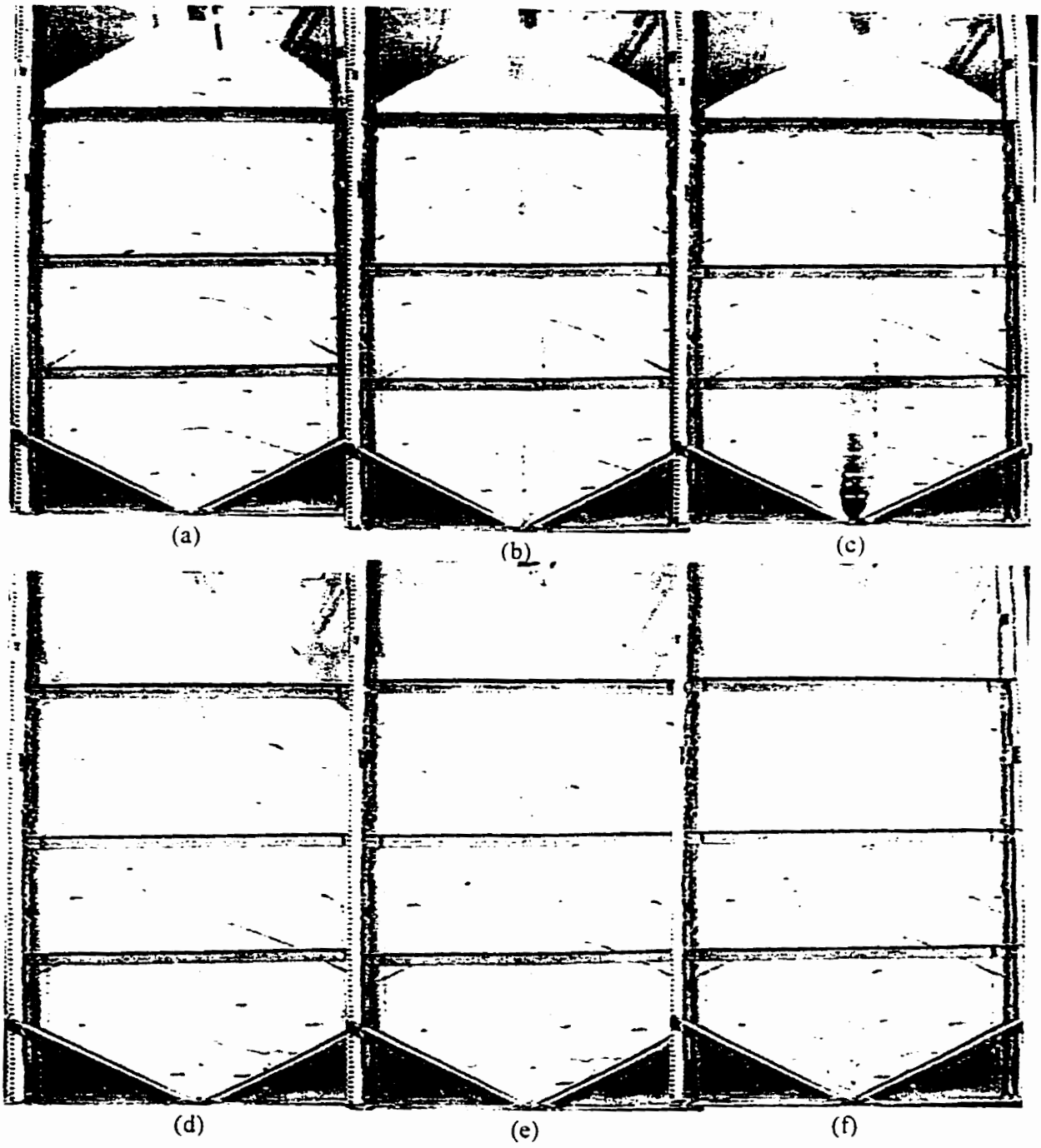

Fig. 5.5 **Typical flow patterns of chop feed in the model bin without an insert, Test PA. a) 0 s, b) 15 s, c) 30 s, d) 50 s, e) 85 s, f) 100 s, g) 104 s, h) 123 s, i) 138 s, j) 153 s, k) 168 s, l) 183 s, m) 189 s, and n) 210 s.**

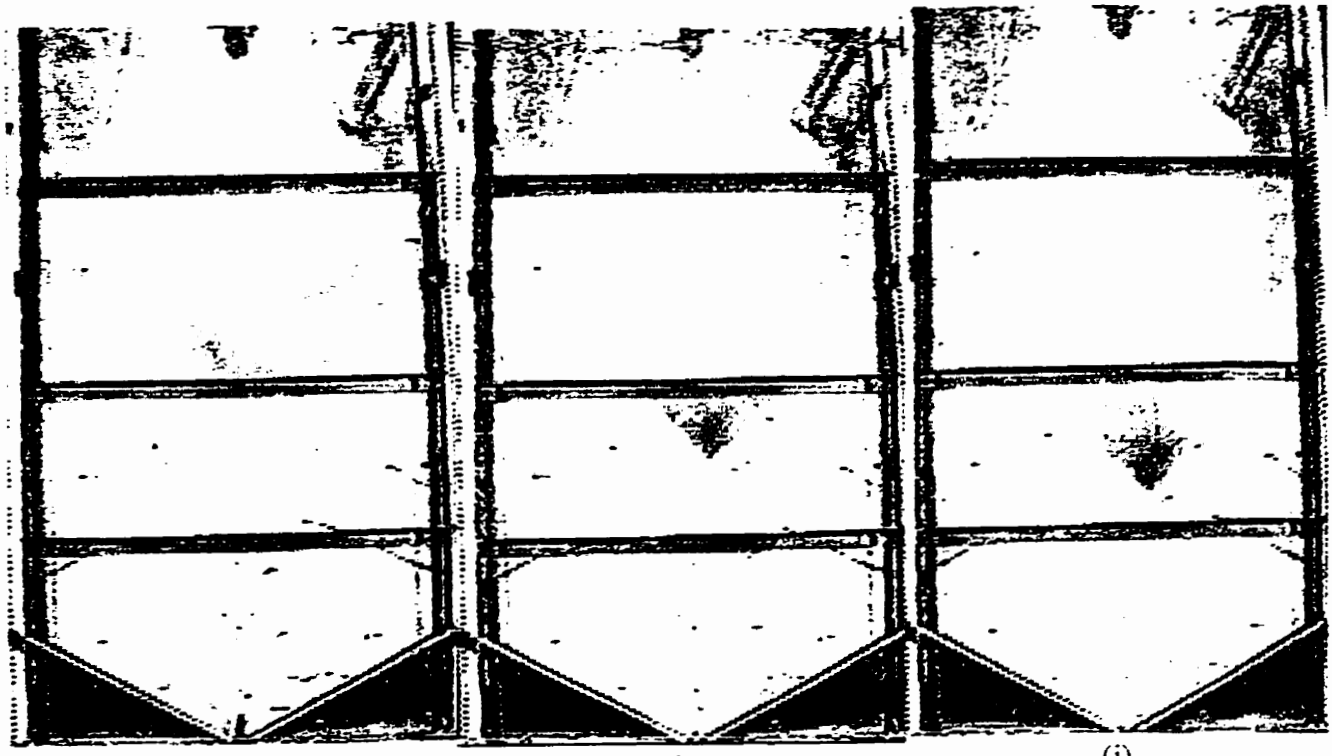

(g) (h) (i)

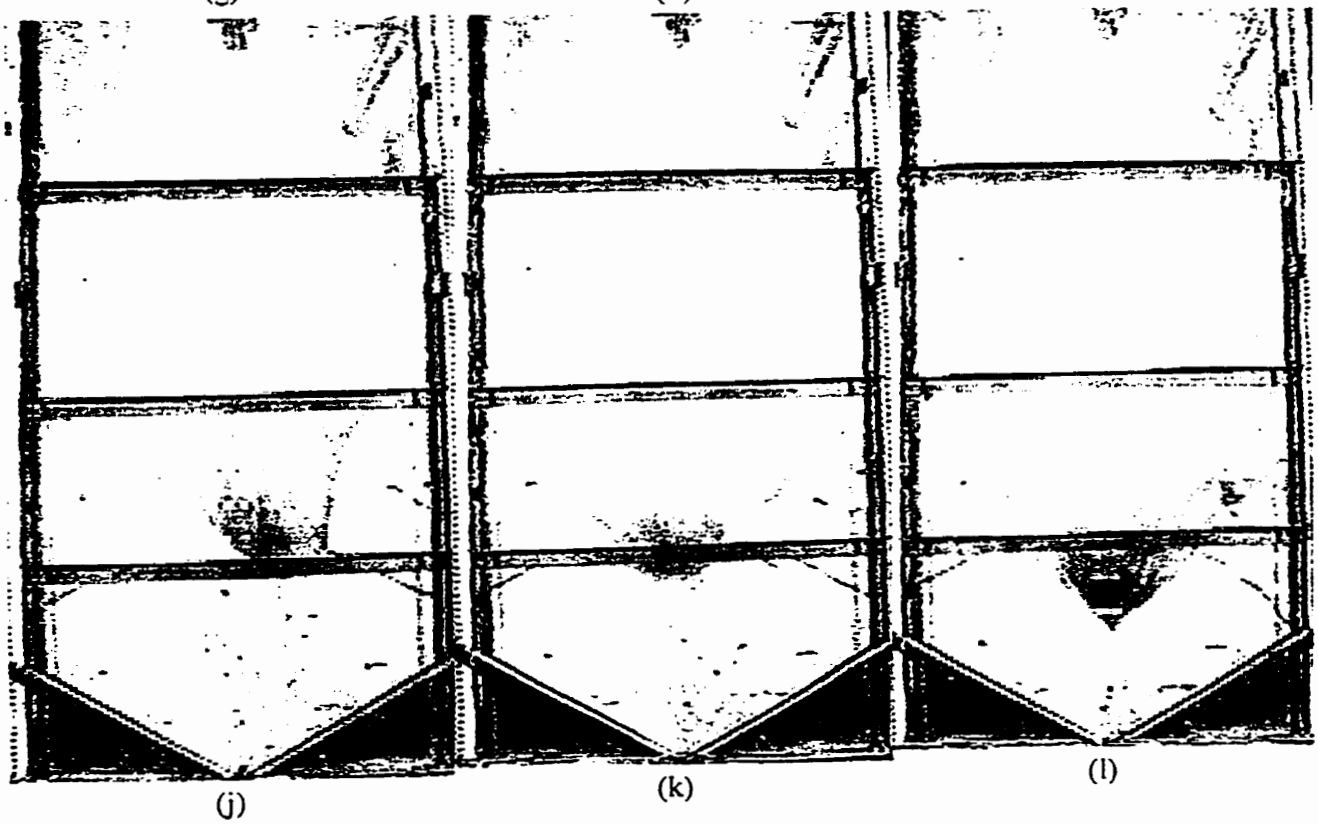

(j) (k) (l)

(m) (n)

thus, impeded the flowability of the chop feed in the hopper. Large hopper opening reduces arching formation. However in this study the dimension of the outlet was deliberately chosen to create flow problems so that the effectiveness of bin inserts could be tested.

5.2.2 Fixed inserts

When a fixed insert was installed in the bin, almost all of the feed in the bin was activated, and feed movement took place along the bin walls. Instead of a central channel flow which appeared in the tests without inserts, two small flow channels developed both sides of the insert (Figs. 5.6a-k, Appendix C and Appendix D). There was only one flow channel when the bin was close to empty (Figs. 5.6d-k).

The velocities in the left three columns were almost equal (Fig. 5.7a), forming a fast flowing channel, while the other two columns formed a slow flowing channel.

The average velocity of 14.05 mm/s in the left channel was 33% higher than 9.46 mm/s in the right flow zone. Therefore, the feed on the left side discharged faster than the right side as shown in Fig. 5.6b. It was also noted that arching occurred frequently in the zone with a lower velocity (Figs. 5.7c-g).

When the fixed insert was installed 83 mm above the discharge outlet, arching occurred at the beginning of discharge for all three tests (Fig. 5.8b). It seemed that the insert placed at a low position produced an obstruction to the flow. With manual intervention the flow resumed, but near the end of discharge an arch was observed again (Fig. 5.8o).

After the initial arching was broken, a mass flow condition was observed from 30 to 60 s of discharge (Figs. 5.8c-d, and Figs. 5.9a-c). The flow velocity in the right side of the bin was greater than the left side (Fig. 5.9a-h). The maximum velocities of 11.7, 21.2, and 22.7

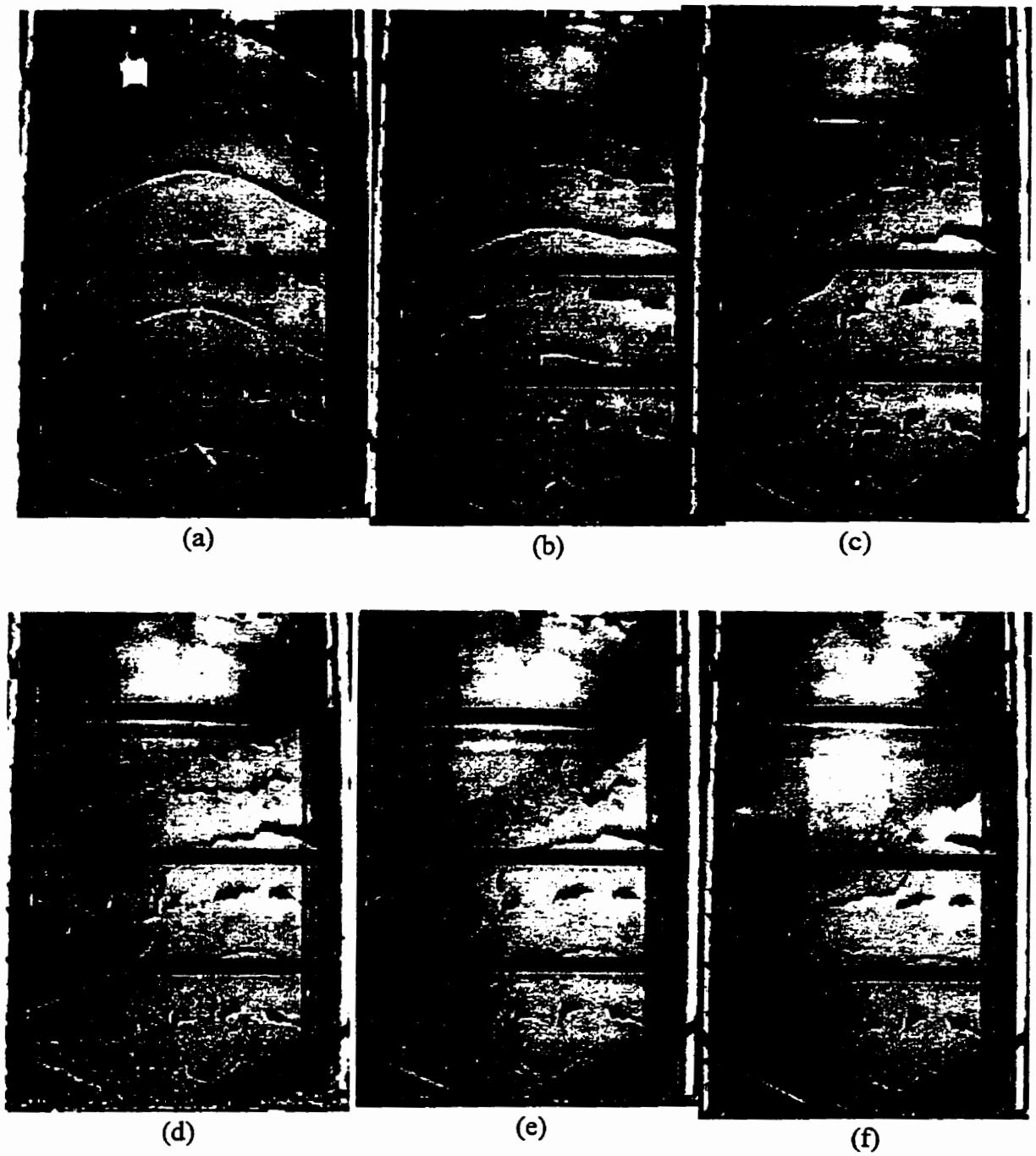

Fig. 5.6 **Typical flow patterns of chop feed in the model bin with a fixed insert, Test F2A. a) 0 s, b) 35 s, c) 50 s, d) 65 s, e) 80 s, f) 90 s, g) 110 s, h) 125 s, i) 140 s, j) 155 s, and k) 170 s.**

(g) (h) (i)

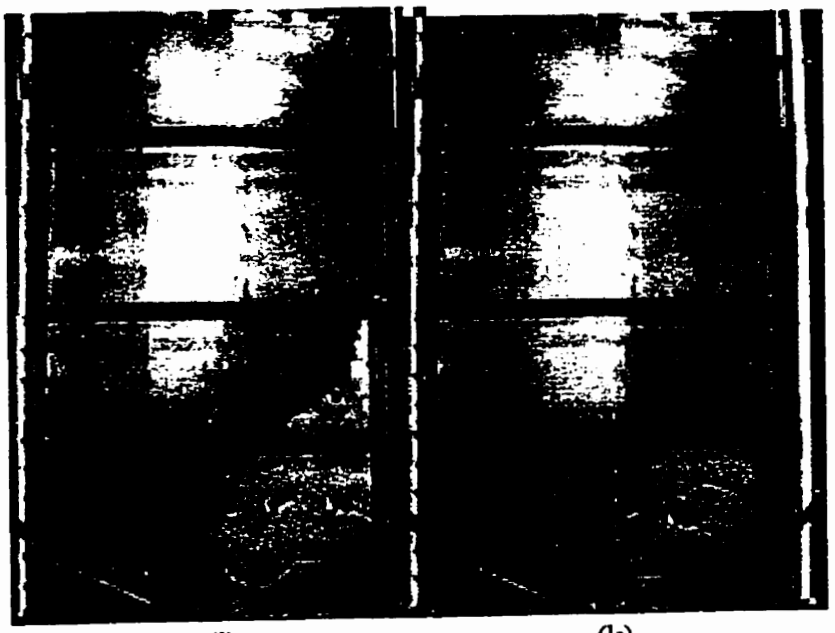

(j) (k)

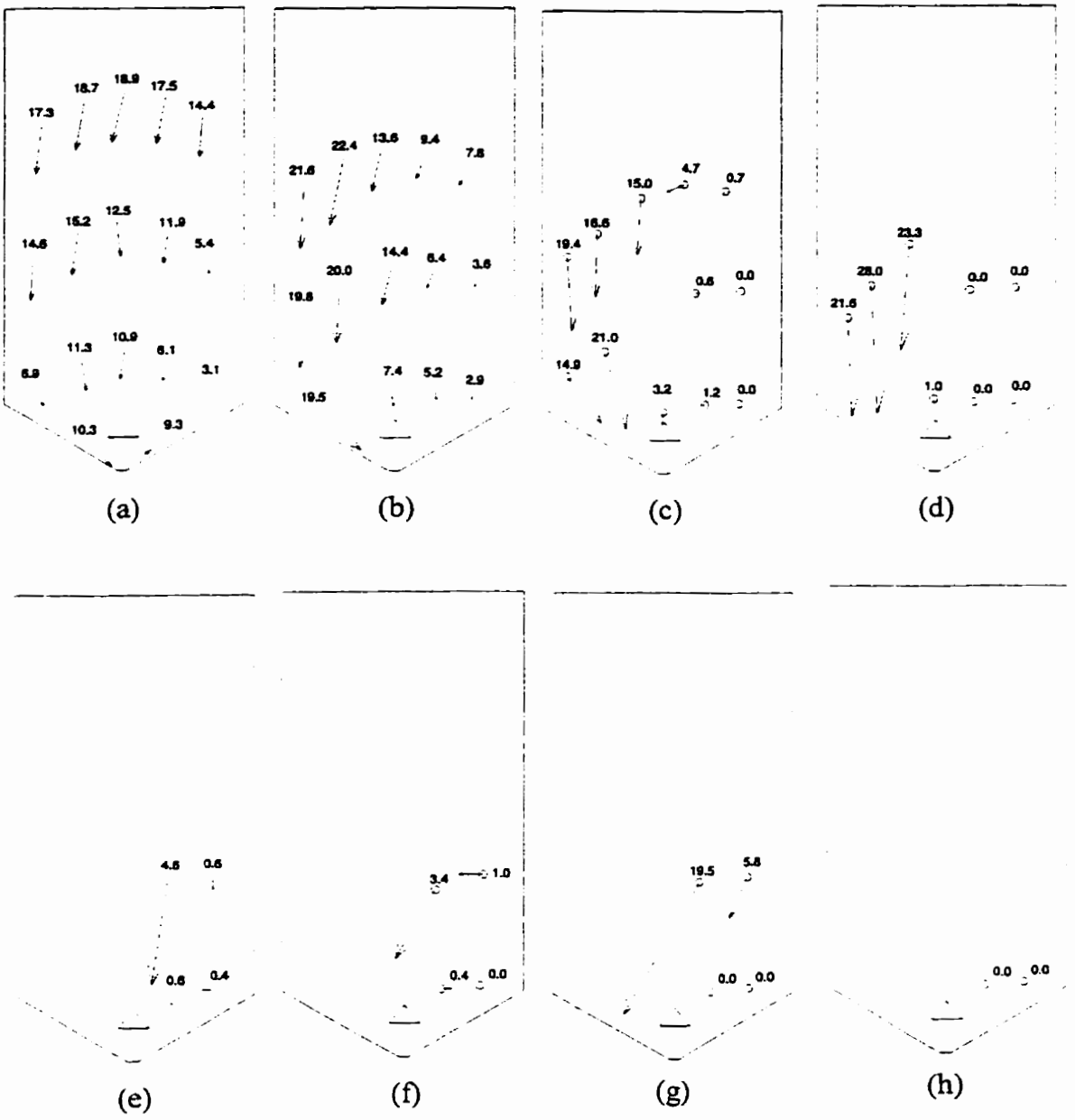

Fig. 5.7 **Typical velocity profiles (in mm/s) in the model bin with a fixed insert, Test F2A. a) 20 s, b) 35 s, c) 50 s, d) 65 s, e) 80 s, f) 95 s, g) 140 s, h) 155 s, i) 170 s, and j) 185 s.**

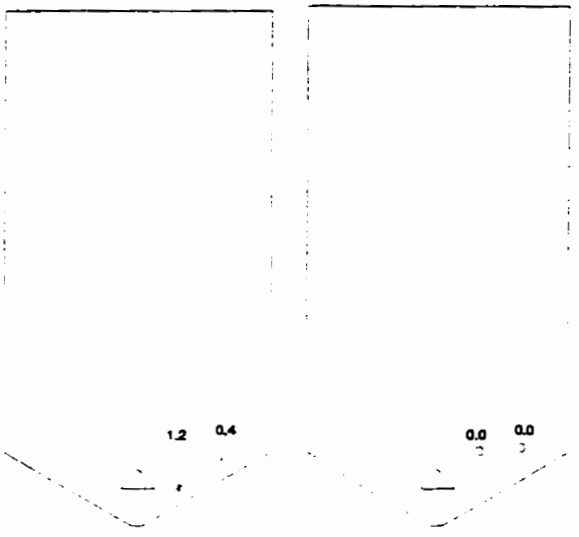

(i) (j)

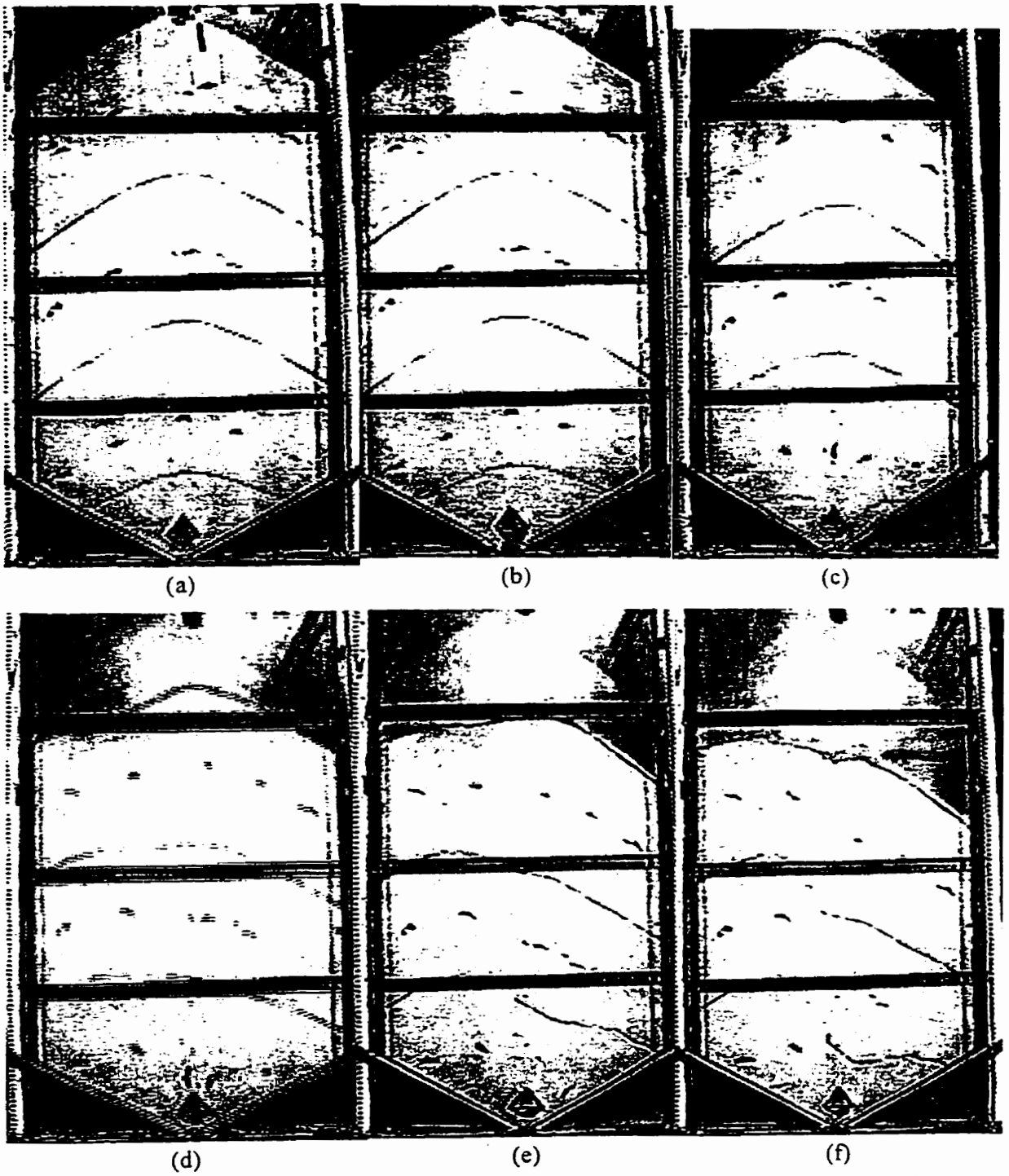

Fig. 5.8 **Typical flow patterns of chop feed in the model bin with a fixed insert, Test F1A. a) 0 s, b) 30 s, c) 45 s, d) 60 s, e) 75 s, f) 90 s, g) 105 s, h) 120 s, i) 135 s, j) 150 s, k) 165 s, l) 180 s, m) 195 s, n) 195 s, o) 210 s, p) 225 s, and q) 238 s.**

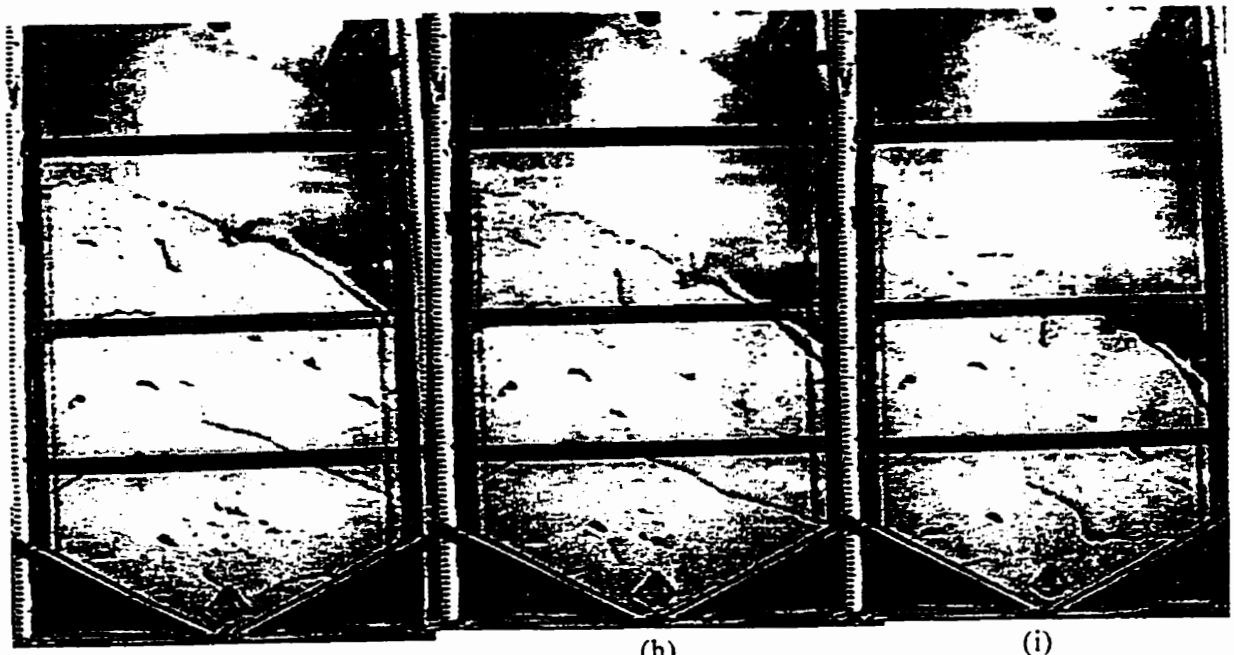

(g) (h) (i)

(j) (k) (l)

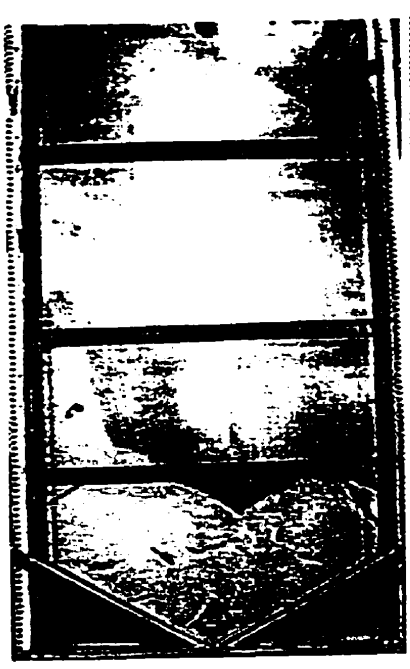

(m)

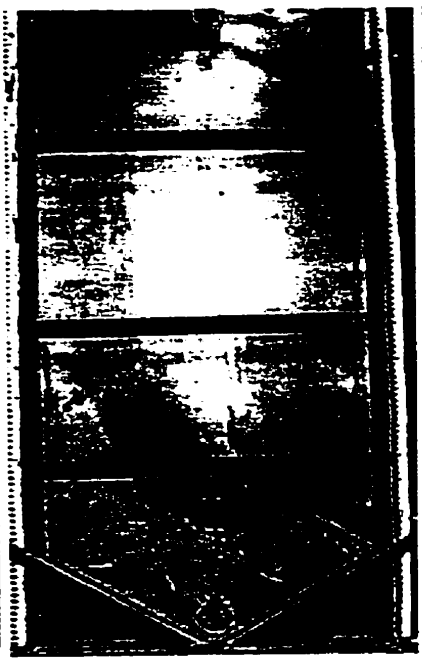

(n)

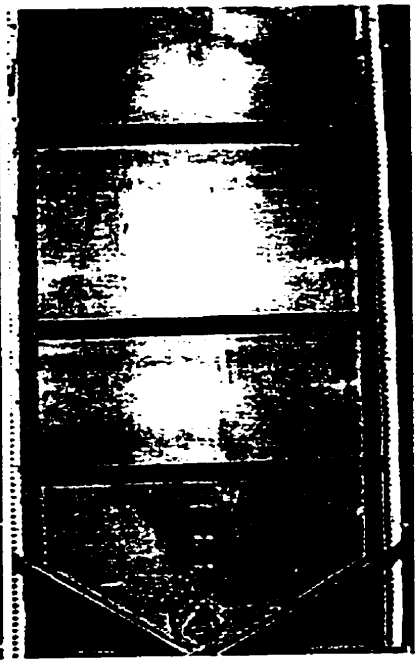

(o)

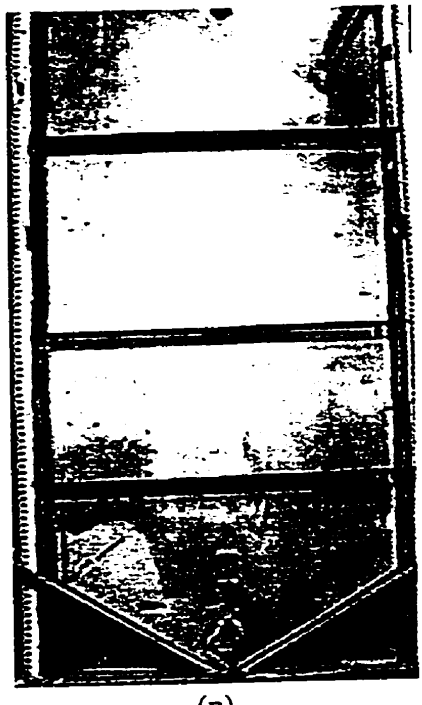

(p)

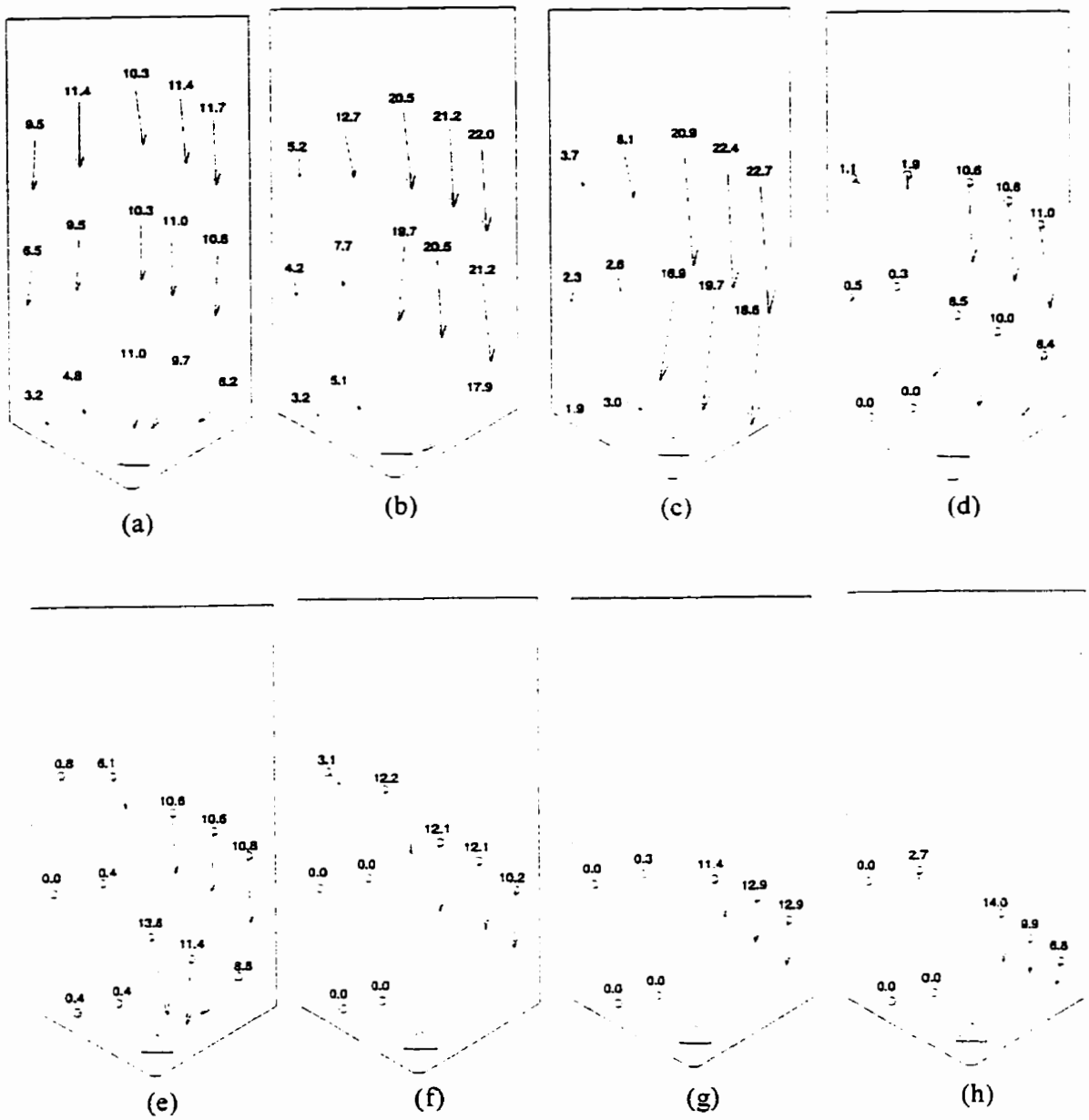

Fig. 5.9 **Typical velocity profiles (in mm/s) in the model bin with a fixed insert, Test F1A. a) 30 s, b) 45 s, c) 60 s, d) 75 s, e) 90 s, f) 105 s, g) 120 s, h) 135 s, i) 150 s, j) 165 s, k) 180 s, l) 195 s, m) 210 s, and n) 225 s.**

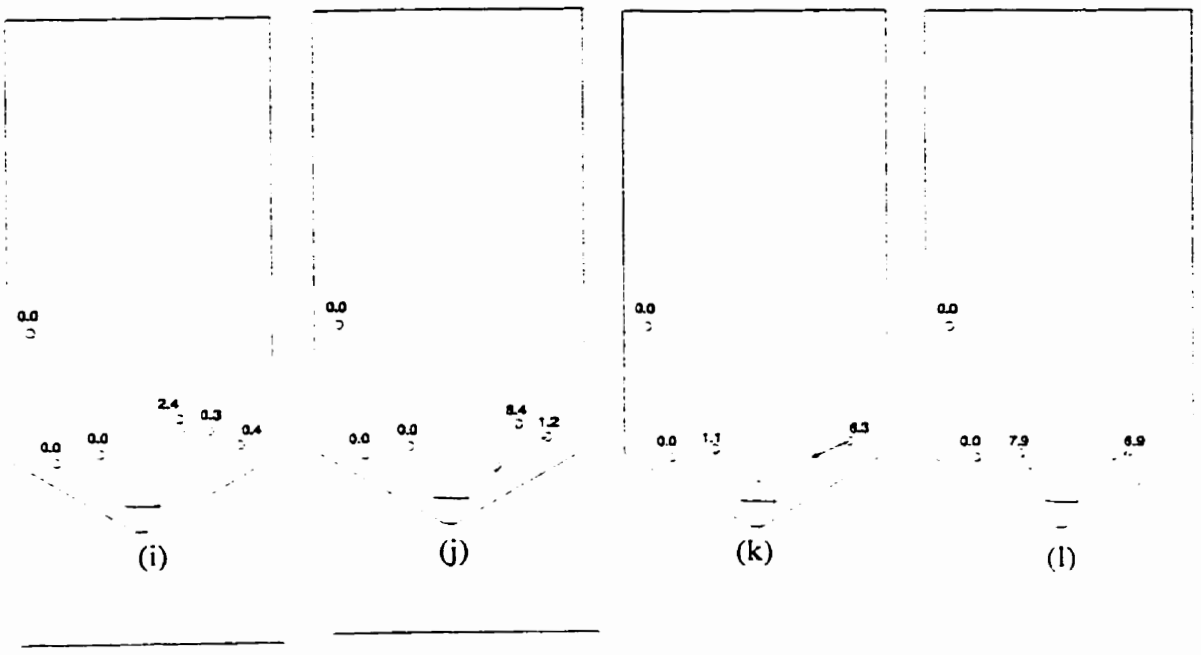
0.0
0.0
0.0
2.4
0.3
0.4
(i)
0.0
0.0
0.0
8.4
1.2
(j)
0.0
0.0
1.1
6.3
(k)
0.0
0.0
7.9
6.9
(l)

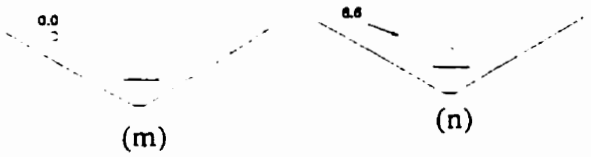
0.0
(m)
6.6
(n)

mm/s were found along the right side wall at 30, 45, and 60 seconds, respectively. The corresponding velocities on the left side were 25.0, 10.7, and 3.7 mm/s. The difference in flow velocity between the left side and the right side increased with time. For example, velocities in columns 2 (left) and 4 (right) at 30 seconds had the same value of 11.4 mm/s (Fig. 5.9a). At 45 seconds the velocity on the right side (V_{14}) became 21.2 mm/s, and velocity on the right side (V_{12}) was 12.7 mm/s, or V_{14} is 1.7 times V_{12}. At 60 seconds V_{14} had a value of 22.4 mm/s and V_{12} 8.1 mm/s, or V_{14} was 2.7 times V_{12}.

The velocity on the left side decreased to zero after 90 s of discharge. In other words, a stagnant zone formed. When a stagnant zone formed, it eventually would collapsed into the flow channel (Figs. 5.9e-g).

For the tests with a fixed insert, two distinct flow channels occurred for all four levels of insert installation. The uniformity of flow was reflected by the difference in velocity between the two channels. This difference varied with the insert location (Fig. 5.10). The difference increased from 3.88 to 7.63 mm/s when the insert was moved from level 1 to level 2, decreased from 7.63 to 3.14 mm/s from level 2 to level 3, and increased again from 3.14 to 4.44 mm/s from level 3 to level 4. The large difference in velocity between the two flow zones caused more collapsing of feed and induced potential flow problems by impacting the feed in the lower portion of the bin. Level 3 produced minimum velocity difference, thus most uniform flow. This result was in agreement with the results of flow rates discussed previously.

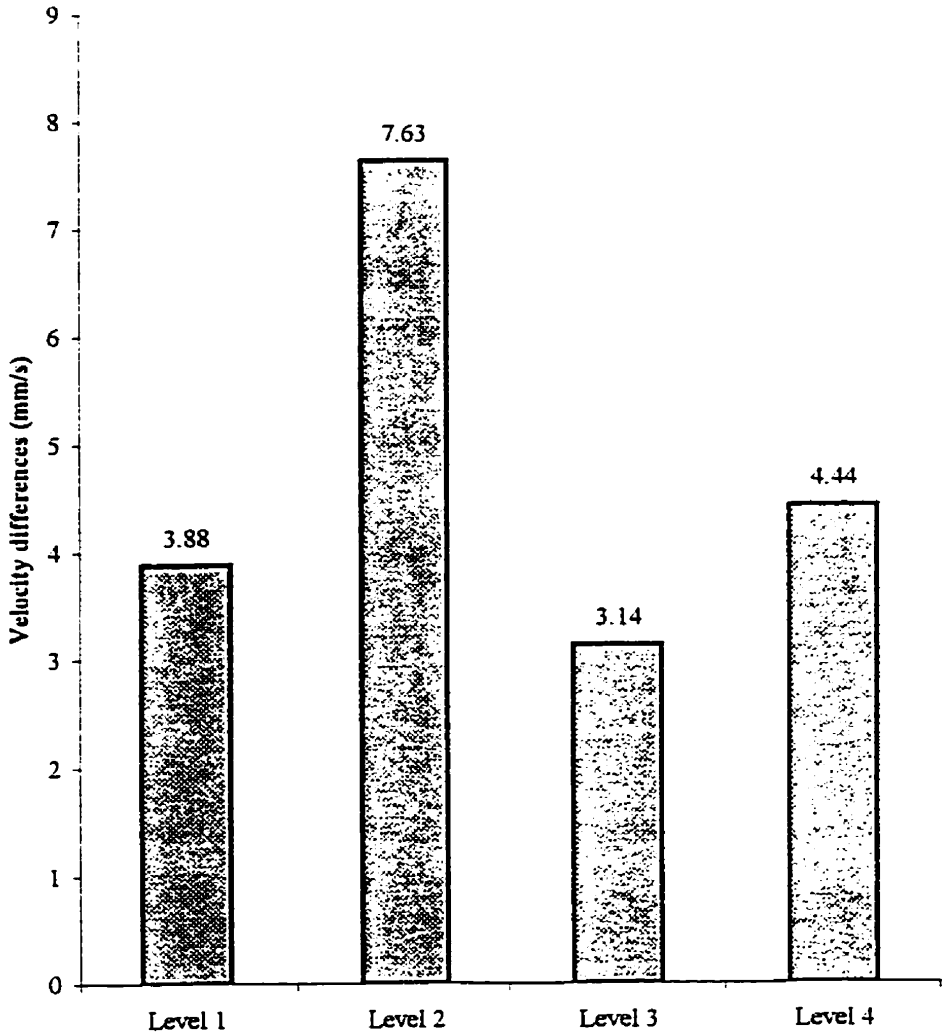

Fig. 5.10 **Velocity differences between two flow channels in the bin for the tests with fixed inserts at four levels.**

5.2.3 Rotating inserts

The test results indicated that when the rotating insert was placed at level 1, the flow could not be enhanced compared to the tests without inserts or the tests with fixed inserts. The reason was the small gaps between the insert and the hopper walls. In this configuration, a gap of 22 mm was formed which was 43% less than the width of the outlet opening of 38 mm.

For the tests with the rotating insert at level 2, mass flow occurred in all of the three tests. No flow stoppage or stagnant zones were observed. In average, the insert rotated ±2° with a standard deviation of 0.5.

Once again, two flow channels were observed (Fig. 5.11a). The velocity in the fast flowing channel (columns 1, 2, and 3) was 19.5mm/s; and 4.9 mm/s in the slow flowing channel (columns 4 and 5). The difference in velocity between the two flowing channels was greater than that in the tests with the fixed inserts.

The uneven flow might be attributed to unbalanced filling of the bin. The inertia of feed leaving the filling auger caused feed to be deposited slightly more on the right side of the bin, even though the spout of the auger was set centrally above the bin. The unbalanced filling caused an 18° clockwise rotation of the insert after the bin was fully filled. Feed was subjected to a greater degree of consolidation on the right side than the left side of the bin. Therefore, feed flowed more easily on the left side than on the right side.

Viewing the recorded video images in slow motion, it was observed that the insert rotated ±2° from the initial position during the first 120 s of discharge. This oscillating motion

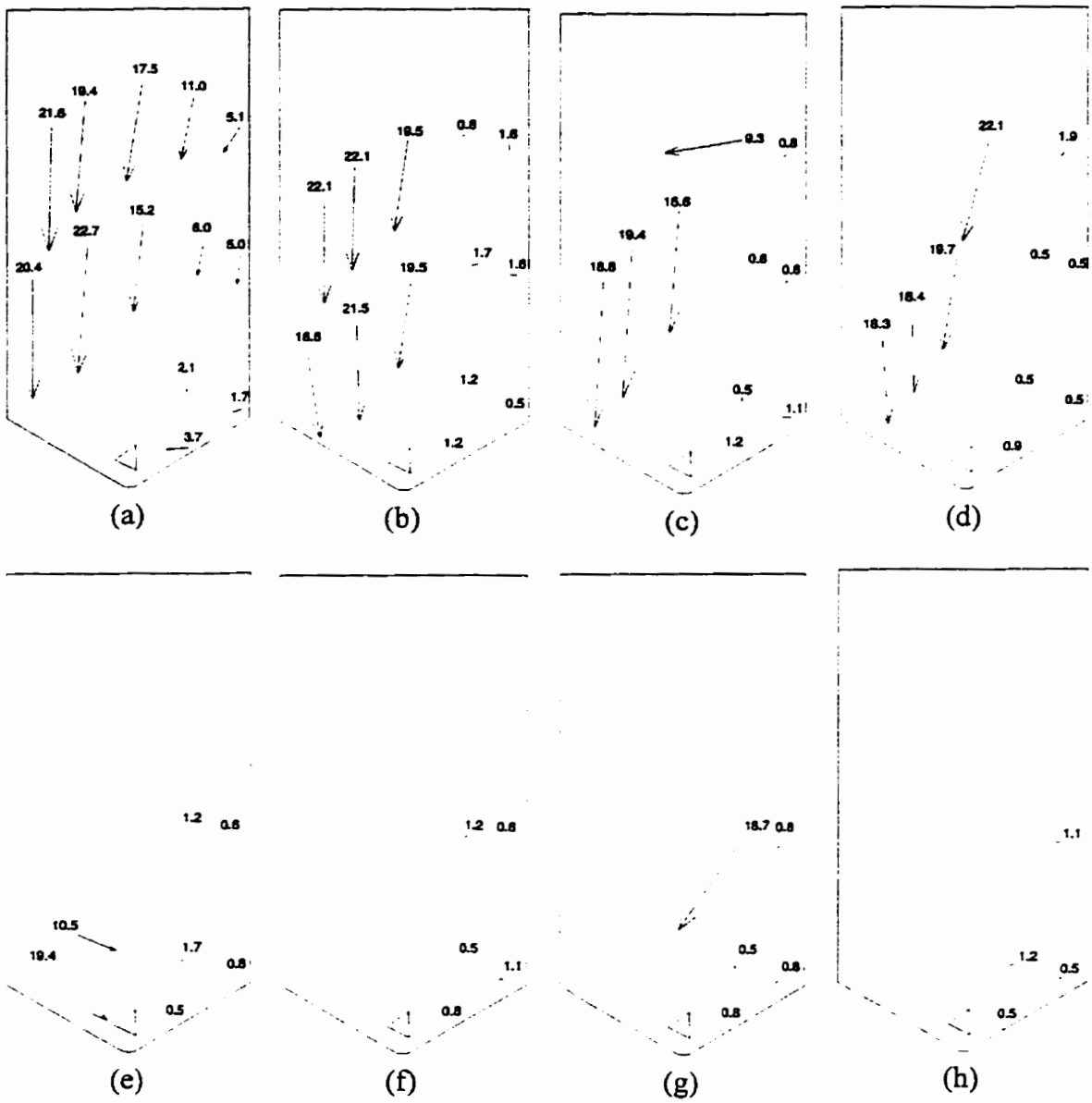

Fig. 5.11 **Typical velocity profiles (in mm/s) in the model bin with a rotating insert, Test R2C. a) 0 s, b) 15 s, c) 30 s, d) 45 s, e) 60 s, f) 75 s, g) 90 s, h) 105 s, and i) 120 s.**

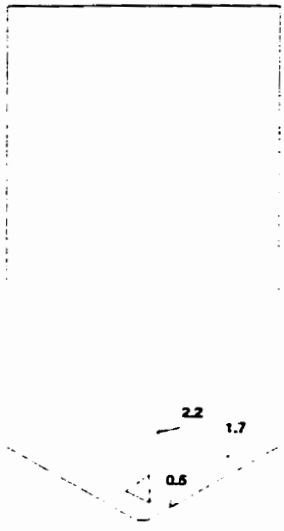

(i)

of the insert helped breaking arching. No noticeable rotation was found after 120 seconds of discharge (Fig. 5.12).

The rotating insert presented a better overall performance in improving the flow than the fixed insert. The most effective location of the rotating insert was 33 % lower than that of the fixed insert.

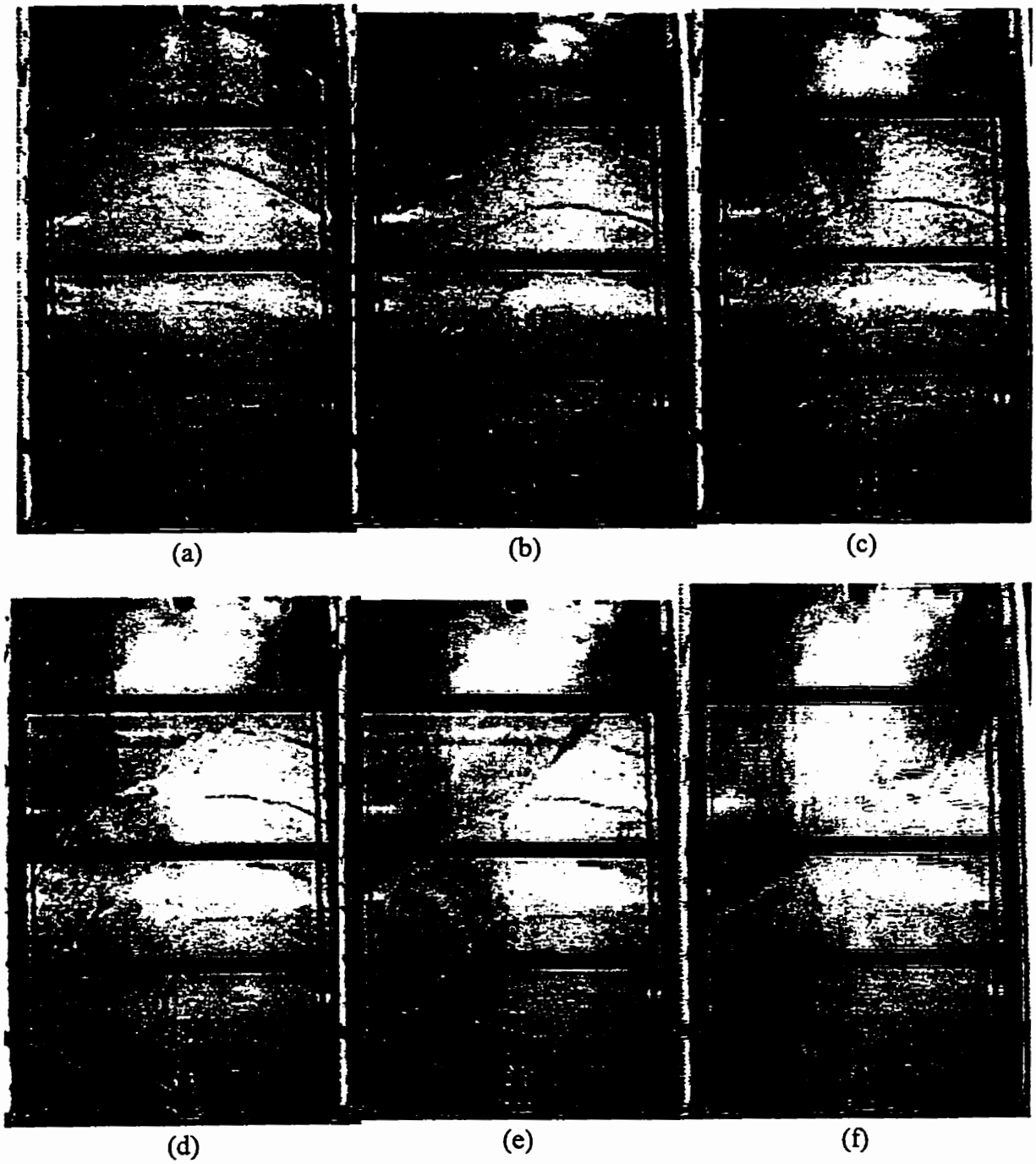

Fig. 5.12 **Typical flow patterns of chop feed in the model bin with a rotating insert, Test R2C. a) 0 s, b) 15 s, c) 30 s, d) 45 s, e) 60 s, f) 75 s, g) 90 s, h) 105 s, i) 120 s, j) 135 s, and k) 150 s.**

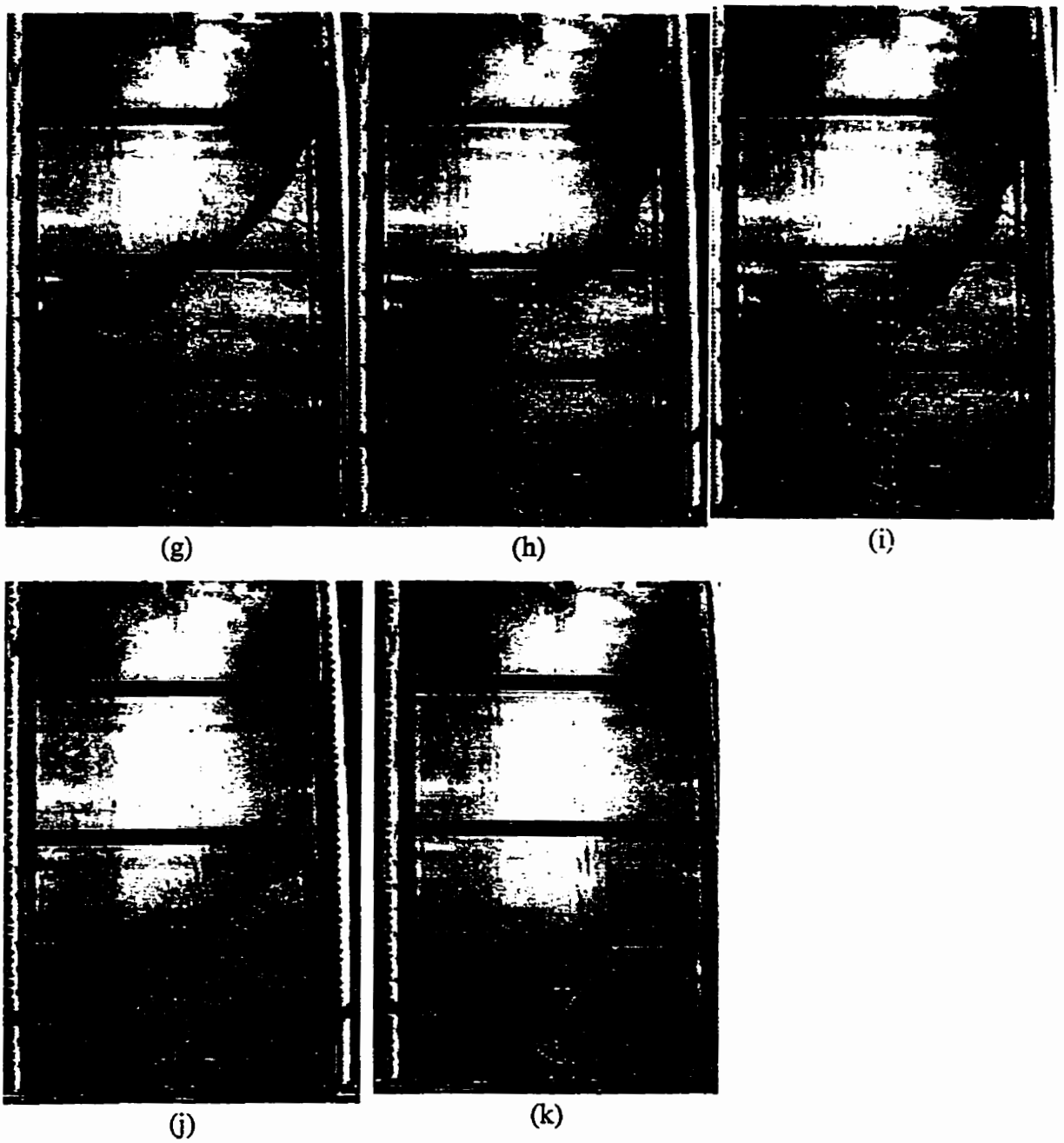

Fig. 5.12 **Typical flow patterns of chop feed in the model bin with a rotating insert, Test R2C. a) 0 s, b) 15 s, c) 30 s, d) 45 s, e) 60 s, f) 75 s, g) 90 s, h) 105 s, i) 120 s, j) 135 s, and k) 150 s.**

6. CONCLUSIONS AND RECOMMENDATIONS

The following conclusions were made based on this study:

1) The introduction of a fixed insert at a height of 216 mm and a rotating insert at a height of 174 mm improved the flow quality of cohesive bulk solids to a point where the bin could be emptied without human intervention. The effectiveness of bin inserts decreased when the insert was mounted too low or too high in the bin.

2) The inserts caused significant changes to flow patterns and velocity profiles. For the tests with a fixed insert, two distinct flow channels occurred for all four levels of insert installation. The large difference in velocity between the two flow zones caused more collapsing of feed and induced potential flow problems by impacting the feed in the lower portion of the bin.

3) The rotating insert was more effective than the fixed insert in improving the flow.

4) The rotating insert oscillated in ±2° during discharge.

Further research was recommended as the following:

1) Full size bin tests should be performed.

2) Other materials should be tested.

3) Tests for different hopper angles, outlet dimensions, insert shapes, and insert sizes should be performed.

7. REFERENCES

ASAE Standards, 35th ed. 1989. EP 433. Loads exerted by free flowing grains on bins. St. Joseph, MI: ASAE.

Bokhoven, W. H. and R. A. Lohnes. 1989. Preconsolidation effects on flow characteristics of soybean meal. Transactions of the ASAE. 32(5): 1779-1783.

Bransby, P. L. and P. M. Blair-Fish.1974. Wall stresses in mass flow bunkers. Chemical Engineering Science. 29: 1061-1074.

Brown, R. L. and J. C. Richards. 1970. Principles of powder mechanics. Pergamon Press Ltd., Headington Hill Hall, Oxford. 10: 95-102.

Brown, R.L. and P.G.W. Hawksley. 1947. The internal flow of granular masses. Fuel 26, 159-73.

Bucklin, R. A., S. A. Thompson, and I. J. Ross. 1991. Flow patterns in model flat bottom grain bins. Transactions of the ASAE. 34(2): 577-585.

Carson, J. W. and J. Marinelli. 1994. To ensure smooth flow. Chemical Engineering. April, 78-90.

Cutress, J. O. 1966. The storage and recovery of particulate solids, London, Institution of Chemical Engineers, 110.

Deutsch, G.P. and L.C. Schmidt. 1969. Pressures on silo walls. Trans. ASME. J. Eng. Ind. (B). 91(1): 450-459.

Endersonby, V.A. 1940. The mechanics of granular-plastic materials, with special reference to bituminous road materials and subsoils. Am. Soc. Test. Mater. 40, 1154-73.

Gaylord, Edwin H. Jr., and Charles N. Gaylord. 1984. Design of steel bins for storage of bulk solids. Prentice-Hall, Inc. Englewood Cliffs, New Jersey.

Giunta, J.S. 1969. Flow patterns of granular materials in flat-bottom bins. Transactions of the ASME, Series B91: 406-413.

Grossman, R. B., H. L. Towne, and T. V. Vogel. 1990. Bulk feed bin challenges. Paper 90-4013. Am. Soc. Agric. Eng., St. Joseph, M. I. 6.

Han, C.; H. Huang, and A. Drescher. 1989. Approximate analysis of unsteady flow of granular materials in bin/hopper structures. Chemical Engineering Science. 44(11), 2545-2552.

Janssen, H. A. 1895. Tests on grain pressure silos, Verein deutscher ingenieure, Zeitschrift 39(8): 1045-1049.

Jenike, A.W. and T. Leser. 1964. A flow no-flow criterion in gravity flow of powders in converging channels. Proceedings of the Fourth Congress on Rheology. Brown University. 125-141.

Jenike, A. W. 1964. Storage and flow of solids, Bull. No. 123, Utah Engineering Experiment Station, University of Utah, Salt Lake City.

Johanson, J. R. 1987. Theory of bulk solids flow-A historical perspective. International Journal of Bulk Solids Storage in Silos. 3(1): 1-15.

Johanson, J. R. and T. A. Royal. 1982. Measuring and use of wear properties for predicting life of bulk materials handling equipment. Bulk solids handling. 2(3):517-523.

Johanson, J. R. 1965. Method of calculating rate of discharge from hoppers and bins, Transaction of the Society of Mining Engineers. 69-80.

Johanson, J. R. 1964. Stress and velocity fields in the gravity flow of bulk solids. ASME, Jnl. Of Appl. Mechanics. 13(3):499-506.

Johanson, J. R. 1966. The use of flow-corrective inserts in bins. Tans. Society of Mining Engineers. 224-230.

Kieper, R. 1992. Interaction between wheat and corrugated steel surfaces. B. Sc. Thesis. The University of Manitoba. Winnipeg. Manitoba.

Kotchanova, I. I. 1971. Experimental and theoretical investigations on the discharge of granular materials from bins. Powder technology. 4:32-37.

Laforge, M. R. and B. K. Boruff. 1964. Profiling flow of particles through hopper openings. Industrial and Engineering Chemistry. 56(2): 42-46.

McCabe, R. P. 1974. Flow patterns in granular material in circular silos, Geotechnique, 24(1):45-46.

McLean, A.G., P.C. Arnord and B. Bravin. 1985. Eccentric discharge silo wall loads. Proceedings of International Reliable Flow of Particulate Solids Symposium, European Federation of Chemical Engineering, Bergen.

Mohsenin, N.N. 1986. Physical properties of plant and animal materials. 2nd edition, Gordon and Breach Science Publishers, New York, NY.

Moriyama, R.1983. The effect of filling method on the flow pattern in a bin. In proceedings Second International Conference On Design of Silos For Strength And Flow. 1:317-331.

O'Callaghan, J. R. 1960. Internal flow in moving beds of granular material. Journal of Agricultural Engineering Research. 5:200-217.

Ooms, M. and A. W. Roberts. 1985. Significant influence of wall friction in the gravity flow silos. Bulk Solids Handling. 5(6):1271-1277.

Pokrant, D. G. 1983. A test facility for grain pressure studies. Unpublished B. Sc. Thesis. University of Manitoba, Winnipeg, Manitoba.

Pieper, K. 1969. Investigation of silo loads in measuring models. Trans. ASME. J. Eng. Ind. (B). 91(1): 365-372.

Reisner, W. and M. V. Eisenhart Rothe. 1971.Bin and bunkers for handling bulk materials: Practical design and techniques. Trans. Tech Publication. Cleveland, Ohio. 1(1): 68-96.

Reynolds, O. 1885. On the dilatancy of media composed of rigid particles in contact: With experimental illustrations, phil. Mag. 5(20): 469-481.

Richards, P.G. 1977. Bunker design - part 1: Bunker outlet design and initial measurements of wall pressures. Trans. ASME. J. Eng. Ind. (B). 99: 809-813.

Roberts A. W., M. Ooms, and S. J. Wiche.1990. Concepts of boundary friction, Adhesion and wear in bulk solids handling operations. Bulk solids handling. 10(2):189-198.

Roberts, A. W.1988. Friction, adhesion and wear in bulk materials handling. In proceedings Antiwear 88, the Royal society, London. Inst. Of metals, I. Mech. E.

Roberts A. W. 1991. Bulk solids handling recent developments and future directions. Bulk solids handling. 11(1):17-35.

Safarian, Sargis S. and Ernest C. Harris. 1985. Design and construction of silos and bunkers. Van Nostrand Reinhold Company Inc. New York, New York.

Schmidt, L.C. and Y.H. Wu. 1989. Prediction of dynamic wall pressures on silos. Bulk Solids Handling. 9(3): 333-338.

Schwab, C.V., I.J. Ross, G.M. White and D.G. Colliver. 1989. Investigation of the grain pressure phenomenon in a full-scale bin, part I: Grain loads and flow characteristics. ASAE Paper No. 89-4007. St. Joseph, MI: ASAE.

Schweds, Jörg. 1983. Evaluation of bulk solids technology since 1974. Bulk solids handling. 3(1):1-3.

Shamlou, P. A. 1988. Handling of Bulk solids: Theory and practice. Anchor Brendon Ltd. Tiptree, Essex, England.

Shan, Yuqin. 1996. Structural loads in a model grain bin during drying of stored grain with near-ambient air. M. Sc. Thesis. The University of Manitoba, Winnipeg, MB. 21-22.

Stewart, Bill R. 1968. Effect of moisture content and specific weight on internal friction properties of sorghum grain. Transactions of the ASAE 11(1): 260-262.

Thompson, S.A. and T.G. Prather. 1984. Dynamic wall loads in a corrugated walled model grain bin. Transactions of the ASAE. 27(3): 875-878.

Thompson, S.A., I.J. Ross, J.N. Walker and L.G. Wells. 1982. Vertical wall loads in a model grain bins. Trans. ASAE. 25(5): 1344-1348.

Thompson, S.A., J.L. Usry and J.A. Legg. 1985. Wall loads as a function of discharge rate in a corrugated model grain bin. Paper presented at the 1985 ASAE Summer Meeting. East Lansing, Michigan. June. Paper No. 85-4003.

Tüzün,U. and R.M.Nedderman .1983. Gravity flow of granular materials around obstacles. Bulk solids handling. V3 no. 3, pp.

Walker, D.M. 1966. An approximate theory for pressures and arching in hoppers. Chem. Eng. Sci. 21:975-997.

Xu. S., Q. Zhang and M. G. Britton. 1993. An endochronic finite element model for predicting loads in grain storage structures. Transactions of the ASAE. 36(4): 1190-1199.

Zenz, F.A. and D.F. Othmer. 1960. Fluidization and fluid particle systems. New York, Reinhold Pub. Corp.

Zhang, Q., V.M. Puri and H.B. Manbeck. 1991. An empirical model for friction force versus relative displacement between maize, rice and soybeans on galvanized steel. Journal of Agricultural Engineering Research. 49:59-71.

APPENDIX A. CALIBRATION RESULTS FOR LOAD TRANSDUCERS

Table A.1 Calibration results for load transducers[1]

Transducer No. (For model bin)	Coefficient με/Kg	R^2
1	2.573	0.9999
2	2.5797	0.99994
3	2.5619	0.99993

[1]All measurements had four repetitions

Calibration equation: S=Coefficient*L

Where: S= Microstrain (με), L=applied weight (kg).

Table A.2 Calibration results for the load cell[1]

Load cell (For shear apparatus)	Coefficient N/mV	R^2
1	130.7025	0.99999

[1]All measurements had three repetitions

Calibration equation: S=Coefficient*mV

Where: S= shear force (N), mV=voltage (mV).

APPENDIX B. CALIBRATION RESULTS FOR THE LINEAR VARIABLE DIFFERENTIAL TRANSDUCER (LVDT)

Table B.1 Calibration results for the Linear Variable Differential Transducer (LVDT)[1]

LVDT No.	Coefficient mm/mv	R^2
1	2.9029	0.99998

[1]All measurements had three repetitions

Calibration equation: D=Coefficient*V

Where: D= deflection of the LVDT (mm), V=voltage (mV).

APPENDIX C. DIGITIZED IMAGES OF FLOW PATTERNS

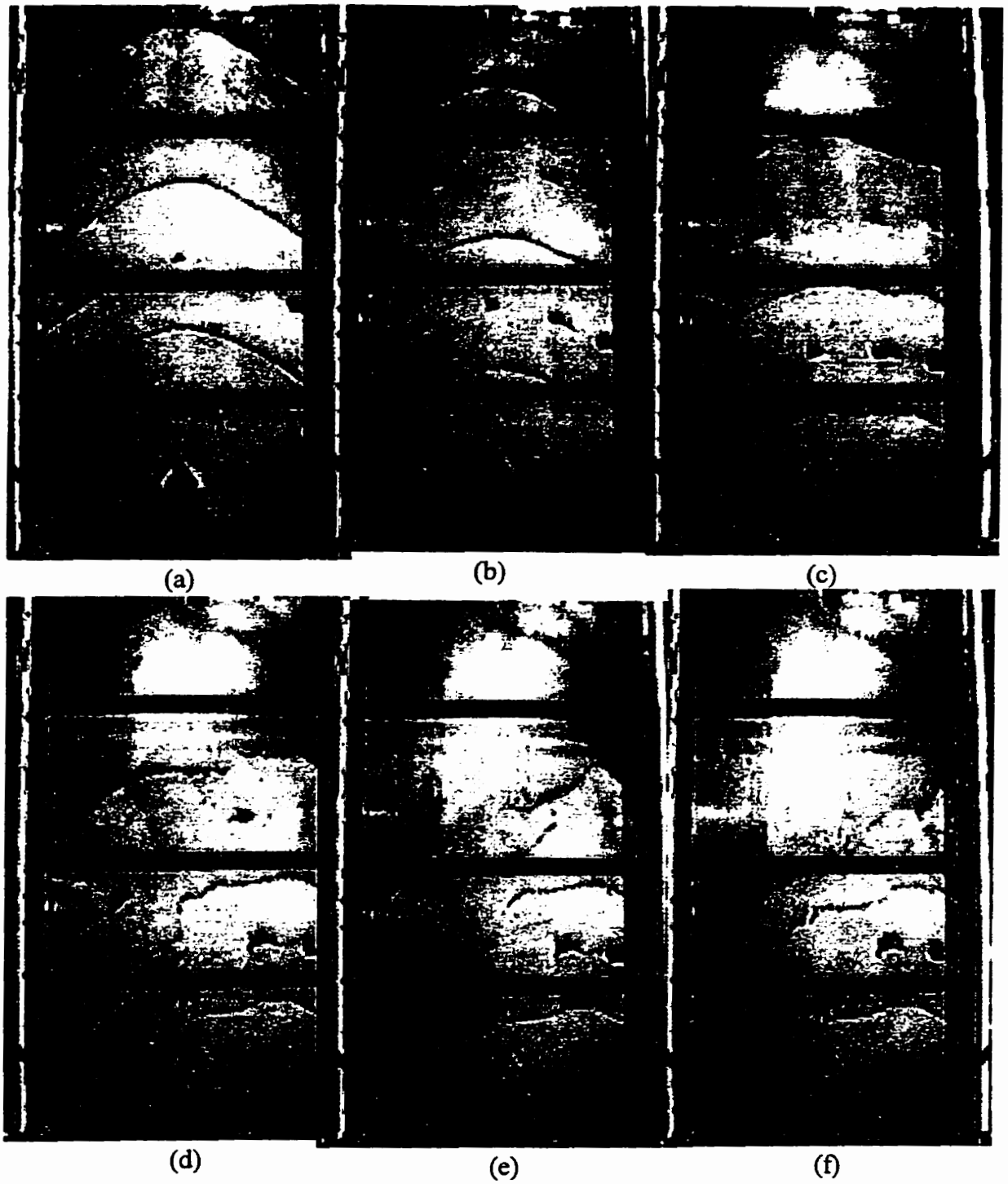

Fig. C.1 **Typical flow patterns of chop feed in the model bin with a fixed insert, Test F3C. a) 0 s, b) 15 s, c) 30 s, d) 45 s, e) 60 s, f) 75 s, g) 90 s, h) 105 s, i) 120 s, and j) 135 s.**

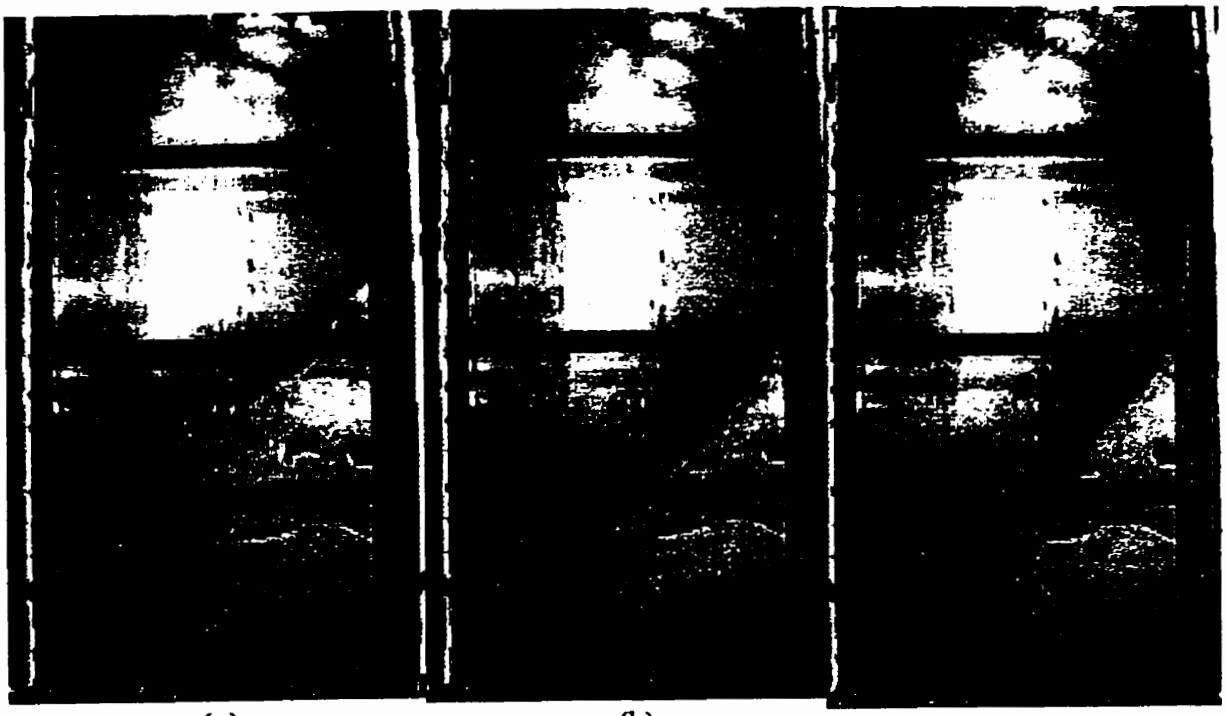

(g) (h) (i)

(j)

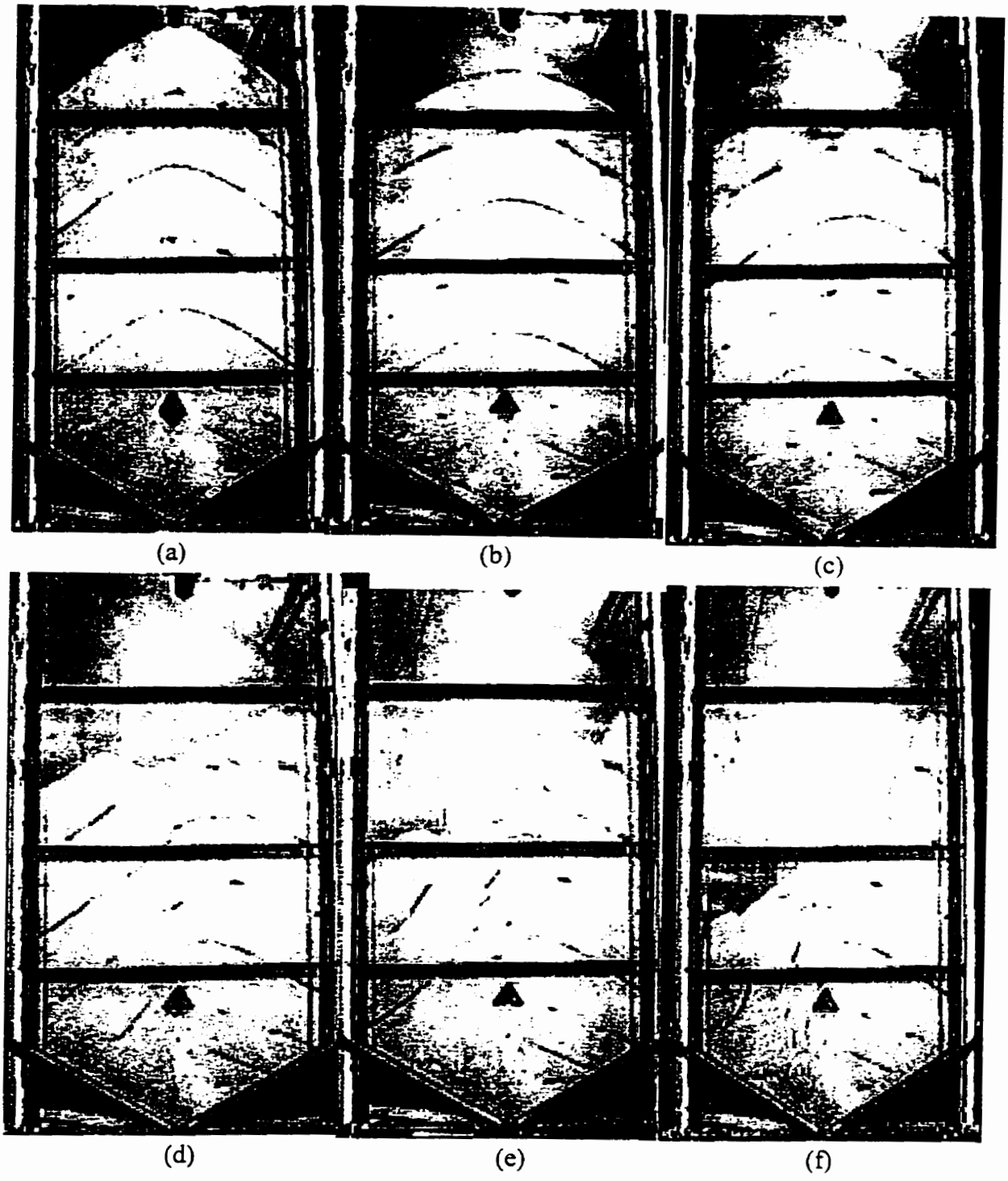

Fig. C.2 **Typical flow patterns of chop feed in the model bin with a fixed insert, Test F4C. a) 0 s, b) 15 s, c) 30 s, d) 45 s, e) 60 s, f) 75 s, g) 90 s, h) 105 s, i) 120 s, j) 135 s, k) 150 s, and l) 165 s.**

(g) (h) (i)

(j) (k) (l)

(a) (b) (c)

(d) (e) (f)

Fig. C.3 Typical flow patterns of chop feed in the model bin with a rotating insert, Test R1A. a) 0 s, b) 45 s, c) 55 s, d) 67 s, e) 68 s, f) 105 s, g) 107 s, h) 215 s, i) 223 s, j) 318 s, k) 325 s, l) 402 s, m) 412 s, n) 423 s, o) 457 s, p) 472 s, q) 580 s, r) 629 s, s) 714 s, t) 720 s, u) 814 s, v) 918 s, and w) 918 s.

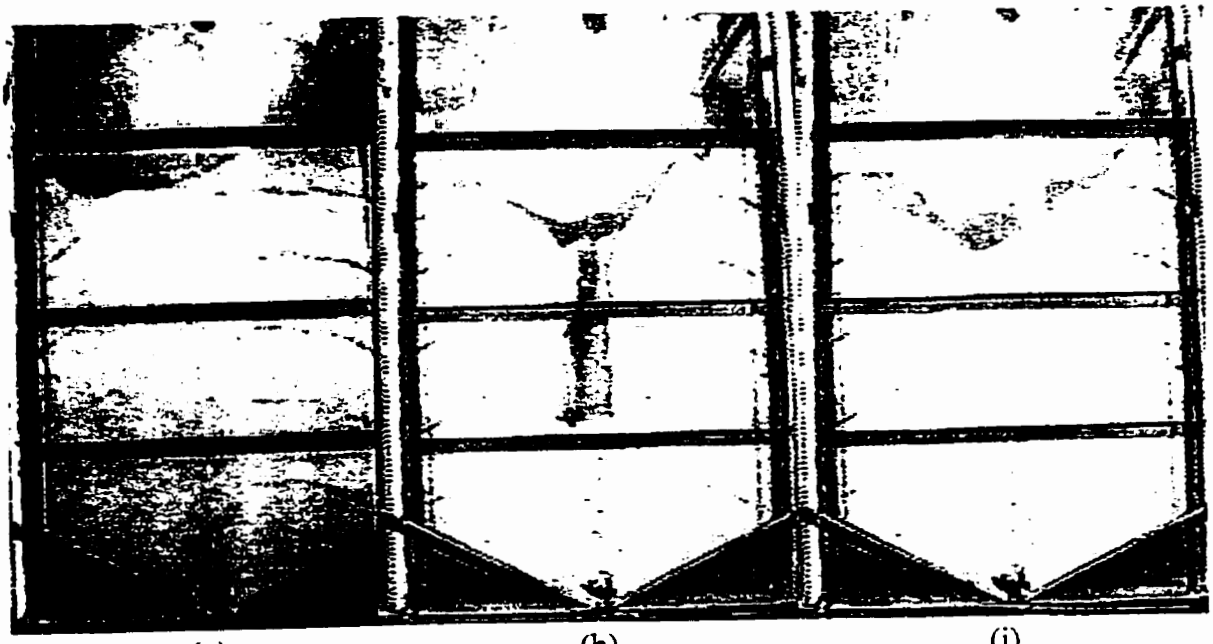

(g) (h) (i)

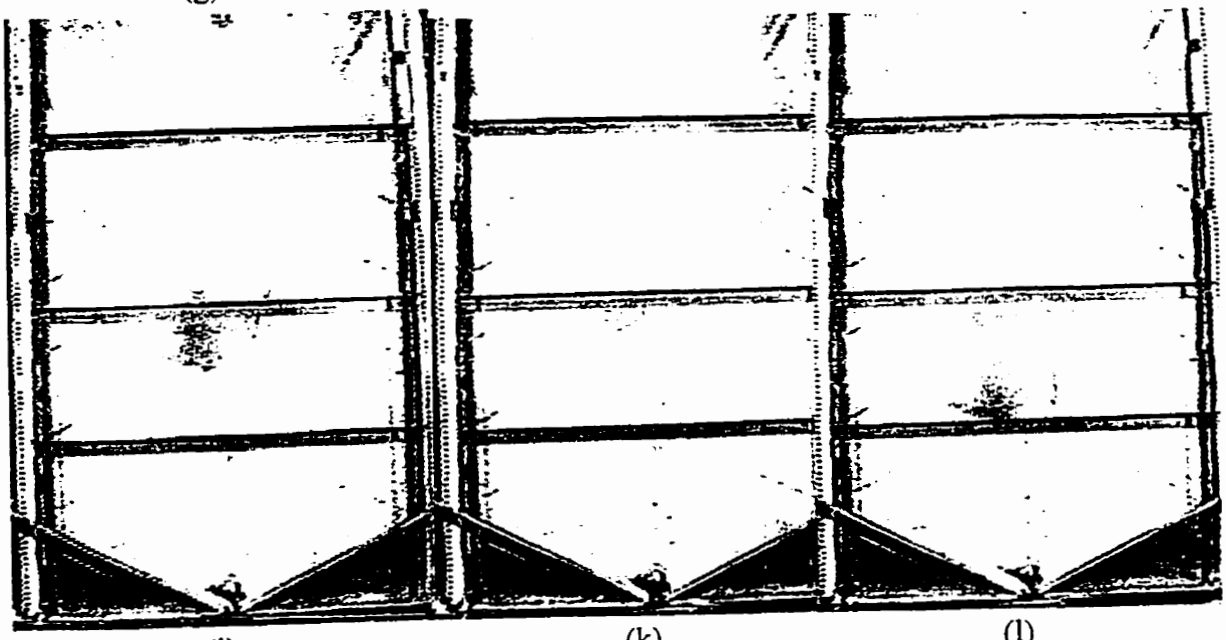

(j) (k) (l)

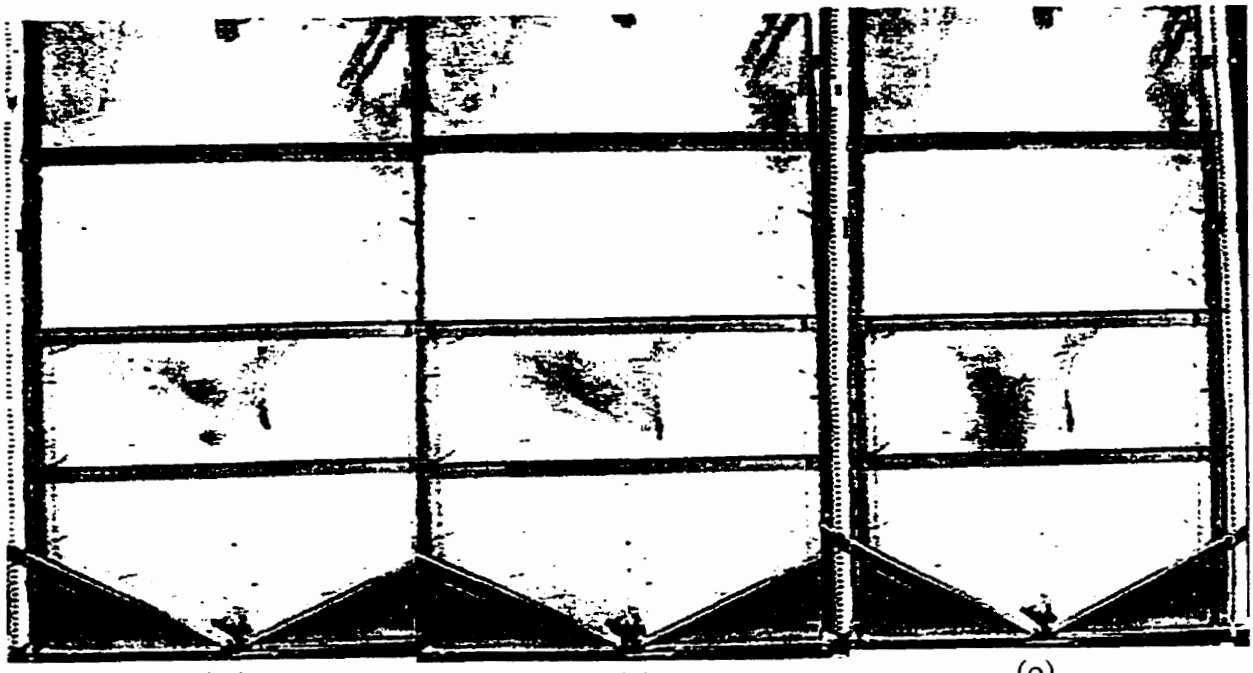

(m) (n) (o)

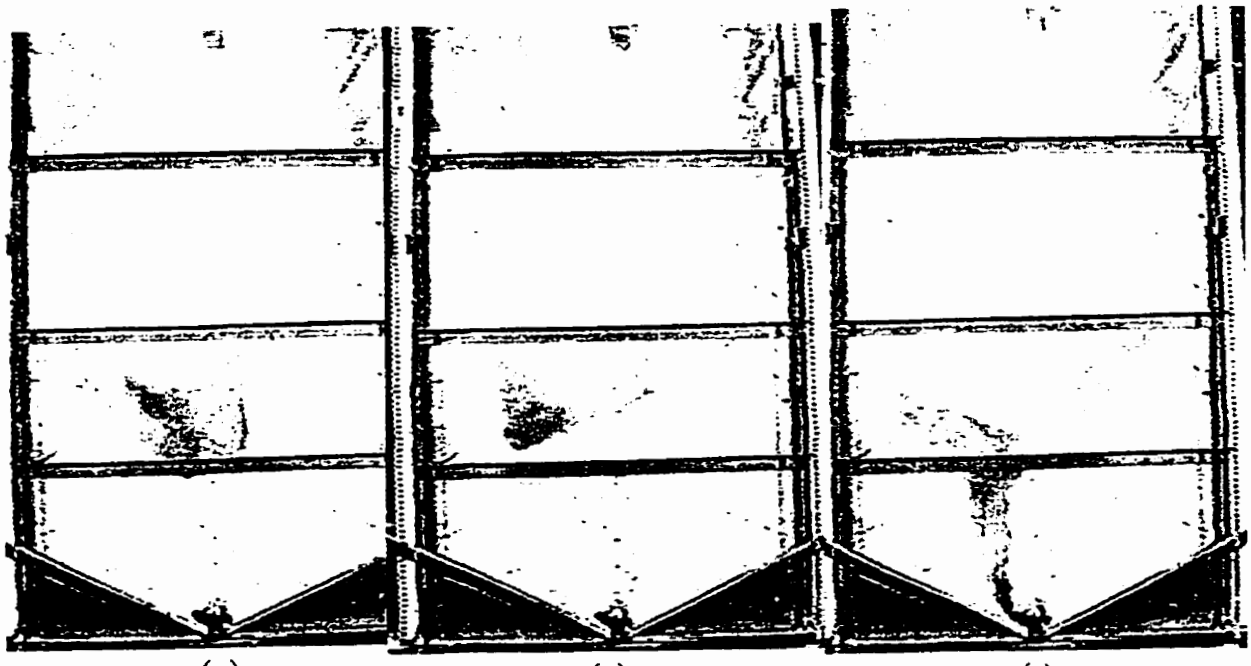

(p) (q) (r)

(s) (t) (u)

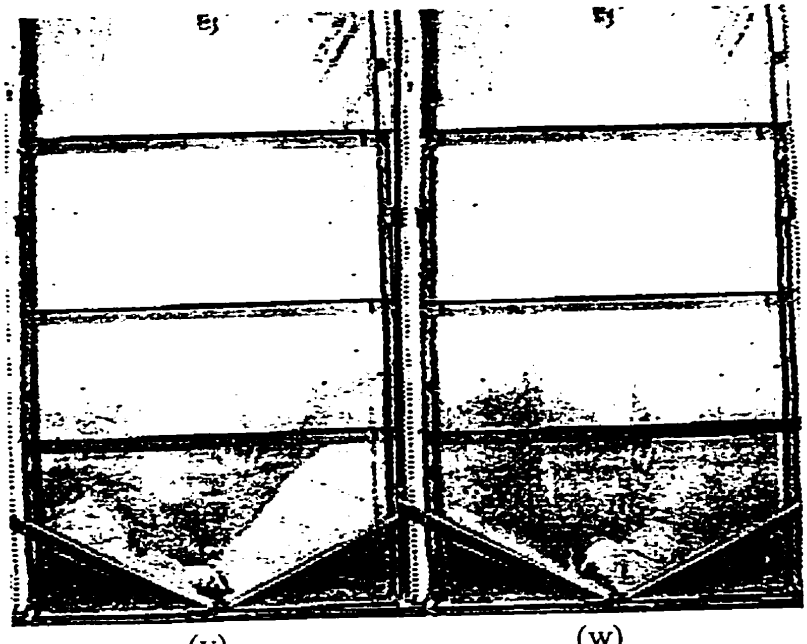

(v) (w)

APPENDIX D. VELOCITY PROFILES

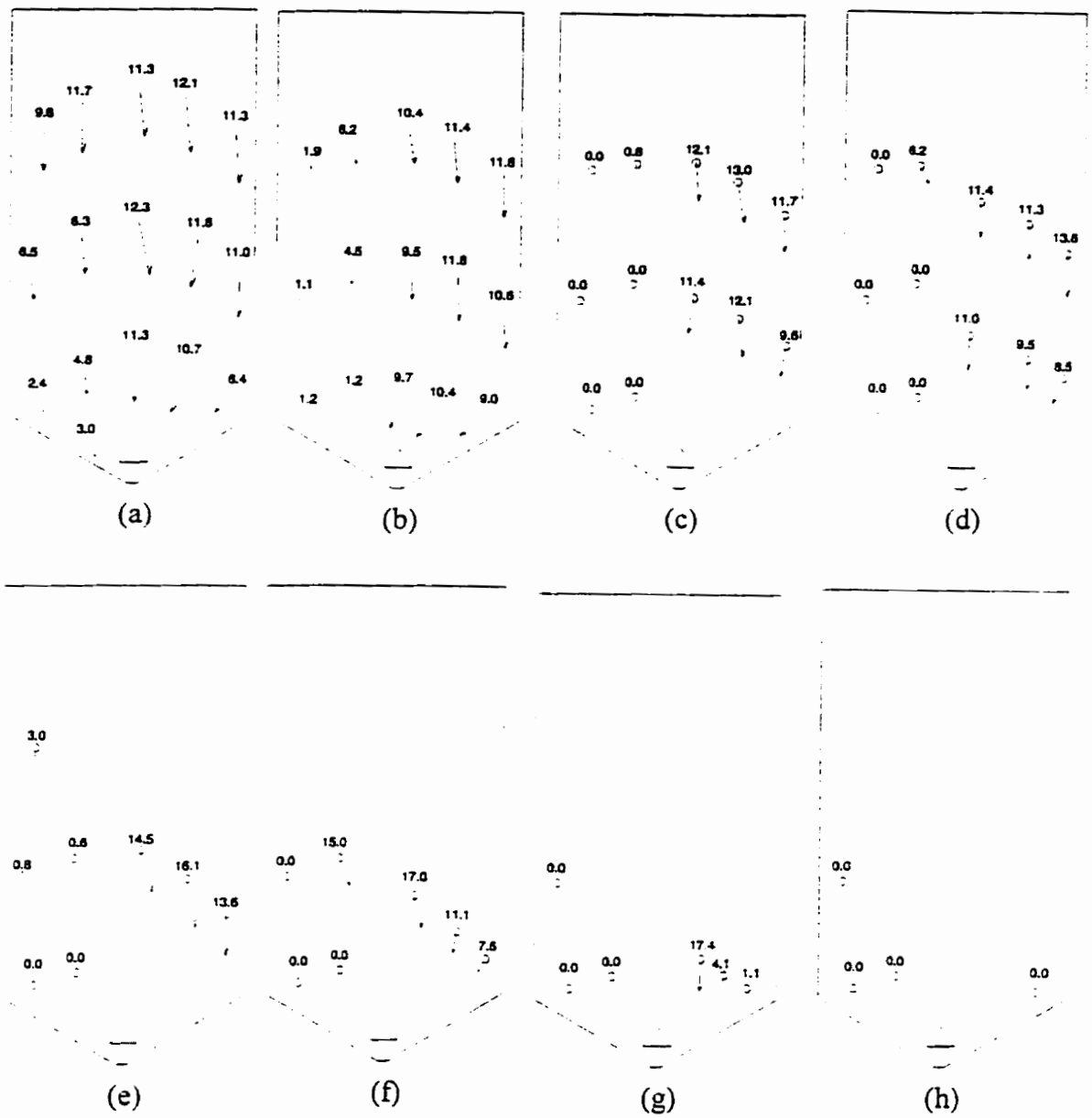

Fig. D.1 **Typical velocity profiles (in mm/s) in the model bin with a fixed insert, Test F1B. a) 25 s, b) 40 s, c) 55 s, d) 70 s, e) 100 s, f) 115 s, g) 130 s, h) 145 s, i) 160 s, j) 175 s, k) 190 s, and l) 205 s.**

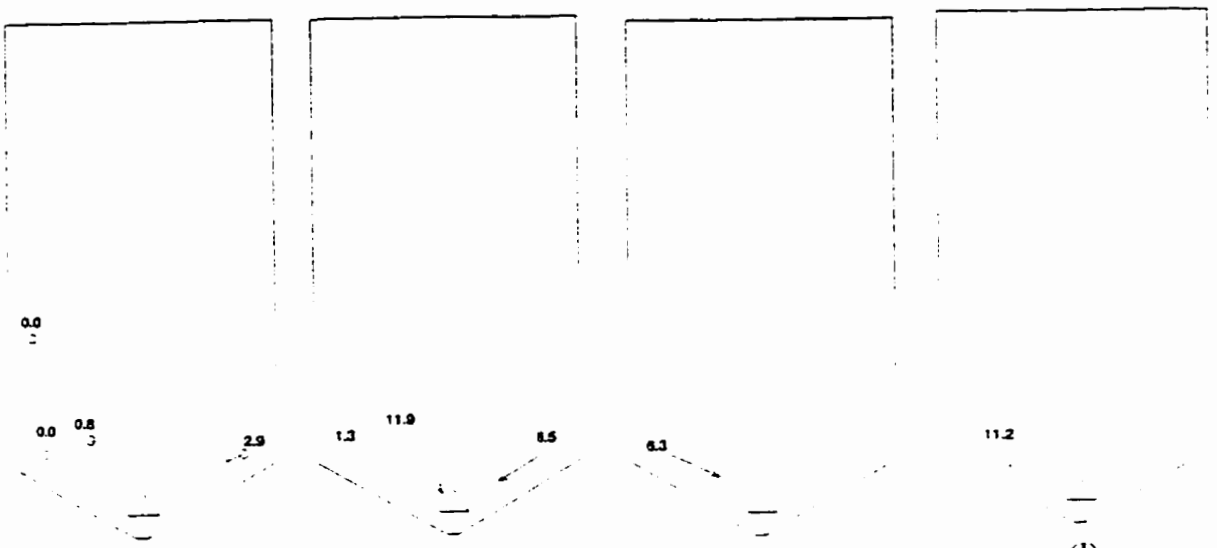

(i) (j) (k) (l)

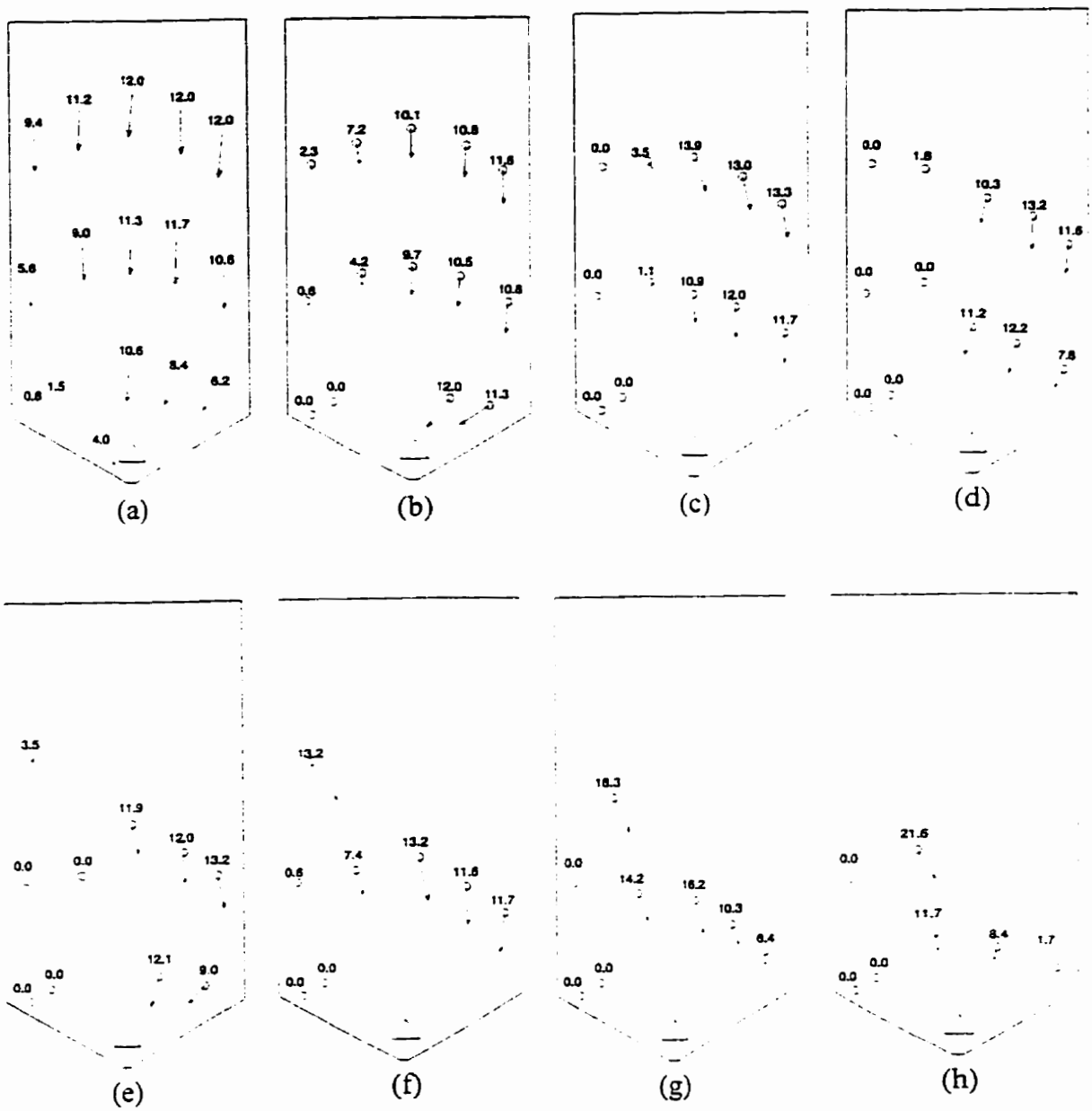

Fig. D.2 **Typical velocity profiles (in mm/s) in the model bin with a fixed insert, Test F1C. a) 10 s, b) 25 s, c) 40 s, d) 55 s, e) 70 s, f) 85 s, g) 100 s, h) 115 s, i) 130 s, j) 145 s, k) 160 s, and l) 175 s.**

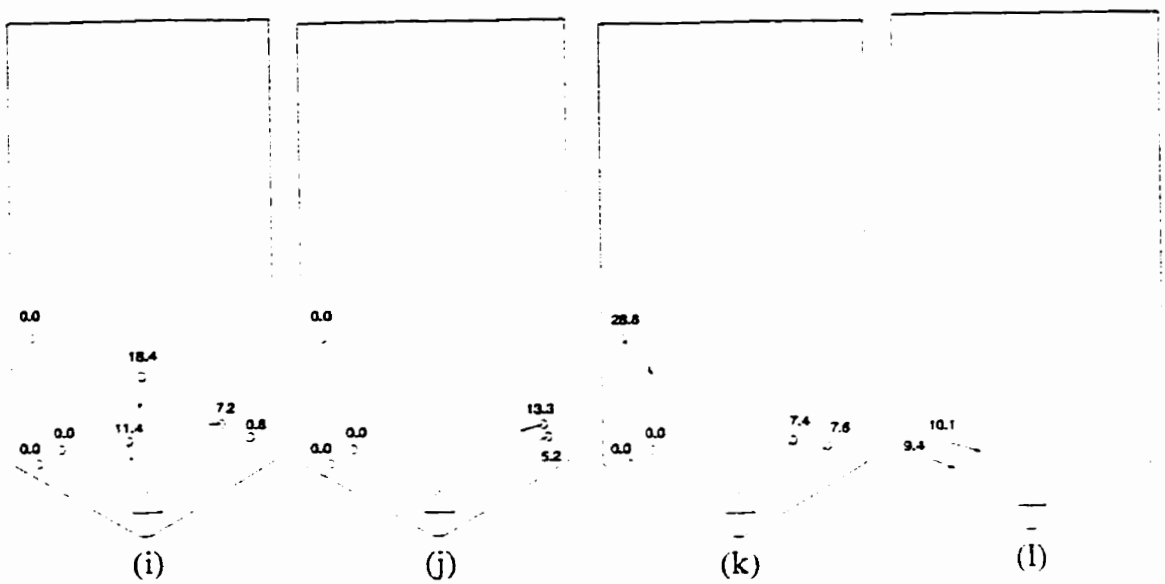

(i) (j) (k) (l)

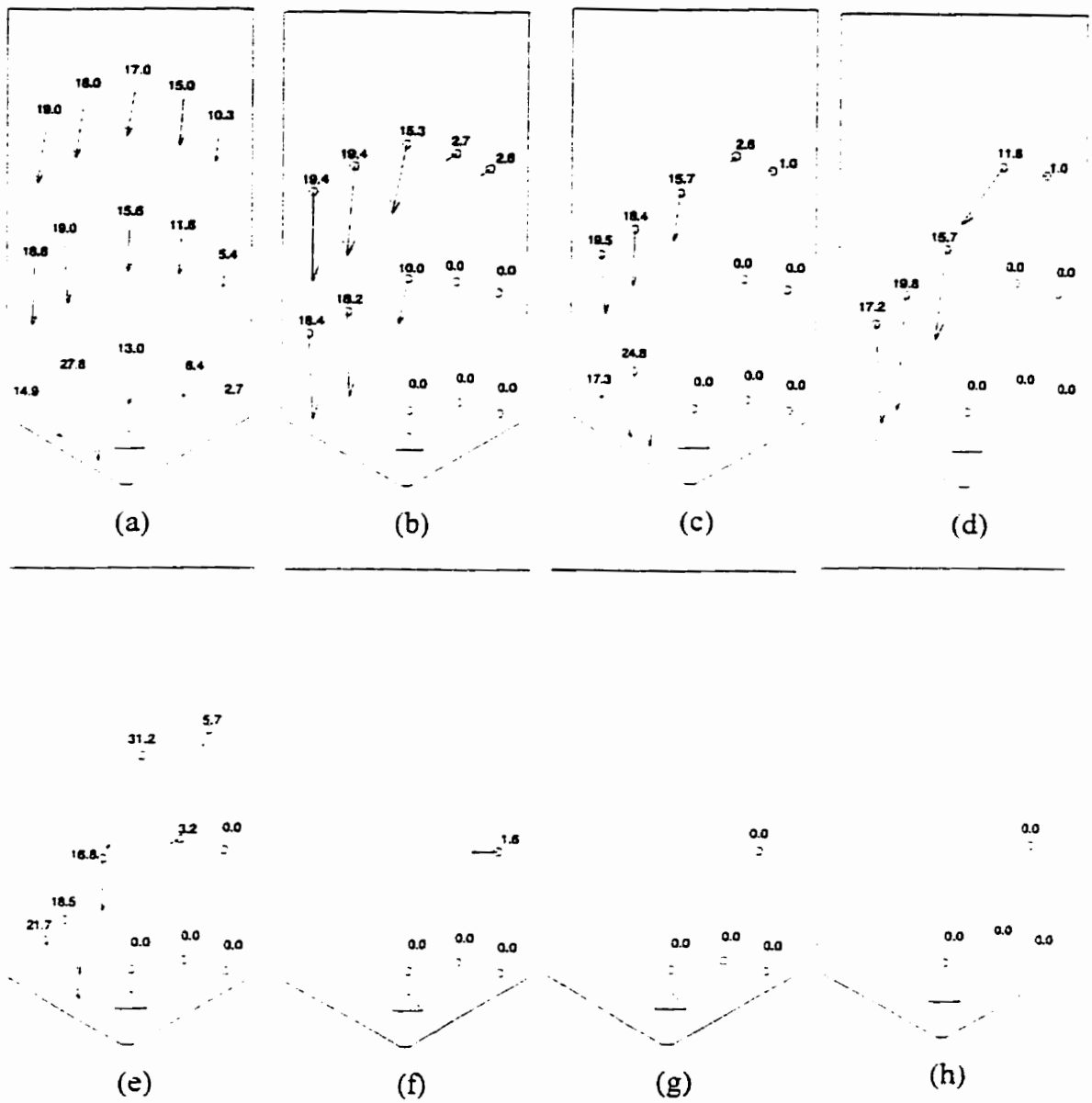

Fig. D.3 **Typical velocity profiles (in mm/s) in the model bin with a fixed insert, Test F2B. a) 0 s, b) 15 s, c) 30 s, d) 45 s, e) 60 s, f) 75 s, g) 90 s, h) 105 s, i) 120 s, j) 135 s, and k) 150 s.**

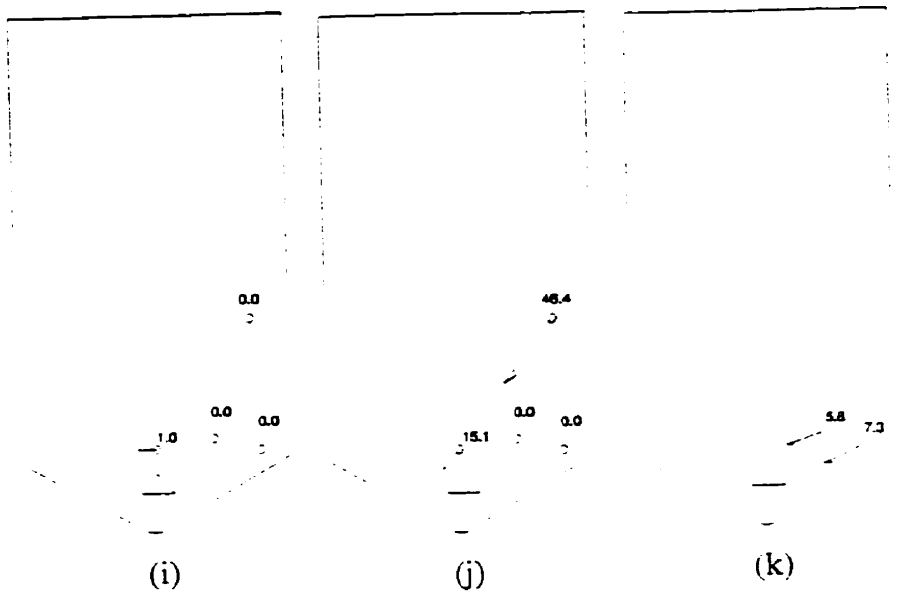

(i) (j) (k)

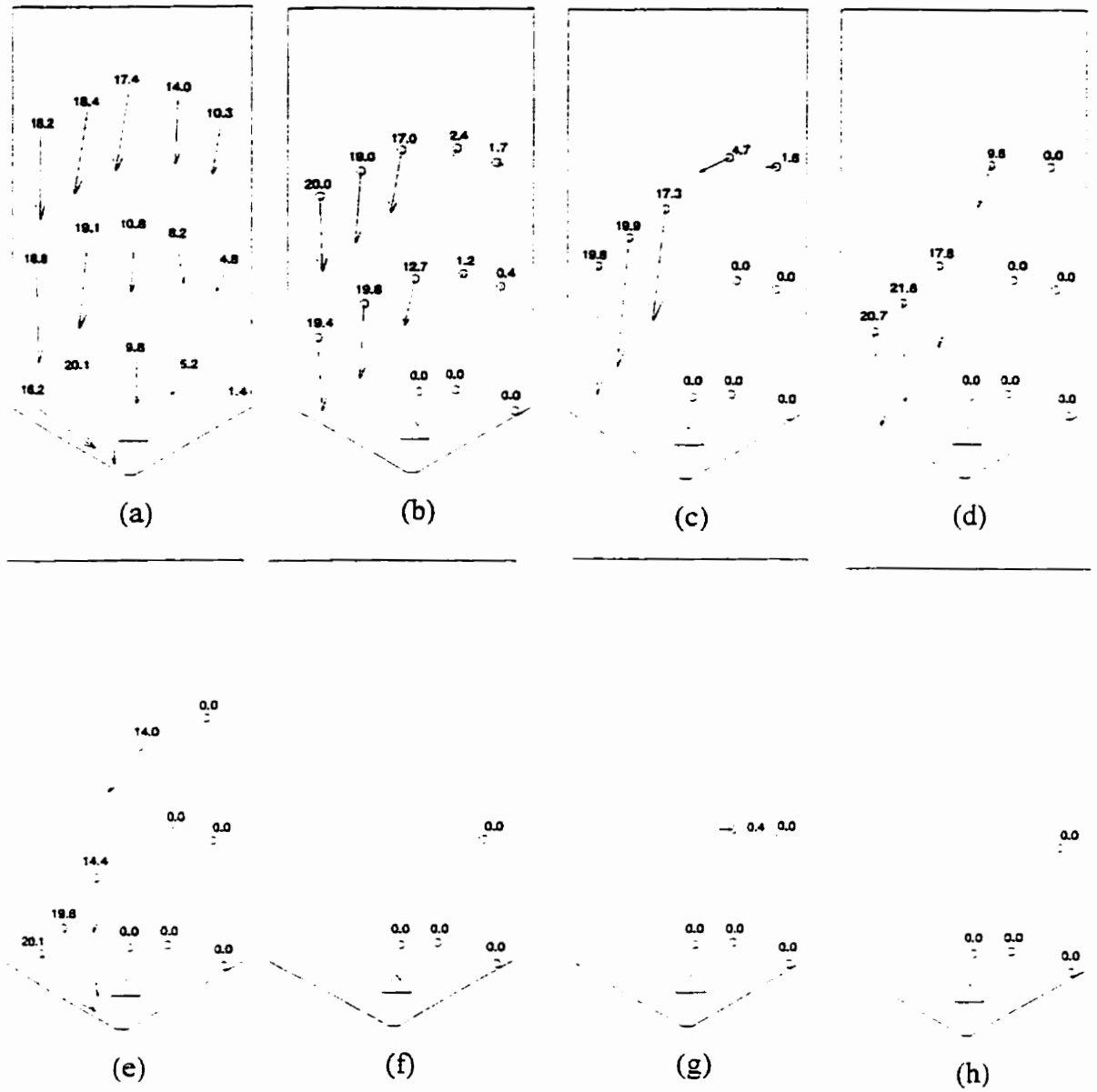

Fig. D.4 **Typical velocity profiles (in mm/s) in the model bin with a fixed insert, Test F2C. a) 0 s, b) 15 s, c) 30 s, d) 45 s, e) 60 s, f) 75 s, g) 90 s, h) 105 s, i) 120 s, j) 135 s, and k) 150 s.**

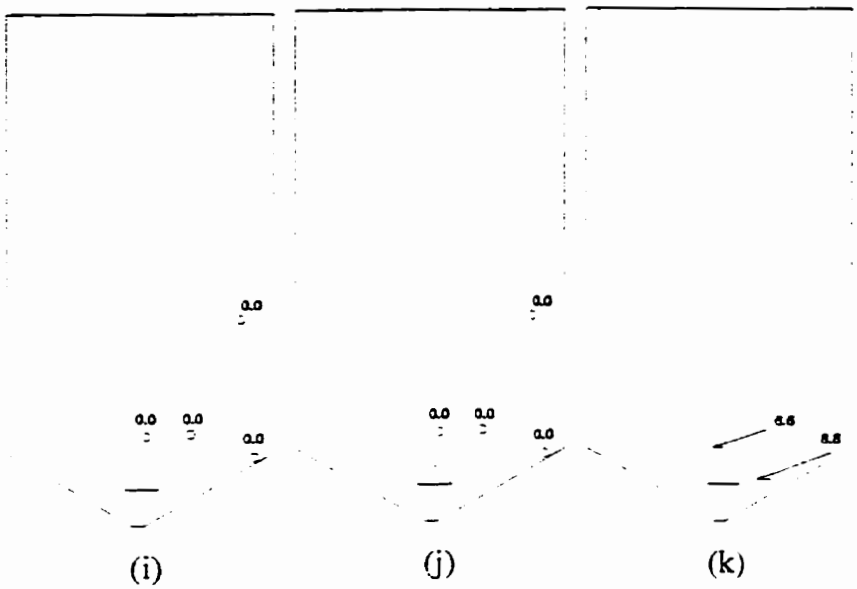

(i) (j) (k)

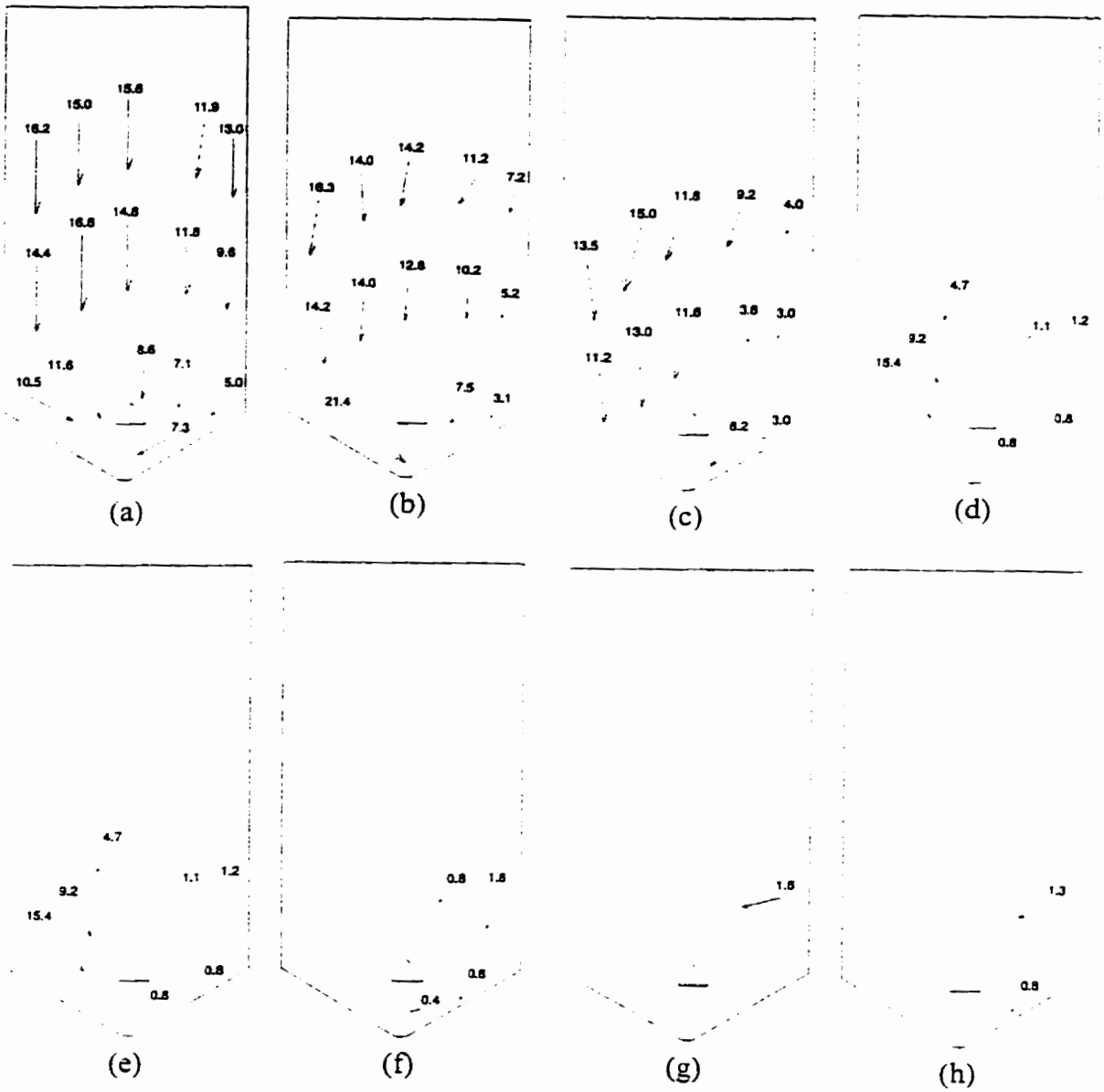

Fig. D.5 **Typical velocity profiles (in mm/s) in the model bin with a fixed insert, Test F3A. a) 0 s, b) 15 s, c) 30 s, d) 45 s, e) 60 s, f) 75 s, g) 90 s, h) 105 s, and i) 120 s.**

(i)

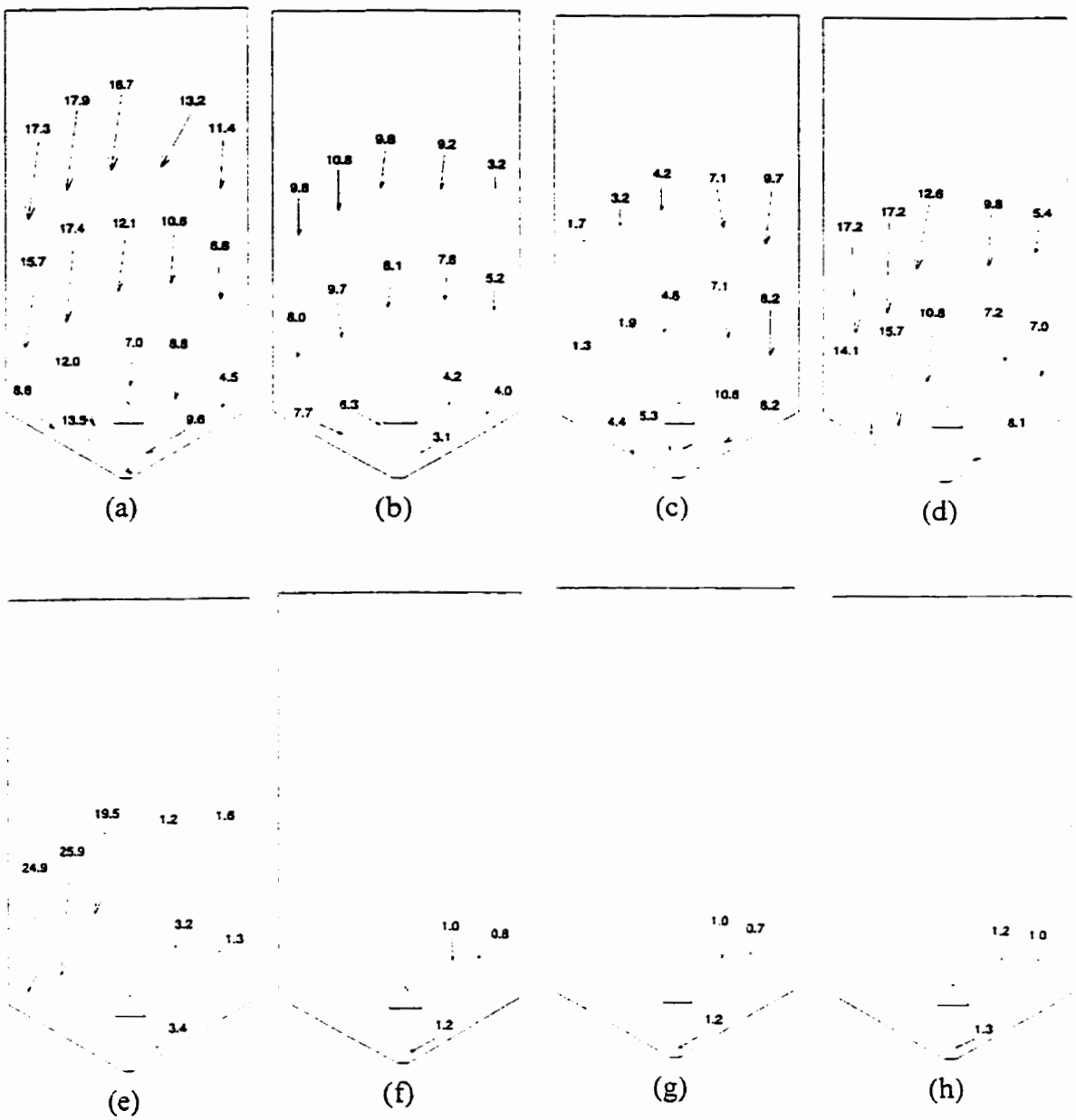

Fig. D.6 **Typical velocity profiles (in mm/s) in the model bin with a fixed insert, Test F3B. a) 0 s, b) 15 s, c) 30 s, d) 45 s, e) 60 s, f) 75 s, g) 90 s, h) 105 s, and i) 120 s.**

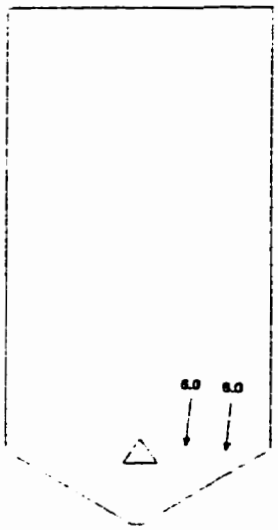

(i)

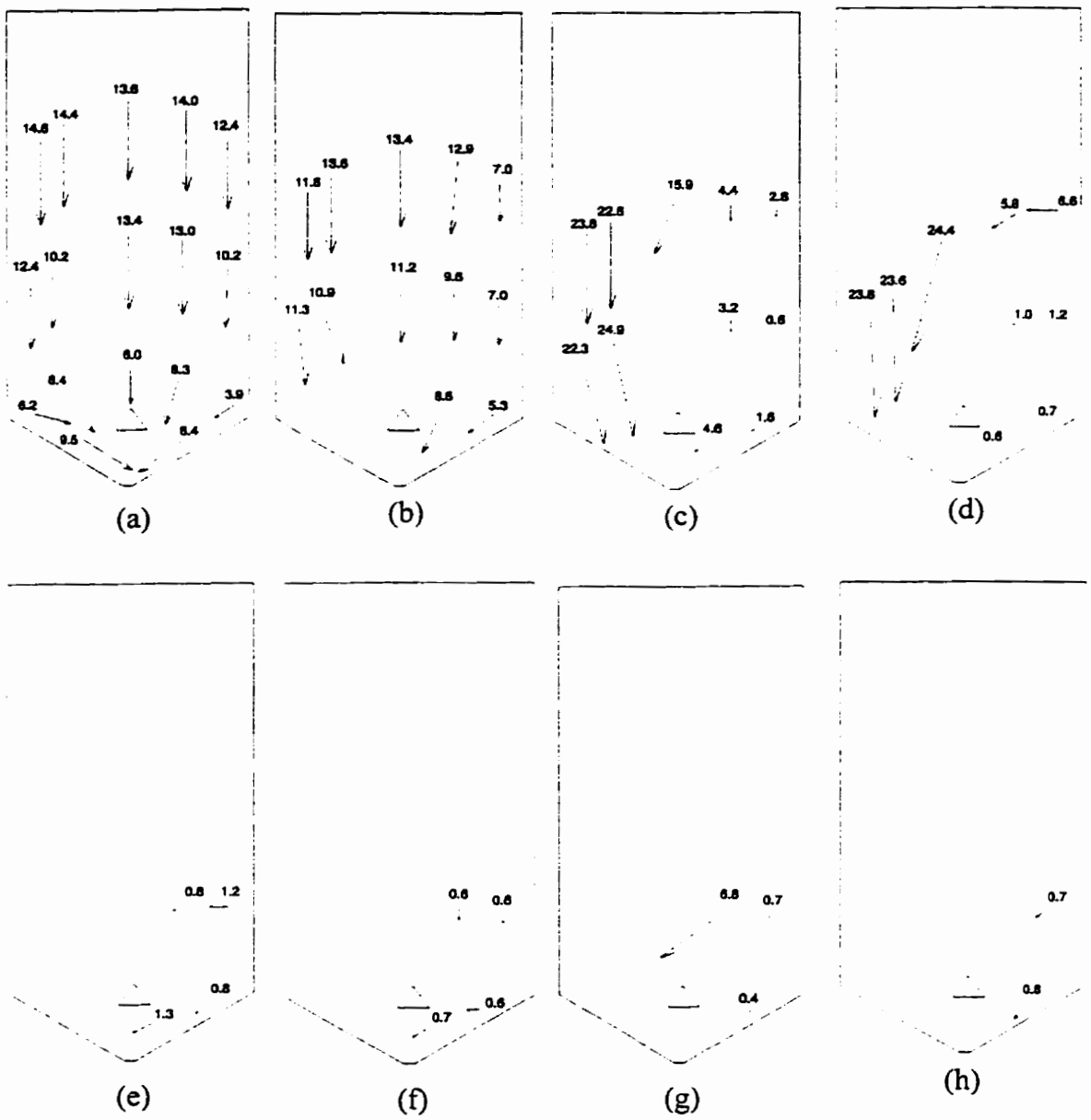

Fig. D.7 **Typical velocity profiles (in mm/s) in the model bin with a fixed insert, Test F3C. a) 0 s, b) 15 s, c) 30 s, d) 45 s, e) 60 s, f) 75 s, g) 90 s, h) 105 s, and i) 120 s.**

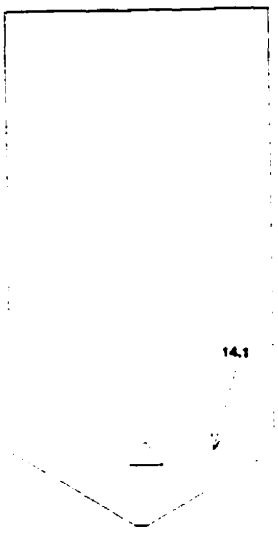

(i)

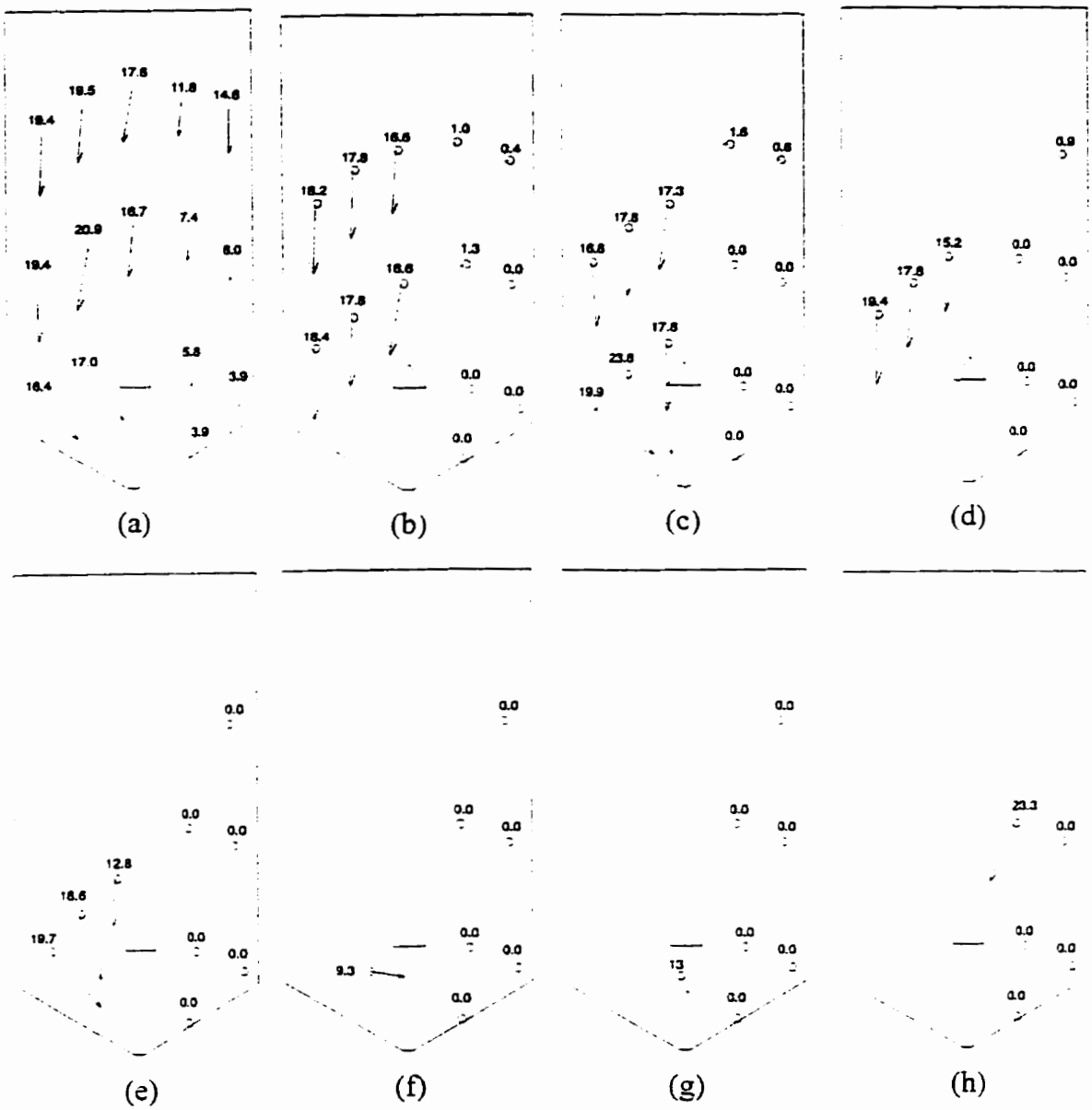

Fig. D.8 **Typical velocity profiles (in mm/s) in the model bin with a fixed insert, Test F4A. a) 0 s, b) 15 s, c) 30 s, d) 45 s, e) 60 s, f) 75 s, g) 90 s, h) 105 s, i) 120 s, j) 135 s, k) 150 s, l) 165 s, and m) 195 s.**

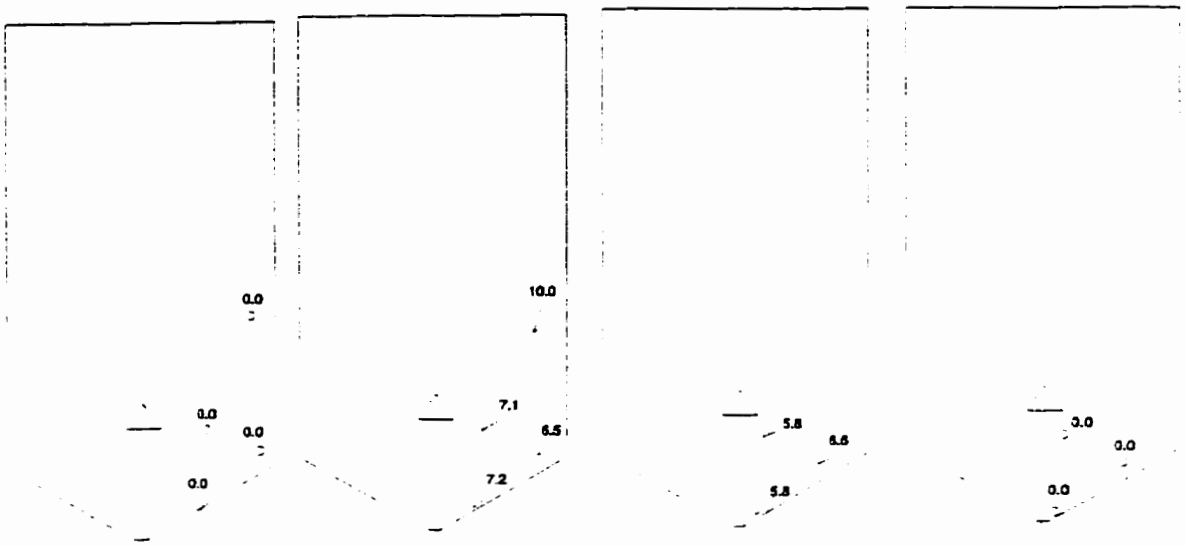

(i) (j) (k) (l)

(m)

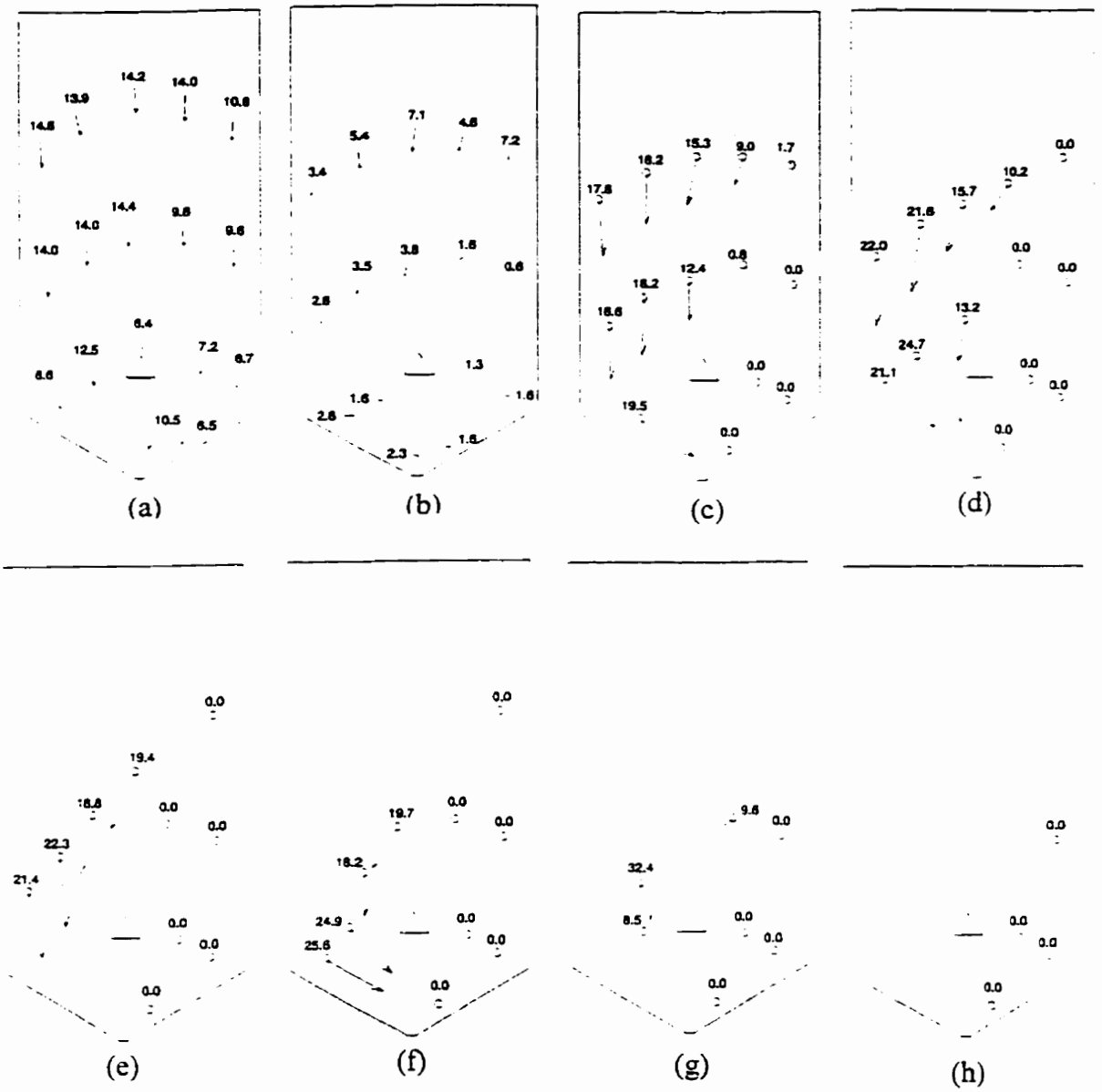

Fig. D.9 **Typical velocity profiles (in mm/s) in the model bin with a fixed insert, Test F4B. a) 0 s, b) 15 s, c) 30 s, d) 45 s, e) 60 s, f) 75 s, g) 90 s, h) 105 s, i) 120 s, j) 135 s, and k) 150 s.**

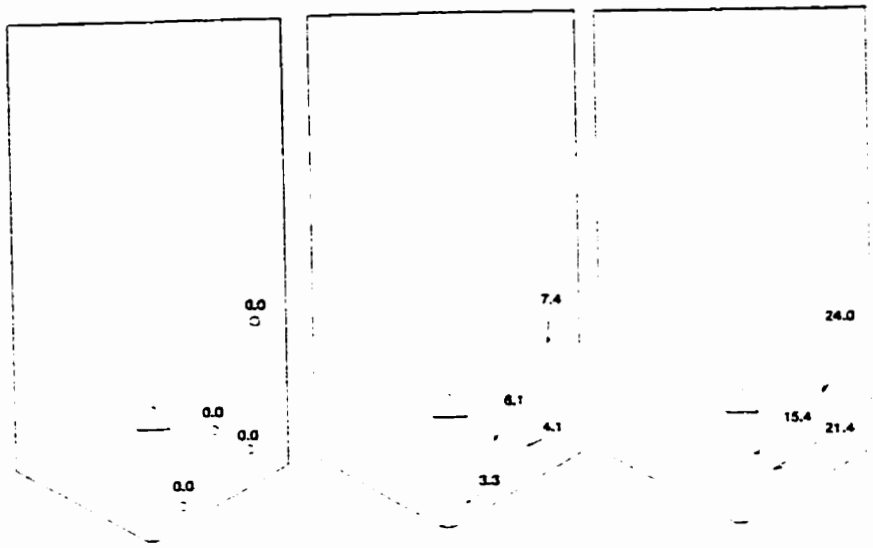

(i) (j) (k)

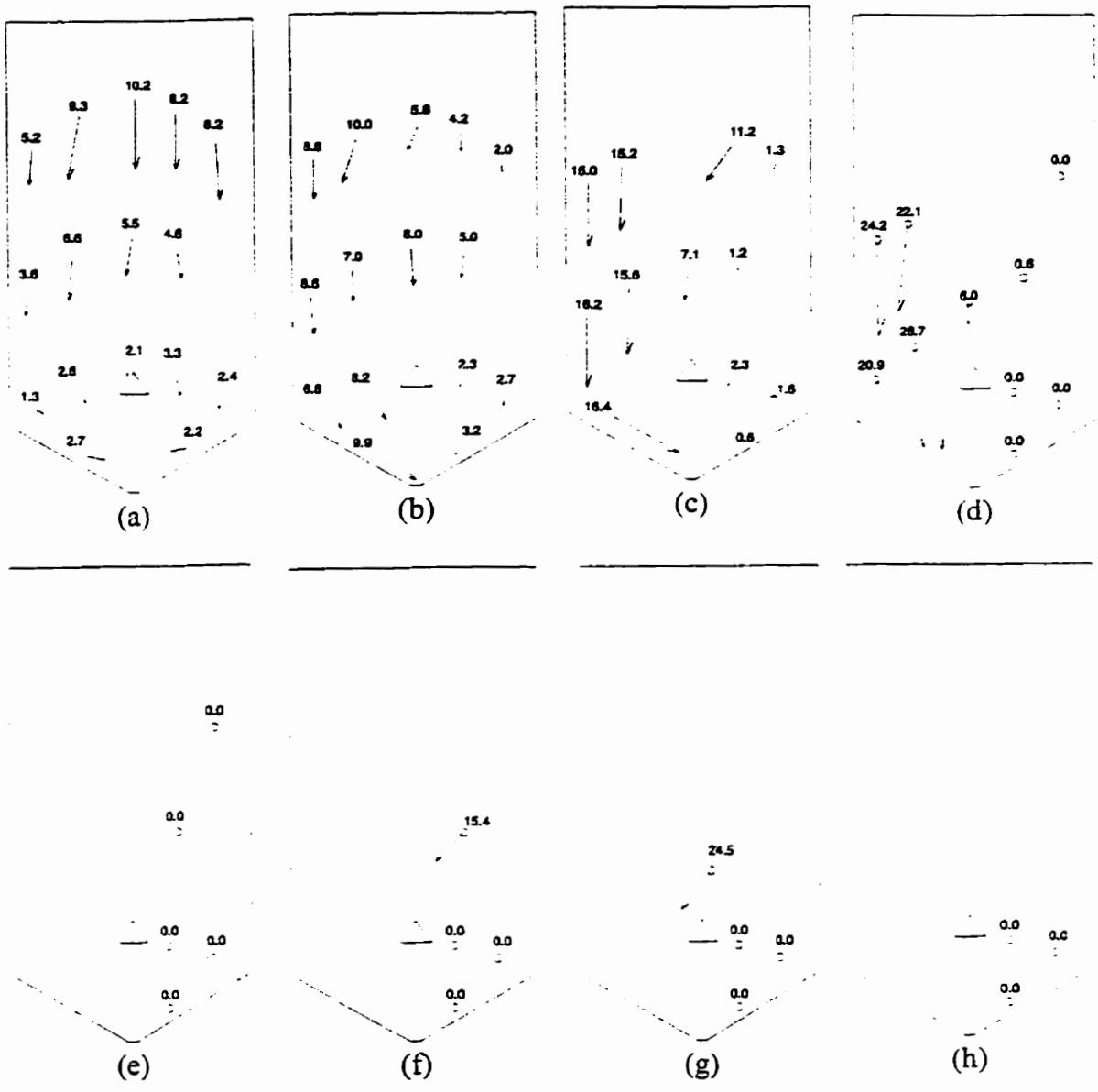

Fig. D.10 **Typical velocity profiles (in mm/s) in the model bin with a fixed insert, Test F4C. a) 0 s, b) 15 s, c) 30 s, d) 45 s, e) 60 s, f) 75 s, g) 90 s, h) 105 s, and i) 120 s.**

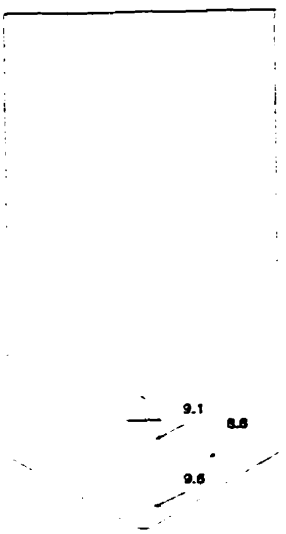

(i)

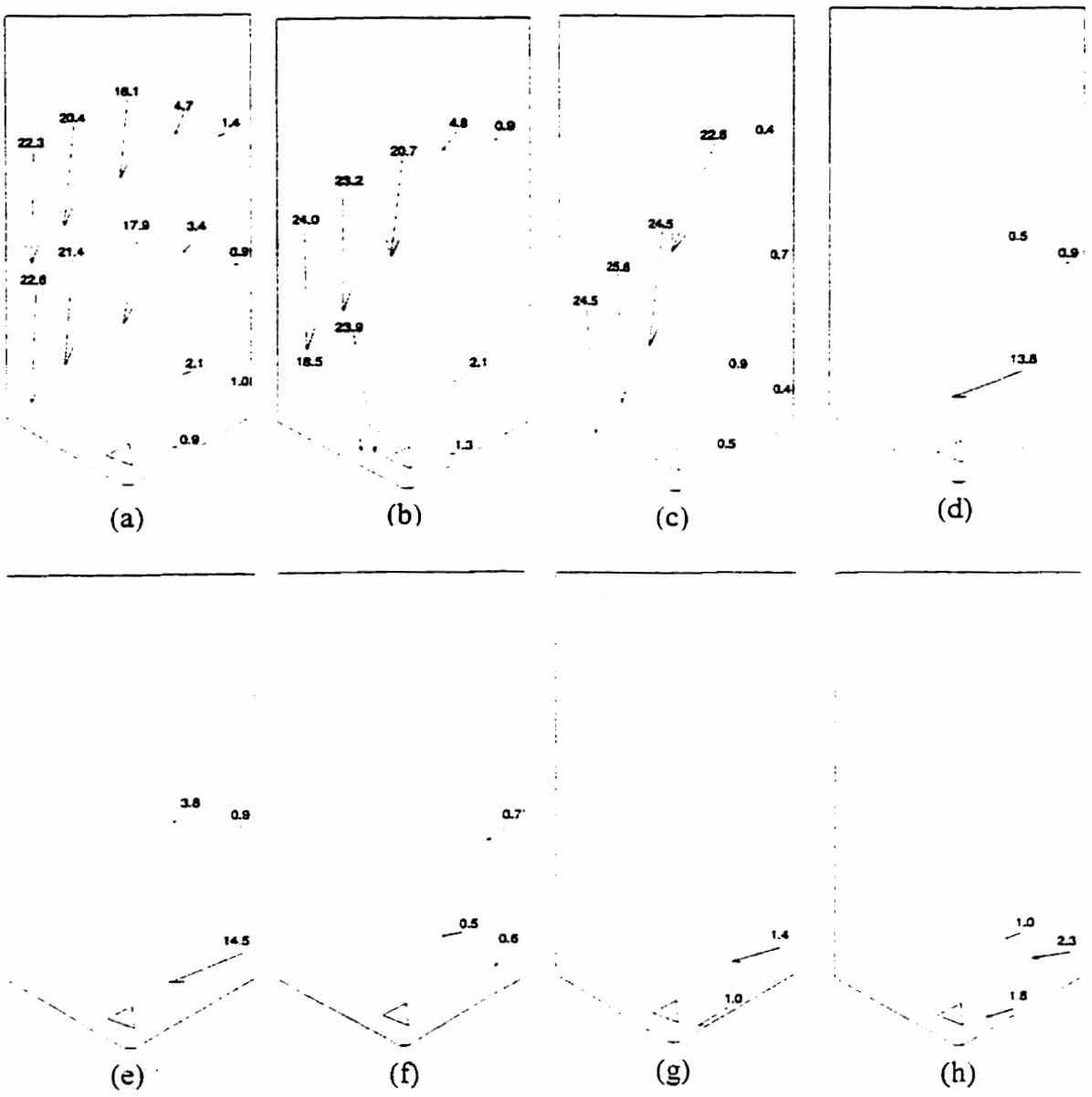

Fig. D.11 **Typical velocity profiles (in mm/s) in the model bin with a rotating insert, Test R2A. a) 0 s, b) 15 s, c) 30 s, d) 45 s, e) 60 s, f) 75 s, g) 90 s, h) 105 s, and i) 120 s.**

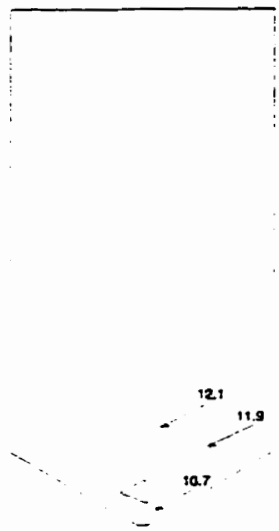

(i)

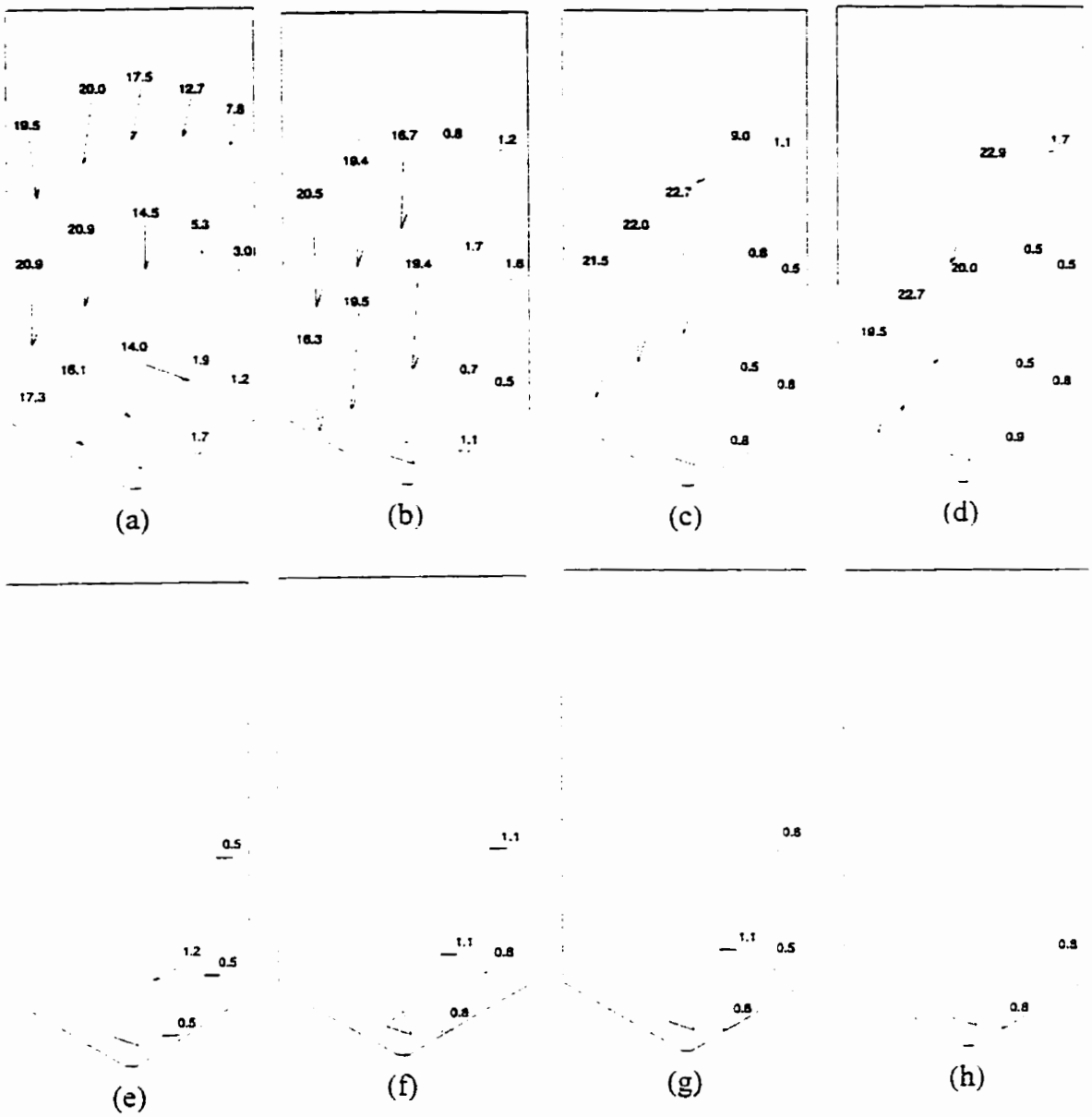

Fig. D.12 **Typical velocity profiles (in mm/s) in the model bin with a rotating insert, Test R2B. a) 0 s, b) 15 s, c) 30 s, d) 45 s, e) 60 s, f) 75 s, g) 90 s, and h) 105 s.**

IMAGE EVALUATION TEST TARGET (QA-3)

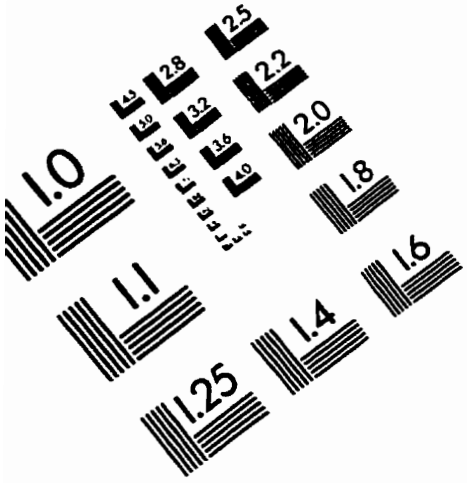

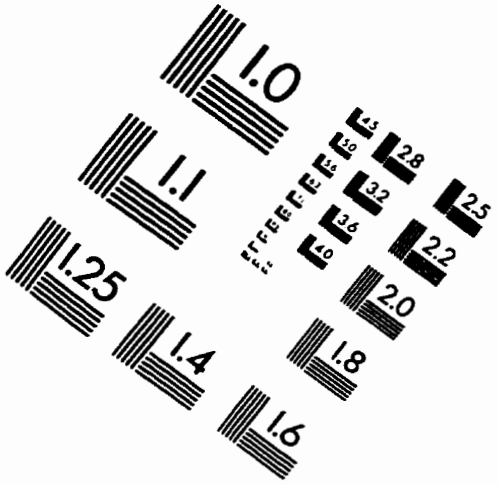

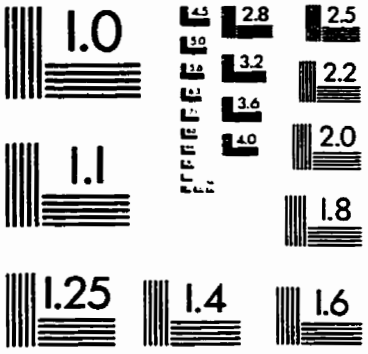

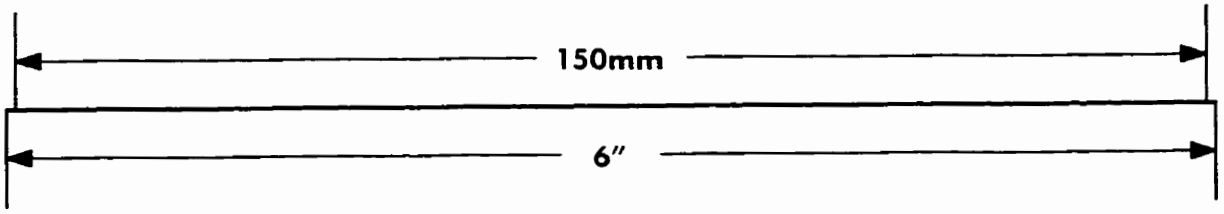

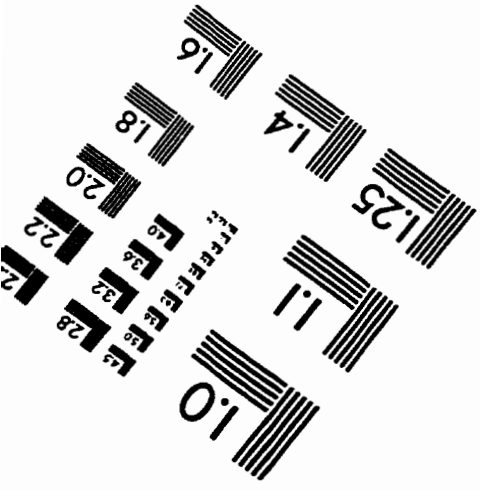

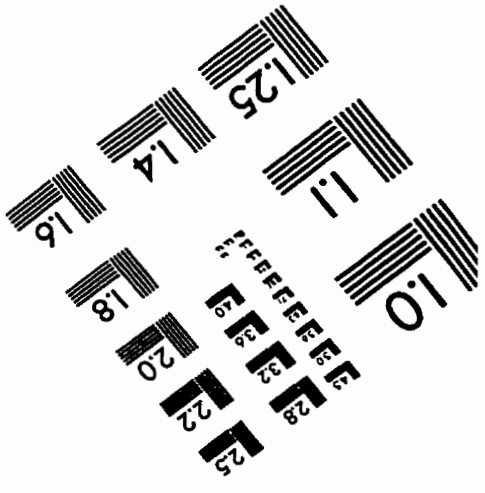

APPLIED IMAGE, Inc
1653 East Main Street
Rochester, NY 14609 USA
Phone: 716/482-0300
Fax: 716/288-5989